EFFECT OF FINES CONTENT ON STRENGTH OF GRANULAR MATERIALS

EFFECT OF FINES CONTENT ON STRENGTH OF GRANULAR MATERIALS

By PAOLO DI TULLIO, B. ENG

A Thesis Submitted to the School of Graduate Studies in Partial Fulfillment of the Requirements

for the Degree Master's of Applied Science in Civil Engineering

McMaster University MASTER'S OF APPLIED SCIENCE (2015) Hamilton, Ontario (Civil Engineering)

TITLE: Effect of Plasticity and Fines Content on Granular Materials AUTHOR: Paolo Di Tullio, B. Eng (McMaster University) SUPERVISOR's: Dr. P. Guo & Dr. D.F. Stolle NUMBER OF PAGES: xiv, 144

Abstract

This study focused on the effect of fines (minus 75 μm) content and type (plasticity) on the strength of granular base materials. Four different sources of crushed rock Granular A materials were selected by the MTO for testing. Routine laboratory tests were carried out on the four Granular A materials including sieve analysis, standard Proctor compaction, Atterberg limits, California bearing ratio, resilient modulus and permeability tests. Fines from an additional source, to be plastic, were selected and used as substitute fines for the Granular A natural fines but were found to have a similar index of plasticity (*PI*).

The influence of fines content on CBR varied for each Granular A source as some increased with increasing fines content and others decreased as the fines content increased. With the similarities in the *PI* of the two fines no clear trend in CBR values between samples with natural and substitute fines was observed.

The resilient modulus (M_R) values were by and large similar when the natural fines were replaced with substitute fines. The M_R decreased as the fines content increased when the water content was below 5 percent but at 7 percent water content some of the tests failed (could not be tested) at higher confining pressures. Energy dissipation was calculated from the resilient modulus tests and it was observed that the energy dissipation decreased as the confining pressure increased, with lower dissipated energies corresponding to higher M_R values. Given that definitive trends could not be identified with respect to the influence of fines and plasticity, the influence of the percent paste (sum of moisture and fines content at the time of compaction) was examined. As the paste increased the resilient modulus decreased and the damping ratio increased.

Results from permeability tests showed that for specimens with no fines present the permeability was much higher than those with fines. There was no significant change observed in permeability for specimens in which natural fines were replaced by substitute fines or as the hydraulic gradient was varied.

Acknowledgements

I would like to express my deepest appreciation and gratitude to my supervisors Dr. Dieter Stolle and Dr. Peijun Guo for their guidance and support throughout the duration of this study. The constant assistance, advice and time that they supplied proved to be instrumental in completing the research. I am also grateful for the uninterrupted financial support that they provided for my Master's studies. I would like to thank Dr. Stolle, Dr. Guo, Dr. Emery and Dr. Tait for being on my committee. Their thoughtful comments and questions were greatly valued.

Funding of this research by the Ontario Ministry of Transportation (MTO) is gratefully acknowledged. I wish to thank the laboratory assistants at McMaster University, Peter Koudys, and Kent Wheeler, for their help in understanding the testing equipment as well as their technical support when a problem occurred. I would also like to express my appreciation to Cong Lou and Joseph Van Der Zalm completing the resilient modulus testing.

I wish to thank Rachelle Szymkiewicz for her continuous help and encouragement during the course of my research. Finally I would like to thank my family, especially my parents, for their love and support over the past few years which have helped me achieve my goal of obtaining my Master's degree.

Table of Contents

List of Tables

List of Figures

List of Symbols

A – Cross- sectional area

b – Y intercept

c – Apparent cohesion

C_c – Coefficient of curvature

C_u – Coefficient of uniformity

D – Damping Ratio

D_{10} – Effective particle size

D_{30} – Diameter corresponding to 30 percent finer

D_{50} – Diameter corresponding to 50 percent finer

D_{60} – Diameter corresponding to 60 percent finer

E – Elastic modulus

h – Hydraulic head

i – Hydraulic gradient

k – Hydraulic conductivity

k_1, k_2 and k_3 – Regression constants

L – Specimen length

M_R – Resilient modulus

m – Slope

p_a – Atmospheric pressure

Q – Discharge volume

S_r – Degree of saturation

S_3 – Total radial stress

S_{max} – Maximum applied axial stress

t - Time

W - Elastic energy

ΔW - Energy dissipated

W_c – Moisture Content

w_{opt} – Optimum moisture content

ϵ – Accumulated strain

ϵ_r – Resilient strain

θ – Bulk stress

ρ_d – Dry density

ρ_{dmax} – Maximum dry density

σ_d − Applied deviator stress

σ_1 – Major Principal stress

σ_2 – Intermediate principal stress

σ_3 – Minor principal stress/confining pressure

τ_{oct} – Octahedral shear stress

ϕ – Friction angle

List of Abbreviations

AASHTO – American Association of State Highway and Transportation Officials

ASTM – American Society for Testing and Materials

CBR – California Bearing Ratio

LL – Liquid Limit

LVDT – Linear Variable Differential Transformers

MTO – Ontario Ministry of Transportation

PI – Plasticity Index

RAP – Reclaimed Asphalt Pavement

RCC - Recycled Crushed Concrete

RLT – Repeated Load Triaxial

UGB – Unbound Granular Base

UGM – Unbound Granular Material

USCS – Unified Soil Classification System

CHAPTER 1 INTRODUCTION

1.1 Background

With current construction activities in Ontario, the reserves of economic, quality aggregates for infrastructure construction have been decreasing, particularly in Southern Ontario and the Greater Toronto areas. To reduce the amount of quality natural aggregates being used in highway construction researchers have conducted studies to identify technologies that allow the use of residuals and by products, and in particular the use of materials such as reclaimed asphalt pavement (RAP) and recycled crushed concrete (RCC) in pavement structures. Within the context of granular base and subbase construction, an alternative strategy could be to relax the specifications set by MTO to allow the use of quarried aggregate that does not meet current physical property requirements, while maintaining proper structural and hydraulic performance of the engineered layers.

Current provincial (MTO) specifications for crushed rock (quarried) Granular A require less than 10 percent material passing the 75 μm sieve, with the material being non-plastic in order to control both moisture and frost susceptibility (OPSS PROV 1010, 2013). In Southern Ontario, many quarries contain carbonate rock with thin shale layers, which when subject to weathering, crushing and processing, can break down to form clay minerals that have plastic properties. From an environmental and sustainability factors, there isj increasing pressure to technically evaluate granular base and subbase aggregate specification requirements for fines content.

1.2 Objective and Scope

The primary objective of this study was to investigate the influence of fines content and type, as well as the effect of water, on the resilient modulus, permanent deformation and permeability properties of quarried crushed, processed rock unbound granular base aggregates. The effect of moisture content on the mechanical properties was also examined. To ensure that the pavement drainage requirements set by MTO are met, the permeability of the four Granular A materials were also considered.

The scope of this study includes the following:

1. Completion of a literature review that focuses on the use, testing and evaluation of unbound granular material with emphasis on the impact of fines and water content on the resilient modulus, permanent deformation and drainage.
2. Performance of routine physical property tests, including sieve analysis, standard Proctor compaction, Atterberg limits, and CBR tests.
3. Carrying out triaxial resilient modulus tests on aggregates containing up to 10 percent fines.
4. Identifying the sensitivity of resilient modulus to the physical characteristics and index properties including, gradation, density, and CBR.
5. Analyzing the experimental data, interpreting the test results and assessing the aggregate containing up to 10 percent fines with regard to influence on M_R and CBR.
6. Providing recommendations for the use of Granular aggregates containing up to 10 percent fines.

I was responsible for completing Proctor compaction, sieve analysis, Atterberg limit, CBR, and permeability tests as well as interpreting the results for these tests along with the results of the resilient modulus tests.

1.3 Outline

This thesis has five chapters including the introductory chapter. Chapter 2 presents a literature review on resilient modulus and the factors that affect the resilient modulus, plastic strain deformation and drainage behaviour of unbound granular aggregates. Chapter 3 describes the materials tested for the experimental component of this study, methodologies of the different tests conducted, and equipment used to evaluate the performance of the Granular aggregates. Chapter 4 summarizes the results from the sieve analyses, standard Proctor tests, the California Bearing Ratio (CBR) and resilient modulus tests at various water contents, percent fines and type of fines. The permeability results for all materials are also summarized in this chapter. Finally, a summary of the observations from this study and final conclusions of the experimental work and recommendations for future work are presented in Chapter 5.

CHAPTER 2 LITERATURE REVIEW

2.1 Introduction

Unbound granular materials (UGM) are generally used for the base and subbase layers in pavement structures. The unbound material may be a natural material like crushed gravel and crushed rock, or it can be a residual or by product material such as slag or crushed concrete. The materials used are of a variety of sizes that fit together through particle interlocking. The quality of the interlocking between materials depends on the shape of the particles, the proportion of particles of each size, and compaction (Commission, 2000). Along with this, almost all granular materials used in road construction contain water.

As granular base and subbase layers generally make up the greatest thickness of a flexible pavement structure, there are several properties that are of interest. These properties include gradation, particle shape, stability, permeability, plasticity of fines, abrasion resistance, and resilient modulus. Base and subbase layers are designed to distribute the load and reduce the maximum stress induced by bus and truck traffic reaching the subgrade. It is important that the subbase layer does not undergo excessive permanent deformation while transferring the stresses. In climates where material is susceptible to frost penetration, these layers increase the distance between the surface and subgrade layers that may have the potential to heave.

To achieve the goals of load distribution and reduction of maximum stress of the base and subbase layers, the resilient modulus and resistance to permanent deformation that is developed due to repetitive traffic loading must be high. This requires that the layers to be free draining and non-frost susceptible. As indicated, current Ontario specifications for crushed rock Granular A require that less than 10 percent material passes through the 75 μm sieve, with the material being non-plastic (OPSS PROV 1010, 2013). Controlling the percentage of fines is important because fines influence the strength and permeability of a material. As the fines content increases the optimum water content tends to increase, the maximum dry density decreases, and the CBR decreases (Ayodele et al., 2009).

Pavement performance depends on the quality and uniformity of materials incorporated into the pavement structure. By carefully monitoring these characteristics during construction, improvements are made to the in-service performance of the pavement.

2.2 Resilient Modulus

In pavement structural design the goal is to use materials that have the necessary strength and drainage properties to support the intended bus and truck traffic ESALs for a given climate and the site subgrade soil conditions. When working with unbound granular materials the elastic modulus (E) is replaced by the resilient modulus (M_R) to describe the 'elastic' behaviour of a material. Resilient modulus, which is expressed as the ratio of the applied deviator stress to the resilient strain, is introduced by Seed et al. (1962).

$$M_R = \frac{\sigma_d}{\epsilon_r} \tag{1}$$

where σ_d= applied deviator stress; and ϵ_r= resilient strain

Resilient modulus is generally obtained by conducting repeated load, triaxial tests on reconstituted/undisturbed samples or can be obtained through correlation equations involving stress state and soil physical properties (George K. P., 2004). Cyclic triaxial tests are performed on pavement structures due to their ability to produce load pulses, which are intended to simulate bus and truck traffic loading. Representative principal stresses σ_1 and σ_3, that develop in a base later due to wheel loading are 51 kPa (7.4 psi) and 14 kPa (2 psi), respectively (George K. P., 2004).The total resilient axial deformation of the specimen is measured and used together with σ_d to calculate the resilient modulus.

The resilient modulus has become a well known measurement of stiffness properties for pavement structure materials, including subgrade, subbase, and base over the past 40 years. With this in mind, it is important to understand what affects the resilient modulus of unbound granular material.

2.2.1 Factors Affecting the Resilient Modulus of Granular Materials

Numerous studies have shown that the resilient modulus of granular base and subbase materials is affected by several factors, including: stress, density, water content, fines content (minus 75 μm), plasticity of fines, gradation and aggregate type. With regard to M_R, of interest in this study are percentage of particles passing the 75 μm sieve, the plasticity Index (*PI*) and liquid limit (*LL*) of the fines, density, water content (w_c). The interactions between these main factors are complex, which has lead to contradictions of research findings that are related to resilient modulus and permanent deformation. Table 2.1 summarizes the different factors that affect resilient modulus from Maree (1982).

2.2.2 Stress Sensitivity

Subgrade materials consisting of mineral particles derive their shear resistance to stress from interparticle interaction. Therefore the stiffness depends on the confining pressure and deviatoric stress. The interparticle friction of granular soils depends on the confining stress. The effects of confining stress are more pronounced on granular, non-cohesive soils when compared to cohesive fine-grained soils (Maher & Bennert, 2000). The effect of confining stress on resilient modulus also depends on the material properties of the aggregate constituents such as density, texture and permeability.

Table 2.1 Factors affecting the resilient modulus of granular base material (Maree, 1982)

Factor	**Change in Factor**	**Influence on**		
		K	***n***	$M_R = K\theta^n$
Duration of load pulse	0.1 to 1.0 s	No effect	No effect	No effect
Frequency of load pulse	0.3 to 1.0 Hz	No effect	No effect	No effect
Number of load cycles	Increase in load cycles	0.20% Higher	No effect to a slight reduction	Up to 20% increase
Load history	-	No effect	No effect	No effect
Density	Increase from 82.6 to 87.5%	100% increase	15% reduction	10% increase
Maximum particle size	19.5 and 37.5 mm	No effect	No effect	No effect
Fines content	Increase in fines	Slight increase	Slight increase	Optimum at 9% fines
Particle shape	Increase in angularity	Not determined	Not determined	Slight increase
Surface texture	More course	Not determined	Not determined	Slight increase
Degree of saturation	Increase from 20 to 90%	Up to 80% decrease	25% increase	Up to 60% decrease

There are various expressions that have been used to describe the resilient modulus of unbound granular materials as a nonlinear function of stress. Hicks and Monismith (1971) developed a non-linear, stress-dependent power function model used to determine the stress dependency of resilient modulus. This *K-θ* model may be expressed as (see List of Symbols for terms involved throughout):

$$M_R = k_1 * p_a(\frac{\theta}{p_a})^{k_2} \tag{2}$$

There are shortcomings with the *K-θ* model (Hicks and Monismith, 1971;Uzan, 1985). The model considers the all-around bulk stress to represent triaxial stress states but does not account for the deviator stress. Uzan (1985) modified the *K*-θ model to include deviator stress, $\sigma_d = \sigma_a - \sigma_r$. The model can be presented as:

$$M_R = k_1 * p_a (\frac{\theta}{p_a})^{k_2} (\frac{\sigma_d}{p_a})^{k_3} \tag{3}$$

The model has been extended for three-dimensional scenarios, where the deviatoric stress is replaced with the octahedral shear stress.

$$M_R = k_1 * p_a (\frac{\theta}{p_a})^{k_2} (\frac{\tau_{oct}}{p_a})^{k_3} \tag{4}$$

The model has been further modified using the Long Term Pavement Performance (LTPP) test data (Yau & Von Qu, 2002) to ensure that M_R does not vanish as τ_{oct} approaches 0:

$$M_R = k_1 p_a \left(\frac{\theta}{p_a}\right)^{k_2} (\frac{\tau_{oct}}{p_a} + 1)^{k_3} \tag{5}$$

where,

p_a= atmospheric pressure (100 kPa)

θ = bulk stress; $\theta = \sigma_1 + \sigma_2 + \sigma_3$

σ_1= major principal stress

σ_2= intermediate principal stress

σ_3= minor principal stress/confining pressure

σ_d = deviator stress = $\sigma_1 - \sigma_3$

τ_{oct} = octahedral shear stress

$$= \frac{1}{3}\sqrt{(\sigma_1 - \sigma_2)^2 + (\sigma_1 - \sigma_3)^2 + (\sigma_2 - \sigma_3)^2}$$

k_1, k_2 *and* k_3 = regression constants

For most granular base/subbase materials, the bulk stress dominates the magnitude of the resilient modulus. With increasing bulk stress the resilient modulus increases; i.e, k_1 and k_2 are greater than zero. Generally, the resilient modulus of clean aggregates are not very sensitive to deviatoric stress while the resilient modulus of fine-grained, cohesive soils tends to decrease with increasing deviatoric stress; i.e, k_3 is less than zero.

Based on the results from various Ontario Granular A aggregates, Stolle et al (2005) found that k_1 lies between 0.52 to 2.05, k_2 between 0.086 and 0.706 and k_3 ranges from -0.432 to 1.595, with k_3 concentrating around 0. The results showed that many of the aggregates are insensitive to deviatoric stress.

2.2.3 Effect of Fines Content

As indicated, there is a restriction on the amount of fines in the granular pavement layers. Owing to differences in research findings, the maximum allowable amount of fines before they have an adverse effect on the performance of these layers is not clear. Hicks (1956) reports that a certain amount of fines content is required for unbound granular base (UGB) materials as the fines assist the binding of particles. He suggests that the fines (minus 75 μm) content should range between 5 percent and 12 percent in UGB material, although fines content over 10 percent can have an adverse affect when the granular material is exposed to freezing and thawing.

Early reports by Haynes and Yoder (1963) show an optimum fines content at 9.1 percent, irrespective of aggregate type; i.e., crushed gravel or crushed rock. The resilient modulus increases with an increase in fines content up to this optimum and any further increase above 9.1 percent results in a reduction of resilient modulus. Hicks and Monismith (1971) later observe that the aggregate type affects the influence of fines on resilient modulus. For crushed aggregate the resilient modulus increases with increasing fines but for partially crushed aggregates the opposite trend can occur.

Barksdale and Itani (1989) note that the resilient modulus can decrease by 60 percent as the fines content increases from 0 to 10 percent. They also observe an increase in plastic strain as the fines content increases. Kolisoja (1997) investigated the effect of different properties on the resilient deformation behaviour. As more fines are added to well-graded materials, a slight decrease in resilient modulus occurs with increasing fines when the material approaches full saturation. Kolisoja (1997) also investigates the effect of the quality of the fines by adding fines from three different origins to two different materials. The results are consistent with the results of Barksdale and Itani (1989) who show a reduction of up to 20 percent in M_R when substituting the fines from one source with that of another.

Maree (1982) reports that the resilient modulus is highest when the fines content is 9 percent. This is similar to the results of Arnold (2004) who finds that the resilient modulus is higher for an aggregate with 10 percent clay fines than material with good quality aggregate and zero clay fines. Richardson's and Lusher's (2009) findings, which are similar to those of Yoder and Witczak (1975), show the optimum fines content for M_R is similar to the optimum fines for maximum CBR in the range of 6 to 9 percent.

Guo et al. (2006) examined the variation of *k*-values with respect to fines content, P_{200}, as seen in Figure 2.1. They find that materials with higher fines content tend to have smaller K_1 and K_3 values compared to materials with no fines, with K_2 decreasing at the same time. In other words, an increase in fines content may result in smaller resilient moduli that are more sensitive to the applied stress owing to the increase in K_2 and decrease in K_3. For aggregates with P_{200} greater than 5 percent, K_3 is generally negative, indicating that the resilient modulus tends to decrease substantially when increasing the deviator stress.

The type of fines, plastic and non-plastic can have an effect on the resilient modulus. Plastic fines tend to reduce the stability of the aggregate structure and thus increase the permanent deformation whereas non-plastic fines at low contents (8 percent) have the potential to reduce permanent deformation of crushed rock aggregates (Mishra & Tutumluer, 2012).

Barksdale and Itani (1989) study the effects of the plasticity of fines on the deformation properties and resilient modulus by replacing a certain percentage of fines with kaolinite or bentonite fines. They report that plastic strain increases from 0 to 75 percent as the content of kaolinite in the fines increases and the plasticity index (*PI*) of fines increases. The resilient modulus decreases with increasing kaolinite content. Their study used preconditioned specimens, 1200 load cycles per test, and multiple load stages of different stress intensity, each comprising of 200 load repetitions. Jorenby and Hicks (1987) also examine the effects of different percentages of plastic fines on crushed aggregates. Their research shows that the resilient modulus is largest at 6 percent plastic fines and decreases thereafter.

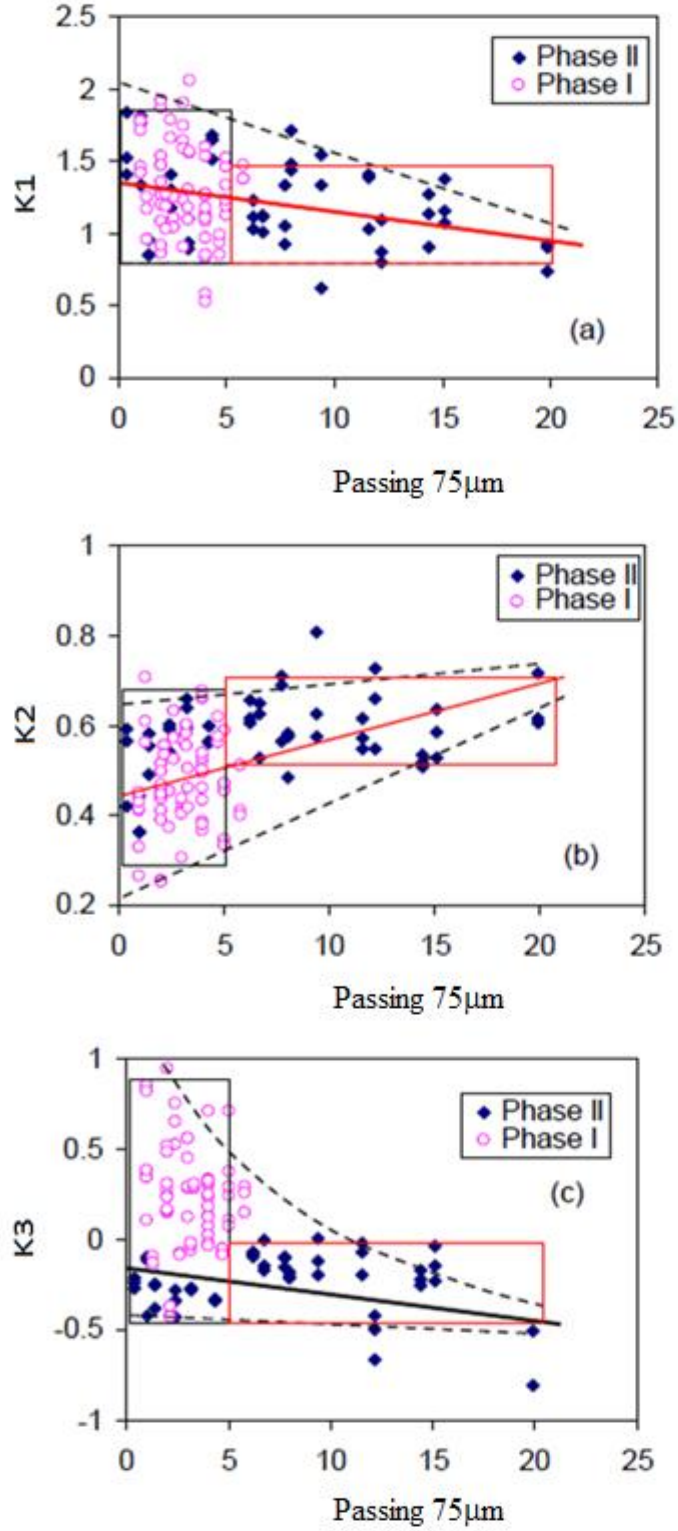

Figure 2.1 Variation of *k*-coefficients with fines content (Guo et al. 2006)

Caicedo et al. (2009) examined the effect of the plasticity index of fines and concluded that the amount of fines produce a greater effect on the resilient modulus than does the plasticity of the fines. As outlined, there is no simple answer to the influence of the fraction of plastic fines and the plasticity index on granular base material because different studies use different bases of comparison. Table 2.2 provides a summary of the findings of all the studies.

2.2.4 Moisture Sensitivity

The water content of UGMs is found to affect the resilient modulus characteristics in both laboratory and field conditions. Researchers, such as Barksdale and Itani (1989), Hicks and Monismith (1971), Haynes and Yoder (1963) and Dawson et al (1996) report a dependency of resilient modulus on the water content with M_R decreasing as water content increases. Haynes and Yoder (1963) observe a 50 percent decrease in resilient modulus in gravel as the degree of saturation increases from 70 to 97 percent and Hicks and Monismith (1971) show a decrease in resilient modulus as the water content increases beyond the optimum water content.

The performance of pavement structures depends on the permeability of the granular material and drainage conditions of the structure. Saturated granular materials may develop excess pore water pressure thereby decreasing the effective stress, leading to a decrease in both the strength and the stiffness of the material. Clean gravels and sands are less sensitive to water content owing to the absence of the small voids that are necessary to develop suction between particles (Maher & Bennert, 2000).

Stolle et al. (2005) conclude that the resilient modulus decreases as the water content increases, where aggregates with non-plastic fines are more sensitive to water content than those containing plastic fines as shown in Figure 2.2. They also find that the resilient modulus of aggregates is sensitive to the compaction method used. A 4 percent increase in water content shows a significant reduction in M_R when compacted by the impact method but only a slight decrease in M_R when the vibration method is used (Stolle et al. 2005).

Table 2.2 Summary of findings of the effect of fines content on M_R

Researcher	Fines Content	Effect on Resilient Modulus
Haynes and Yoder (1963)	9.1%	Increase in M_R up to this fines content and decrease in M_R above 9.1%
Hicks and Monismith (1971)	Increasing fines content in crushed aggregate	M_R increases with increasing fines
Hicks and Monismith (1971)	Increasing fines content in partially crushed aggregate	M_R decreases with increasing fines
Maree (1982)	9%	M_R is highest
Jorenby and Hicks (1987)	6%	M_R is largest at 6% but decreases thereafter
Barksdale and Itani (1989)	0-10%	M_R decrease by 60%
Barksdale and Itani (1989)	Kaolinite Fines (plastic fines)	M_R decreases with increasing fines
Kolisoja (1997)	Increasing fines content	Slight decrease in M_R
Arnold (2004)	10% clay fines	M_R higher than material with 0% clay fines
Richardson and Lusher (2009) Yoder and Witczak (1975)	6-9%	M_R is at highest

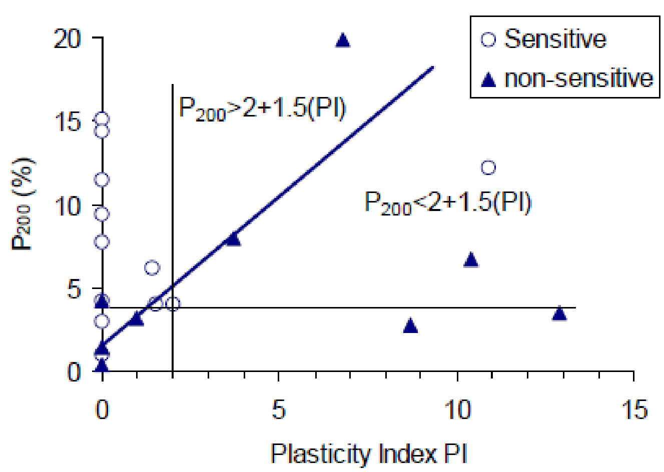

Figure 2.2 Fines content, plasticity index and the water sensitivity of M_R for Ontario aggregates (Stolle et al. 2005)

Kolisoja (1994), performed repeated load tests on aggregate that had five different gradings Based on the results the influence of the degree of saturation of a material having a high fines content is shown to be important. Well-graded materials are most affected by this, in which the resilient modulus decreases once the optimum water content is exceeded. The change in water content changes the effective stresses in fine-grained soils as a result of the changes in soil suction. As the water content decreases, the suction along with the effective stress and soil stiffness increase until very low water contents are reached. Fine-grained soils are especially problematic because the creation of excess pore pressure leads to a decrease in effective stress, excess permanent deformation and reduction in resilient modulus.

2.2.5 Effect of Density

When studying the effect of dry density of a compacted material on resilient modulus there are several factors that it depends on, including the grain size and shape and the amount of fines, as well as external factors like the compaction method. Barksdale and Itani (1989), Kolisoja (1994), Hicks and Monismith (1971) and many others all find that density plays a dominant role on the resilient response of materials. Hicks and Monismith (1971) report that the effect of density decreases with increasing fines content. Nevertheless the general trend is that the resilient modulus increases as the dry density increases. Rounded aggregates achieve higher dry densities than angular aggregates (Uthus, 2007). This indicates that the dry densities depend on the compatibility and the ability to fill voids in the structure.

The method adopted when compacting a granular material has a significant effect on the resistance to permanent deformation and long term stability (Austin, 2009). The grain size also has an influence. Different results are obtained when triaxial testing is completed on specimens that are fabricated using a vibration hammer when compared to the results obtained from

Modified Proctor compaction. Stolle et al. (2005) find that due to different compaction methods and compaction efforts (vibratory compaction and Proctor compaction) for fabricating the M_R test specimens, the optimum water content for vibratory compaction is lower resulting in different M_R results.

The dry density of a material is influenced by the amount of fines content in the material up to a certain percentage and plays an important role in the limiting of permanent deformation (Uthus, 2007). Dry density with high fines content may be important for dry of optimum conditions. However, as the fines content continues to increase, the optimum water content increase overrides the effect of dry density of the samples.

2.2.6 Effect of Grain Shape, Surface Texture and Aggregate Type

In a study conducted by Heydinger et al. (1996), natural, uncrushed gravel aggregate is shown to have a higher resilient modulus than crushed limestone. However, Barksdale and Itani (1989), Hicks and Monismith (1971), Allen and Thompson (1974) and others all find that crushed aggregate provides better load spreading properties and higher resilient modulus than uncrushed gravel. Barksdale and Itani (1989) find that the resilient modulus of angular crushed material is higher than that of rounded gravel by a factor of 50 percent at low mean normal stress and 25 percent at high mean normal stress, contradicting the results of Uthus (2007).

Different grain shapes for unbound granular material and fines can exist for the same material. These different shapes are shown in Figure 2.3. For high levels of stress the cubical rounded materials display the highest resilient modulus values. Cubical angular materials are however less sensitive to an increase in stress as the resilient modulus does not increase as much for higher stress levels (Uthus, 2007). Cubical angular materials display a higher resistance to permanent deformation when compared to cubical rounded aggregates, which is attributed to the interlocking of the particles and the higher internal friction. Lower internal friction causes less resistance to permanent deformation and rutting.

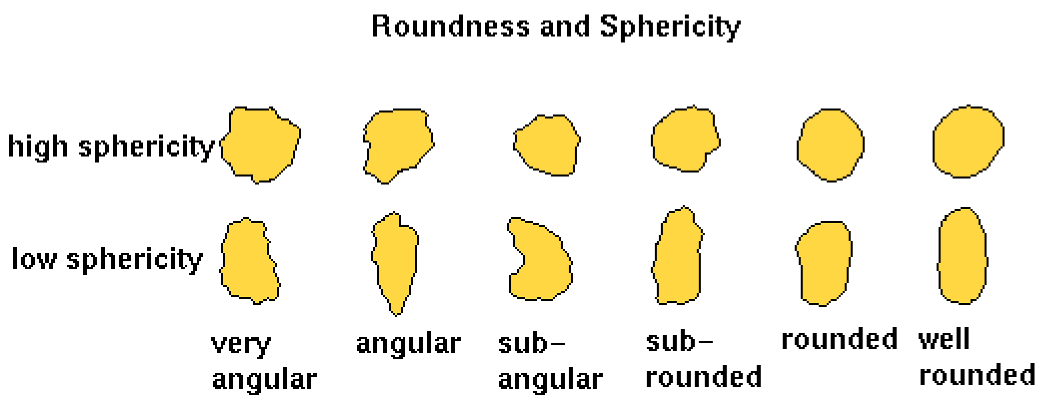

Figure 2.3 Particle shapes (Reeves, 2006)

Material can also be flaky angular and flaky cubical. The resilient modulus for both such materials is similar, although the dry density of flaky rounded material is higher than that of flaky angular material.

2.3 Resilient Modulus Correlations

2.3.1 Correlations between CBR and M_R

Simple correlations are used to routinely estimate the resilient modulus properties of subgrades and bases given standard CBR tests, R-value and physical soil properties (George, 2004). Heukelom and Klomp (1962) report a correlation between the Corps of Engineer CBR and the resilient modulus of soil. Another correlation is given in the AASHTO 2002 Design Guide (Stolle et al. 2005). It should be noted that the equation given by AASHTO is only applicable for fine-grained soils and fine sands (with CBR < 20) rather than for granular materials. Table 2.3 presents the two correlations however there are several other correlations equations which have been developed.

Table 2.3 CBR correlation equations

Researcher	**Equation**
AASHTO	$M_R\ (MPa) = 10.3\ CBR$
Corps of Engineering	$M_R\ (MPa) = 37.3\ CBR^{0.71}$

2.3.3 Correlations between Physical Properties and M_R

Correlations between M_R and physical properties are usually based on regression analyses of limited available experimental data. The majority of the existing relationships have been developed for subgrade soils.

Carmichael and Stuart (1978) propose a regression model for fine-grained soils and course grained soils based on the Highway Research Information Service database. Their goal was to establish correlation equations for predicting subgrade modulus from basic soil tests; for example for course-grained material:

$$\log M_r = 0.523 - 0.025w + 0.544(\log\theta) + 0.173(SM) + 0.197(GR) \qquad (6)$$

where M_R = resilient modulus (ksi); w = water content (%); θ = bulk stress (psi); SM = 1 for SM soils = 0 otherwise; GR = 1 for GR soils (GM,GW,GC, or GP) = 0 otherwise;

Rahim and George (2004) investigated the relevance of soil index properties used for predicting the resilient modulus of Mississippi soils. Their equation for course-grained soil is given by:

$$M_r(MPa) = 307.4\left(\frac{\rho_s}{w}\right)^{0.86}(P_{200}/\log C_u)^{-0.46} \qquad (7)$$

where ρ_s = dry density/maximum dry density; P_{200} = fines content passing #200 sieve; and C_u = uniformity coefficient.

Guo et al. (2006) correlated the k-coefficients of a constitutive model and the physical properties of 41 Ontario aggregates. The expression for the coefficient k_i, i = 1, 2 and 3, takes the form:

$$k_i = a_i P_4 + b_i P_{200} + \frac{c_i w}{w_{opt}} + d_i\left(\frac{\rho_{dr}}{\rho_{opt}}\right) + e_i w_c + f_i \rho_{dr} + g_i w_{opt} + h_i \qquad (8)$$

where a_i through h_i are regression coefficients, P_4 = percentage passing #4 sieve; P_{200} = fines content passing #200 sieve; w = water content (%); w_{opt} = optimum water content of soil (%); ρ_{dr} = dry density (kg/m^3); and ρ_{opt} = optimum dry density (kg/m^3). Using this regression expression, the calculated M_R is found to be in the range of +/- 30 percent of the experimental M_R values. The variables that have greatest effect on M_R are w/w_{opt} and $\rho_{s/}\ \rho_{opt,}$ which can indicate that the compaction method used for preparing the resilient modulus may play an important role. Equation (8) does not take into account the influence of the plasticity of fines. The regression constants a_i through h_i are listed in Table 2.4 with Figure 2.4 comparing the experimental k-coefficients with those calculated from the regression model.

Table 2.4 Regression constants defining M_R-physical properties relations (Guo et al., 2006)

Variable	Coefficient	K_1	K_2	K_3
P_4 (%)	a	0.00098	-0.00222	0.005059
P_{200} (%)	b	-0.01104	-0.00033	-0.01451
w/w_{opt}	c	0.114106	-0.34213	0.676475
$\rho_{dry} / \rho_{dry\ opt}$	d	-0.27318	-0.05079	0.084806
W (%)	e	-0.07785	0.060897	-0.1237
ρ_{dry} (kg/m^3)	f	0.000338	3.88E-05	0.000712
w_{opt}	g	0.080172	-0.04438	0.045166
	h	0.577858	0.930883	-2.07516

2.4 Plastic Strain Deformation

The development of the plastic strain of unbound granular material under traffic loading has received considerable attention in pavement engineering. Deformation is characterized by recoverable (resilient) deformation and residual (permanent) deformation. The plastic strain accumulates as the loading continues until the material rearranges into a stronger structure or failure occurs (Uthus, 2007). The deformation of granular material may be characterized by the stress-strain relation. Figure 2.5 shows that as the stress increases the material's resistance to further deformation decreases. At low levels of stress, the stiffness of the material increases as the stress increases (strain hardening), causing the particles to rearrange and move closer together. As the stress level continues to increase the strain behaviour softens (strain softening) with an additional increase in stress resulting in collapse in the extreme case.

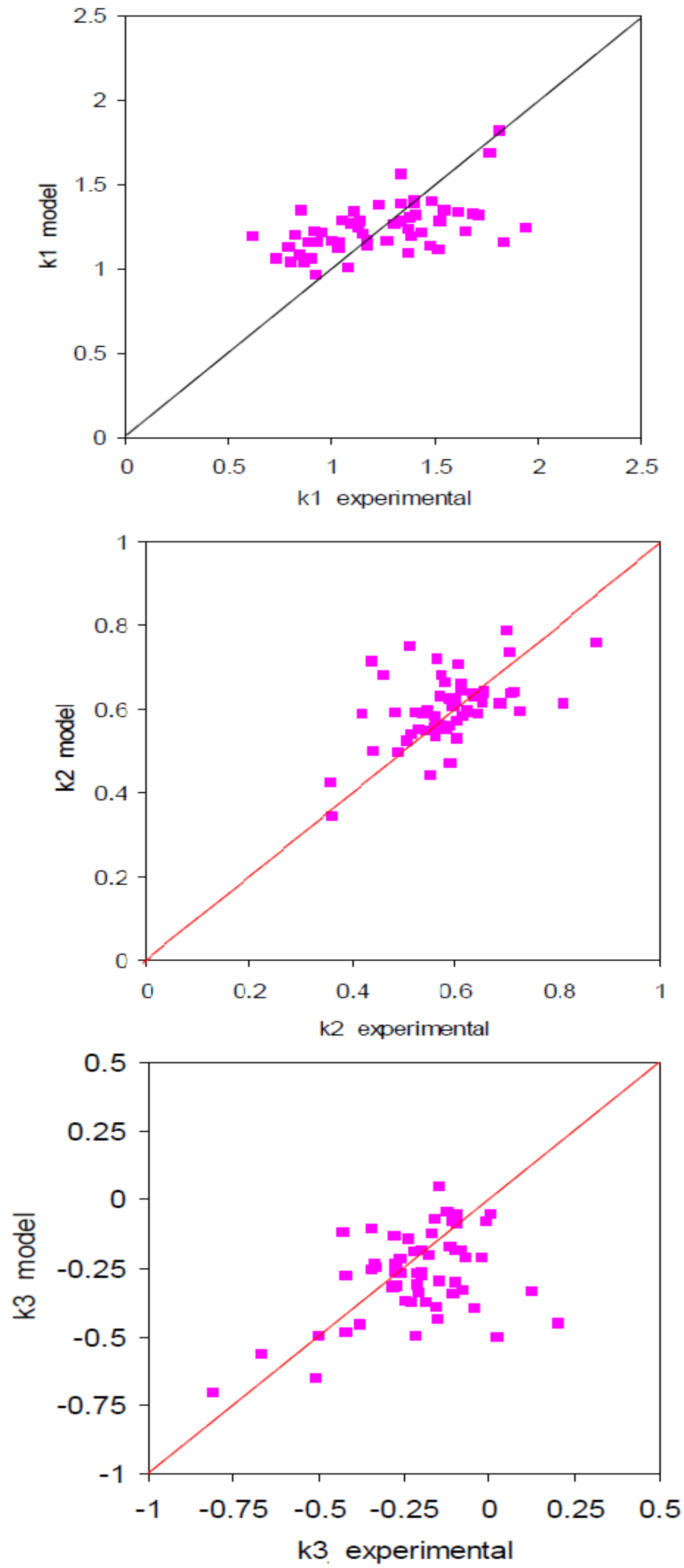

Figure 2.4 *k*-coefficients from Equation (8) (Guo et al., 2006)

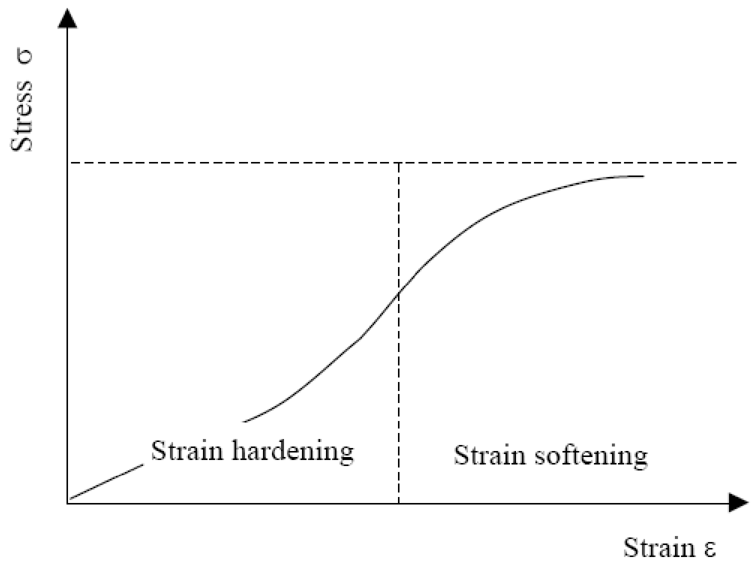

Figure 2.5 Stress strain behaviour of UGM's (Werkmeister et al., 2004)

Pavement structures are subject to large numbers of loading during their service life. The strain development in pavement structures is highly complex due to the interaction between resilient and permanent strains. The resilient deformation recovers after each load cycle, whereas the permanent deformation accumulates with each load cycle (Austin, 2009). The accumulation of deformation depends on the material properties, stress level, and loading conditions (Austin, 2009). Under cyclic loading the stress-strain behaviour follows a non-linear relation that is characterized by a hysteresis loop. A general idea of what a single strain hysteresis loop looks like is depicted in Figure 2.6. When several loops are plotted together, the loops become narrower at increasing cycles, showing a decrease in permanent deformation. Barksdale (1991) proposes an equation which can be used to track the strain accumulation:

$$\epsilon = a + b \log N \tag{9}$$

where ϵ is the accumulated strain, a and b are parameters that depend on the deviator and confining stress and N refers to load cycle.

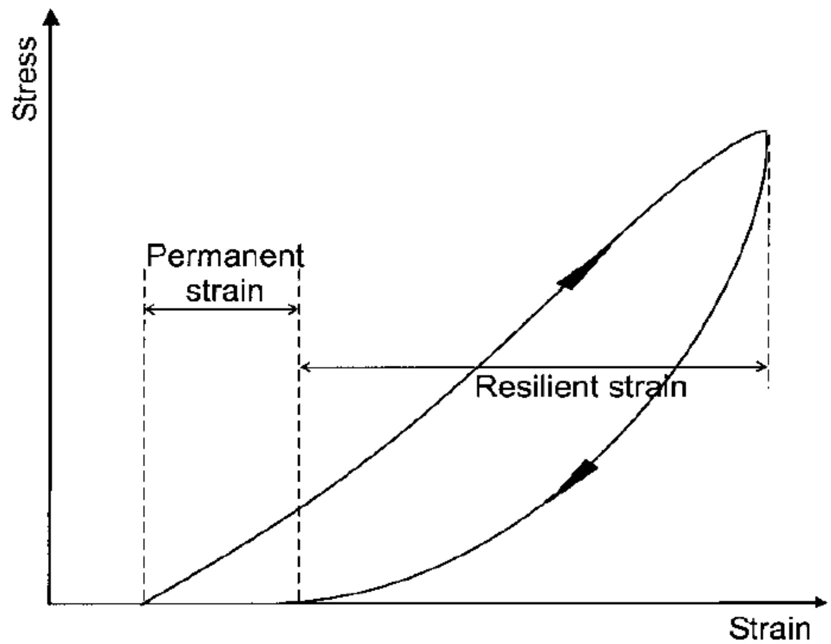

Figure 2.6 Hysteresis loop for one cycle of loading (Lekarp F. , 1997)

Stress sensitivity maybe taken into account via a relation that includes stresses,

$$\epsilon = f(\theta, \tau_{oct}, \phi, c) \tag{10}$$

in which θ = bulk stress, τ_{oct} = octahedral shear stress, ϕ = friction angle and c = apparent cohesion. An example of permanent deformation development of a specimen is presented in Figure 2.7. The plastic strain accumulation is sensitive to many of the factors that influence resilient modulus, including: deviatoric stress, confining pressure and water content. An important conclusion that can be taken from the Austin (2009) study is that resilient modulus cannot be used to evaluate permanent strain resistance.

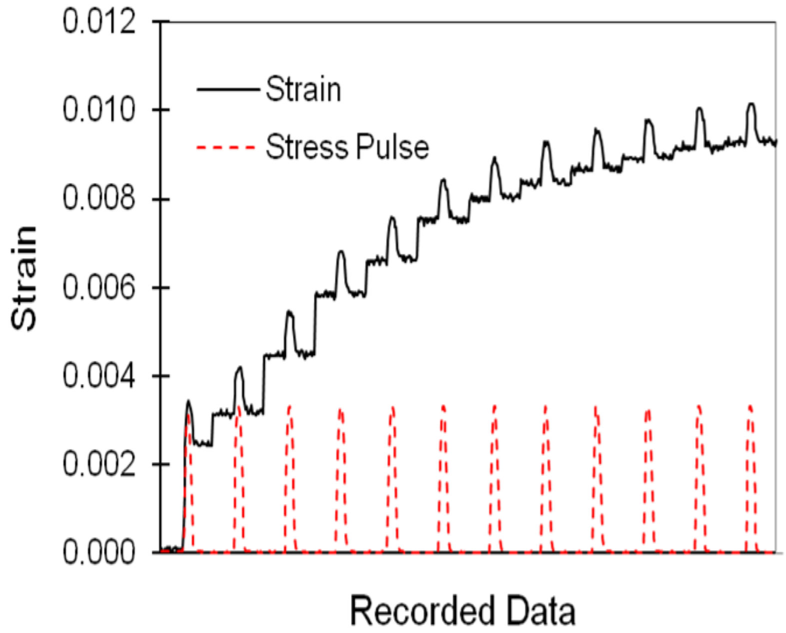

Figure 2.7 Schematic of permanent deformation on a specimen (Stolle et al., 2014)

It is generally accepted that an increase in the fines content leads to an increase in the magnitude of permanent deformation in cyclic triaxial compression tests (Barksdale R. D., 1991) (Mishra & Tutumluer, 2012). Dodds et al. (1999) report that materials containing 10 percent fines produce the highest deformations. They also observed high pore water pressure development for materials with higher fines content. As a result of the high pore water pressure, the effective stress reduces and thus the level of confinement reduces.

Some research shows that with lower amounts of non-plastic fines, approximately 8 percent, the permanent deformation of crushed rock aggregate is lower than the deformation with plastic fines (Mishra & Tutumluer, 2012). On the other hand, Kolisoja (1997) and Belt et al. (1997) observe significantly high permanent strains for aggregates containing a high content of fines (>15 percent), as well as at low fines content. Based on their results, this suggests that there is an optimum fines content that will produce a low permanent strain. As the research on the effects of fines content on permanent deformation is inconsistent and varies from researcher to researcher, an overall conclusion cannot be drawn at this time.

2.5 Permeability

Based on Darcy`s law, the conventional property that describes the ease of flow of water through a soil is hydraulic conductivity, which in engineering is referred to as permeability. At the same time granular bases are not generally saturated and irrotational flow conditions are not developed (Commission, 2000). Designers aim to have roads drain sufficiently well to ensure that steady state saturated flow does not develop.

Although the Darcy approach cannot be applied to granular materials with any confidence, this does not mean the materials cannot act as a drainage media (Cedergren & Godfrey, 1974). It was concluded that 80-90 percent of severe and premature damage to pavement is caused by excess water. Ring (1974) reports that less than 0.5 in. (12 mm) of rain, if able to access the pavement structure, has the potential to fill all voids in a 6 in. (150 mm) thick open granular base course. As the weight and number of axle loads increase, the influence of water contributes to more damage of pavements including pumping and degradation along with the loss of shear strength (Huang, 1993). More recently, Dawson (2008) stated the presence of water in a pavement due to infiltration of rainwater through pavement surface defects reduces the effective stress. Hence, the stress as well as the elastic and plastic stiffness of the pavement material decreases. The rate of traffic-induced deterioration of the road increases during this time.

The movement of water in pavement structures is caused by gravity, capillary action, and/or vapour pressure. In fine-grained soils the flow of water is mostly by capillary action, whereas the flow in coarse-grained soil is due to gravity (Huang, 1993). The damaging effects of water on pavements are controlled by preventing it from entering the pavement, or by providing drainage to quickly remove it. Drainage systems can be classified as either surface systems or subsurface systems. Surface drainage systems remove rainwater flow from a road's surface and can be divided into transverse drainage and longitudinal drainage (Dawson, 2008). Subsurface drainage systems take care of groundwater or water that infiltrates through the pavement surface. The location of the drainage layer in a pavement structure can be in either the base course or on top of the subgrade. If the drainage layer is added on top of the subgrade, the permeability of the base and subbase must be greater than the infiltration rate so that the water can flow freely to the drainage layer (Huang, 1993). Sealing surface cracks is an important maintenance strategy to reduce the amount of water entering a pavement structure, thus mobilizing the resilient modulus of the granular layers and reducing permanent deformation.

The permeability, which controls drainage, is influenced by gradation. Aggregates with fines have lower permeability. For example, Emery and Lee (1977) report that the permeability of a Granular A crushed limestone decreases from 3.41×10^{-2} cm/s to 1.26×10^{-4} cm/s when 10 percent fines are included. Similar findings with Ontario experiences can be found in Senior et al. (2008). On the other hand, there is evidence that permeability is not an issue as long as the fines content is less than 10 percent (Senior et al. 2008; OPSS PROV 1010, 2013).

The relation between the mechanical properties and drainage is important as the stress-strain-load cycle behaviour is sensitive to the degree of saturation and ability of the granular material to rapidly dissipate any generation of excess pore pressure. In dense, well-graded materials where the pores are very small, surface tension forces tend to yield significant suction pressure (Commission, 2000). The suction holds the granular particles together, increasing the effective stress but as the pores become more and more filled with water, the surface tension decreases, reducing the suction. Lam (1982) finds that when the moisture content is in the range of $w_{opt} \pm 2\%$ the drainage condition for resilient modulus samples has negligible influence on M_R, indicating that no significant excess pore water pressure develops even under undrained conditions.

For granular materials there is a residual water content, which is the point where the granular material is in balance with the hydraulic environment (Commission, 2000). Sufficient water occupies the pores to generate suction and the water neither rises nor drains, but is held in equilibrium. When the residual water content is too high in a pavement structure, the suction is usually low and the mechanical capacity of the granular material decreases. Defects in the upper pavement layers may allow rainwater to penetrate into the granular layer, thus decreasing suction from a beneficially high value to a low value, which leads to a decrease in the mechanical capacity of the material.

CHAPTER 3 METHODOLOGY

This chapter presents a description of the four Granular A aggregates supplied by the MTO and a separate substitute plastic fines selected for this study and detailed information about the equipment and experimental testing procedures used in this study for the gradation, Atterberg limits, and standard Proctor compaction tests of the materials involved.

3.1 Test Program

An experimental testing program was developed to investigate the behaviour of unbound granular base for four Granular A quarry sources. The physical properties of each aggregate type were determined first, including sieve analysis (AASHTO T27), Atterberg Limit (AASHTO T89 and T90) and Proctor compaction (AASHTO T99). CBR testing (AASHTO T193-99) was then completed to evaluate the strength and stiffness characteristics of the materials. Permeability testing (ASTM D2434) was also carried out on the aggregates taking into account changes of the fines content as well as the plasticity of the fines.

Resilient modulus tests (AASHTO T307-99) were conducted on all selected aggregates at different fine contents and different water contents. A summary of the testing standards involved is presented in Table 3.1.

3.2 Material Tests

Four Granular A manufactured (crushed stone) aggregates from different sources, Sources 1, 2, 3 and 4, were tested in the laboratory to determine the effect of plastic and non-plastic fines on the resilient modulus of typical Southern Ontario (crushed stone rock) Granular A aggregates. The plastic fines, shown in Figure 3.1, were obtained from a separate source.

Aggregate previously tested at McMaster University, from various MTO regions, were used for comparison, where applicable. Table 3.2 shows the different material sources and the tests that each material were subjected to.

Table 3.1 Summary of testing procedures

Laboratory Tests	Test Method
Sieve Analysis of Fine and Coarse Aggregates	AASHTO T27
Determining the Liquid Limit of Soils	AASHTO T89
Determining the Plastic Limit and Plasticity Index of Soils	AASHTO T90
Standard Method of Test for Moisture-Density Relations of Soils Using a 2.5-kg (5.5-lb) Rammer and a 305-mm (12-in) Drop	AASHTO T99
Standard Method of Test for The California Bearing Ratio	AASHTO T193-99
Standard Test Method for Permeability of Granular Soils (Constant Head)	ASTM D2434
Standard Method of test for Determining the Resilient Modulus of Soils and Aggregate Materials	AASHTO T307-99

Table 3.2 Summary of tests

Test / Material	Sieve Analysis	Atterberg Limit	Proctor Compaction	Permeability	CBR	Resilient Modulus
Source1- F1 Natural Fines	Yes	Yes	Yes	Yes	Yes	Yes
Source 1- F2 Substitute Fines	Yes	Yes	Yes	Yes	Yes	Yes
Source 2 - F1 Natural Fines	Yes	Yes	Yes	Yes	Yes	Yes
Source 2 – F2 Substitute Fines	Yes	Yes	Yes	Yes	Yes	Yes
Source 3 – F1 Natural Fines	Yes	Yes	Yes	Yes	Yes	Yes
Source 3 – F2 Substitute Fines	Yes	Yes	Yes	Yes	Yes	Yes
Source 4 – F1 Natural Fines	Yes	Yes	Yes	Yes	Yes	Yes
Source 4 – F2 Substitute Fines	Yes	Yes	Yes	No	No	Yes

All four aggregates were rough textured and angular. Figure 3.2 shows the materials used in this study.

Figure 3.1 Substitute fines

Figure 3.2 Aggregates from Sources 1 to 4 (Top to Bottom)

All material was first placed into an oven and dried at a pre-specified temperature, 110°C, for a minimum of 15 hours. The quantity of dried material depended on the test being performed. Thereafter, the material was left out on the counter for a day for the material to cool down to room temperature before any tests were performed. Thereafter, the materials were subdivided using a splitter box and quartered according to the specifications in AASHTO T248-02 (AASHTO, 2011).

3.2.1 Sieve Analysis

Sieve analyses were conducted on all four aggregates. The particle distribution curves of each aggregate can be seen in Figure 3.3 and are also presented in Table A.1 of Appendix A. Included on the curves are the limits for Granular A aggregates set by the MTO (OPSS PROV 1010, 2013). Using the USCS soil classification, ASTM Standard D 2487-06 (ASTM, 2008), it can be seen that Source 1 is a well-graded sand with clay and gravel (SW-SC). Source 2 and Source 4 are both classified as well-graded gravel (GW) and Source 3 is well-graded gravel with silt and sand (GW-GM). A summary of the classifications along with the coefficient of uniformity and curvature can be seen in Table 3.3.

Table 3.3 Aggregate classification

	Source 1	Source 2	Source 3	Source 4
D_{10} (mm)	0.10	0.37	0.20	0.40
D_{30} (mm)	1.20	2.10	1.80	2.90
D_{60} (mm)	5.00	7.80	7.90	8.00
C_u	50.00	21.08	39.50	20.00
C_c	2.88	1.52	2.05	2.63
USCS	SW-SC	GW	GW-GM	GW
AASHTO	A-2-4	A-2-4	A-2-4	A-2-4
MTO	Granular A	Granular A	Granular A	Granular A

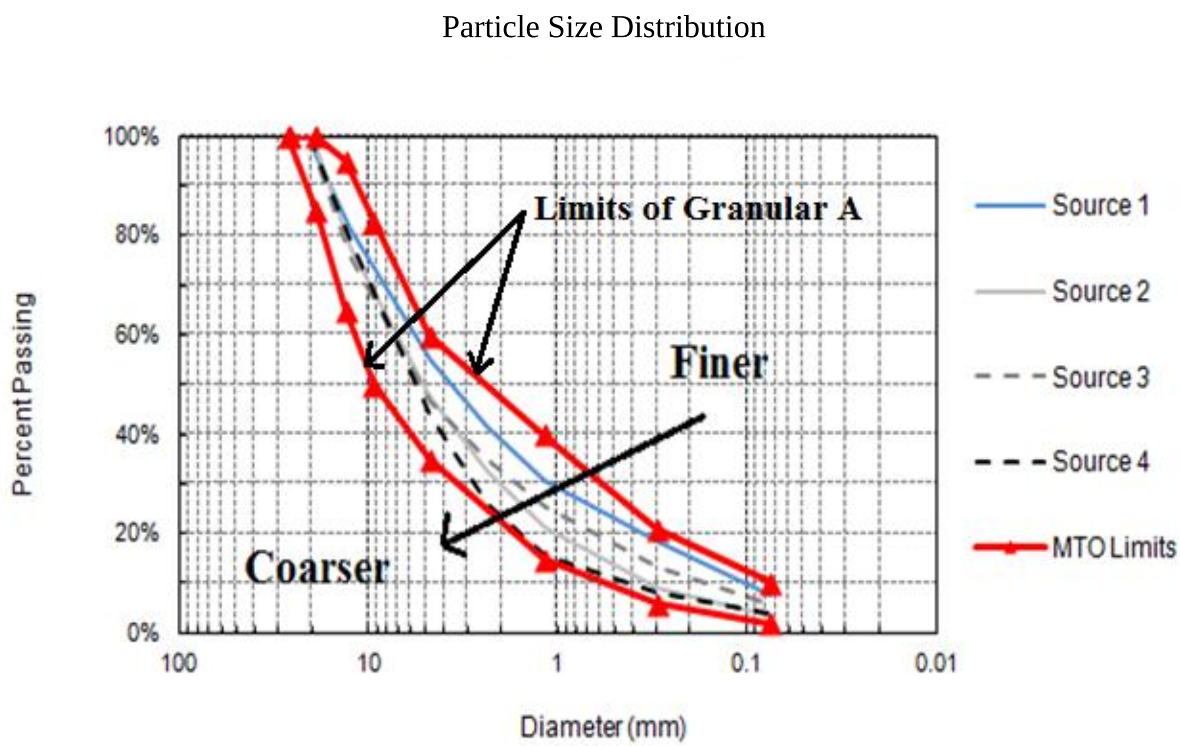

Figure 3.3 Particle size distributions

3.2.2 Atterberg Limits

Atterberg limit tests were subsequently carried out on the four sources to characterize the plasticity of the fines in accordance to AASHTO T89 and T90 (AASHTO, 2011). The fines were obtained from the material passing the 425µm sieve. Figure 3.4 shows the setup of an Atterberg test and Table 3.4 summarizes the results. It can be seen that Source 1 and Source 2 fines are clays (CL), according to USCS Soil Classification (ASTM, 2008). Source 3 fines are silt (ML) and Source 4 fines are silty clays (CL-ML). The substitute fines were also examined with material passing the 425µm sieve and 75 µm sieves. The fines passing the 425 µm sieve are silty clays (CL-ML), similar to Source 4 and the fines passing the 75 µm sieve are clays (CL), the same as Source 1 and Source 2 fines. Overall the difference between the *PI* of fines passing the 425μm sieve and 75 μm sieve is small. As the difference in *PI* is small the fines will be referred to as substitute fines instead of plastic fines.

Figure 3.4 Atterberg limit test (Liquid Limit on left, Plastic Limit on right)

Table 3.4 Atterberg limit test results (minus 425μm)

	Source 1		Source 2		Source 3		Source 4		Substitute Fines		Substitute Fines Passing 75 μm	
LL (%)	28	27	29	30	18	18.5	22	21	24	24	30	29.5
PL (%)	19.1	19.7	19.0	20.0	15.6	15.9	14.6	14.5	17.4	17.4	19.1	19.7
PI	8.9	7.4	10.0	10.0	2.4	2.7	7.4	6.5	6.6	6.6	10.9	9.8
USCS	CL		CL		ML		CL-ML		CL-ML		CL	

Figure 3.5 is the same as Figure 2.1, which shows the plasticity index and water sensitivity of different Ontario aggregates, now including the test results for each source of this study. The plasticity indexes of the sources in this study tended to be relatively high compared to those from the previous study.

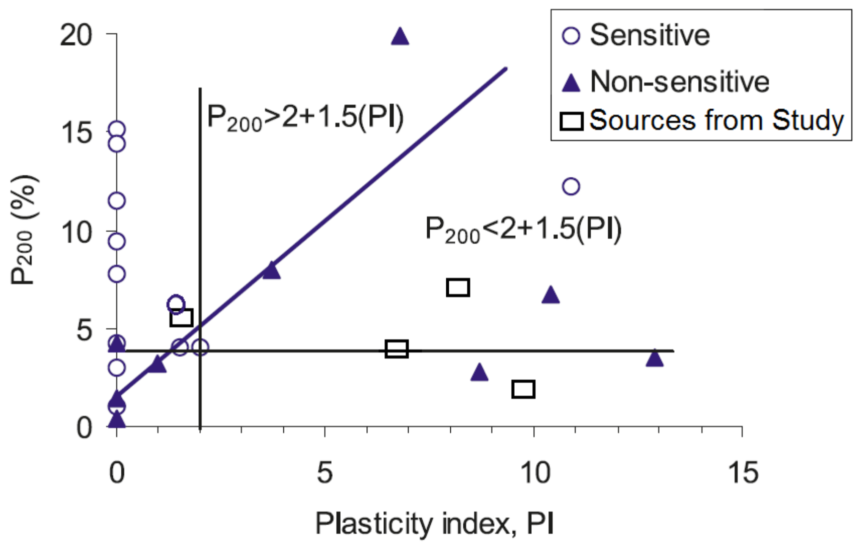

Figure 3.5 Fines content, plasticity index and water sensitivity for various sources (Stolle et al., 2005)

3.3 Proctor and CBR Preparation and Compaction

The samples for the CBR and standard Proctor tests were prepared in the same manner; i.e., in accordance with the procedures from AASHTO T99 Method C (AASHTO, 2011) . For both tests only material passing a 19.0 mm (3/4-in) sieve was used and any material retained on the 19.0 mm sieve was removed and replaced by an equal amount of material retained on the 4.75 mm sieve. For the Proctor test a sample size of 5 kg was prepared for testing, whereas for the CBR 7 kg was used. The mold sizes for the Proctor and CBR tests were 101.6 mm and 152.4 mm in diameter, respectively.

3.3.1. Impact Compaction

Impact compaction was adopted for the Proctor and CBR sample compaction. For the purpose of this study only the standard Proctor compaction was used to determine the optimum water content and the dry density of each material. It should be noted that many agencies use modified Proctor compaction and this would have provided better results but due to MTO recommendations standard Proctor compaction was used. For the standard method the weight of the hammer is 2.5 kg (5.5 lb) and the height of the drop is 305 mm (12 in). The number of layers for both the standard Proctor and CBR test is 3, however the number of blows per layer is different. The standard Proctor test requires 25 blows per layer, which is done manually with a compaction hammer, whereas the CBR test requires 56 blows per layer. Unlike the Proctor test, the CBR test compaction was completed using a compaction machine, which is shown in Figure 3.6. The dry density-water content curves are provided in Figure 3.7 with a summary of the optimum water content and dry density of each material presented in Table 3.5. The material with the highest density is Source 3, which is considered to be a high quality aggregate. Sufficient fines exist to help fill the voids, which may explain why Source 3 aggregate was found to be more sensitive to water content when compared to other aggregates.

Figure 3.6 Compaction machine

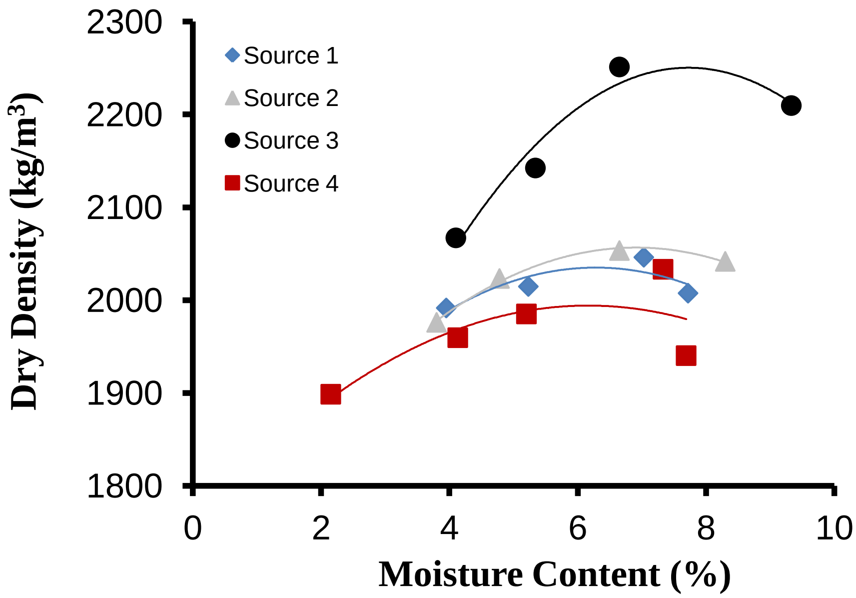

Figure 3.7 Standard Proctor compaction results

Table 3.5 Summary of optimum water contents and dry densities

	Standard Proctor Compaction			
	Source 1	**Source 2**	**Source 3**	**Source 4**
Optimum Water Content (%)	6.64	6.70	7.95	6.30
Maximum Dry Density (kg/m^3)	2035	2057	2250	2055

We can see that the optimum water content for all is within the range of 6.3 and 8 percent. Figure 3.8 compares the optimum water content and maximum dry density results of this study to the results obtained by Guo et al. (2006). The data points that are circled are considered to be outliers. The results from this study follow the same trends as the results from the previous study. P_{200} has little effect on the maximum dry density, ρ_{max} however the optimum water content tends to increase with fines content.

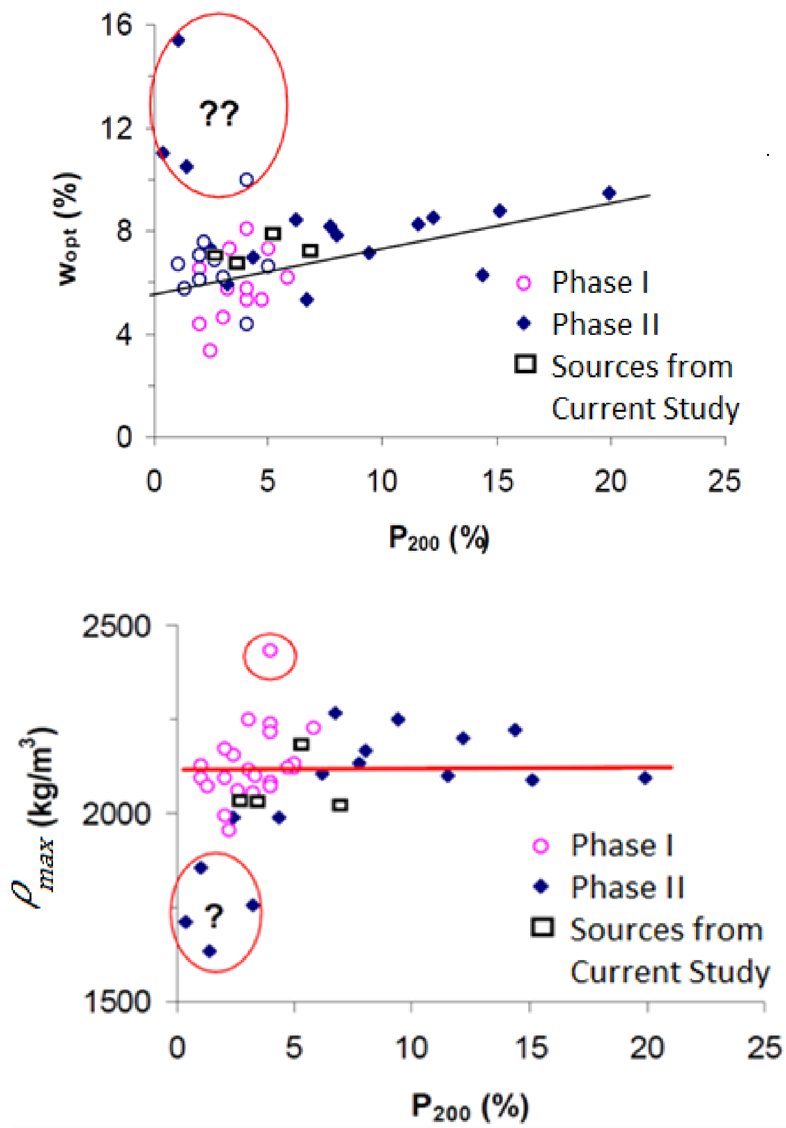

Figure 3.8 Variation of w_{opt} and ρ_{max} with fines content (Guo et al., 2006)

3.3 CBR Test

The laboratory California Bearing Ratio test method is intended for evaluating the potential strength/stiffness of subgrade, subbase, and base course materials for use in road and airfield pavements. The test setup is shown in Figure 3.9. Following the standard procedure, AASHTO T193-99 (AASHTO, 2011), the rate of penetration was set to 1.3 mm/min (0.05 in/min).

Prior to evaluating the penetration, some CBR specimens were soaked. The specimens were immersed in water for a period of 24 hours. An initial dial reading and final dial reading, at the end of the soaking period, were taken on the soaked specimens to calculate the swelling as a percentage. Soaked CBR tests were not completed on all test specimens, since the objective was to compare the CBR and M_R results under similar conditions.

When calculating the CBR, the values at both 2.5 and 5.0 mm (0.1 and 0.2 in) penetration were recorded and the load values were corrected when the stress-strain curves had a concave upward shape. For each material at each water content and fines content the CBR test was conducted twice to ensure repeatability in the results. If the results varied significantly a third test was completed. It should be noted that the samples were not soaked prior to the penetration tests.

For this study, both controlled heat source (oven drying) and uncontrolled heat source (microwave oven) drying methods were used to determine the water content of the aggregates. The procedures for determining the water contents are described in AASHTO T 265 (AASHTO, 2011). For the uncontrolled drying method, a minimum of 500g of material depending on the maximum particle size was required. Once the material was gathered it was placed in the microwave for five minutes. The microwave was 1.6 ft^3 with 950 Watts of power. After the five minutes the material was weighed and the sample was placed in the microwave for an additional two minutes and weighed again. If the change in water content was greater than 0.1 percent change, the sample was placed in the oven for additional heating until constant mass was reached.

3.4 Repeated Load Triaxial (RLT) Test

RLT tests were used to determine the resilient modulus of base, subbase and subgrade materials. According to standard procedures, AASHTO T307-99 (AASHTO, 2011), repeated axial cyclic stress of fixed magnitude for a duration of 0.1 seconds was be applied to the sample specimen followed by a 0.9 second rest period. The materials were tested with varying water content, and fines, both type and amount, changing one parameter at a time.

Figure 3.9 CBR test machine

3.4.1 Test Apparatus

The resilient modulus loading system used for this study was a closed-loop, servo-controlled electro-hydraulic MTS testing machine. Figure 3.10 shows the loading frame with the triaxial chamber, the transducers, including a load cell and two linear variable differential transformers (LVDT's), along with other key components of the RTL apparatus. The triaxial cell held a specimen of 152.4 mm (6 in) diameter and 304.8 mm (12 in) height.

For the 152.4 mm diameter specimen, the load-cell capacity, required to obtain accurate measurements of the applied load and the resulting deformation of the specimen, is 11.12 kN, and the LVDT ranges are 5 mm as specified by AASHTO T307-99 (AASHTO, 2011). The capacities for both the load cell and the LVDTs were slightly smaller than required by AASHTO T307-99 to allow for more accurate measurements.

3.4.2 Preparation and Compaction

AASHTO T307-99 describes the manner in which the resilient modulus test material is to be prepared. The materials tested for this study were Type 1 Granular A aggregate. Type 1 materials include untreated granular base and subbase materials, which contain less than 70 percent passing the 2.00 mm (No.10) and less than 20 percent passing the 75 µm (No.200) sieve and have a plasticity index of 10 or less (AASHTO, 2011). A split mold with a 152.4 mm diameter mold was used to fabricate specimens with a height ranging from 295 mm to 330 mm and using 15 kg of prepared material.

A rubber membrane was placed within the split mold while a vacuum was applied to draw the membrane to the inside of the mold. After the appropriate water content was achieved, the sample was compacted in six layers. Following the compaction of the final layer a metal spacer was placed on top of the sample to ensure a level surface. A second membrane was applied once compaction was completed to ensure the correct confining pressure could be maintained during a test and a vacuum was attached to draw the membrane to the inside of the mold.

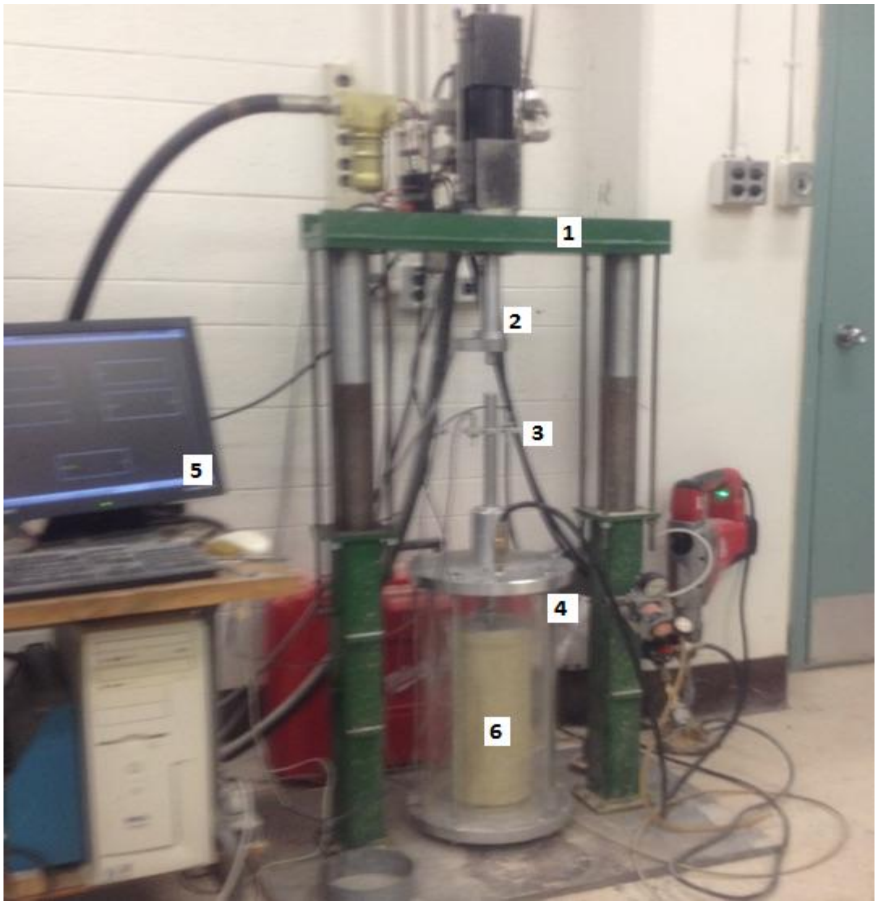

Figure 3.10 Repeated Load Triaxial apparatus 1-Load Frame; 2-Load Cell; 3-LVDT; 4-Triaxial Cell; 5-Data Acquisition Machine; 6-Soil Specimen

3.4.2.1 Vibratory Compaction

To compact a resilient modulus specimen a vibratory hammer was used. Compaction forces were generated by the hammer without kneading action, using a 152.4 mm (6 in) diameter tamping foot to minimize damage to the membrane. To achieve uniform compaction throughout the specimen the height of each layer was compacted to approximately 50 mm. Before a new layer of material was placed in the mold, the top surface of the pervious layer was lightly scratched to roughen the surface for better bonding between the layers as stated in AASHTO T309-99. The vibratory hammer and split mold is shown in Figure 3.11 and a compacted specimen is shown in Figure 3.12.

3.4.4 Resilient Modulus Test

Following the preparation and compaction of the specimen, it was placed in the triaxial chamber. The recording devices, that is the LVDTs and load-cell, were adjusted before conditioning. The conditioning process began by setting the cell pressure to 103.4 kPa (15 psi) and a minimum of 500 repetitions of a load equivalent of axial static stress of 103.4 kPa (15 psi) and a corresponding cyclic axial stress of 93.1 kPa (13.5 psi) were applied. Conditioning the sample helped to provide uniform contact between the top and bottom platens and the soil specimen. Conditioning also aided in the minimizing the effects of initially imperfect contact between the test specimen and the sample cap and base plate and the test specimen.

Figure 3.11 Vibratory hammer and split mold

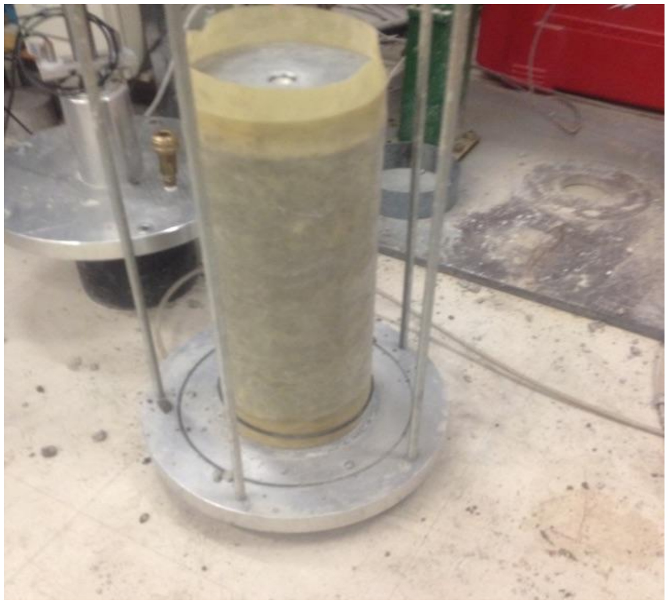

Figure 3.12 Compacted specimen

After completion of the conditioning, each resilient modulus test was performed according to the loading sequences presented in Table 3.6. The readings for each LVDT and the load-cell for the last five cycles of each loading sequence were recorded to calculate the corresponding resilient moduli.

3.4.5 Data Acquisition

Figure 3.13 shows a typical repetitive load pulse that is generated from a resilient modulus test system where each load cycle consists of 0.1 seconds loading time and 0.9 seconds of rest period. Following AASHTO T307-99 a minimum of 200 data points from the load cell and each of the two LVDT were recorded per cycle.

Table 3.6 Resilient modulus testing sequence

Sequence No.	Confining Pressure S_3		Max. Axial Stress, S_{max}		Cyclic Stress, S_{cyclic}		Constant Stress, $0.1S_{max}$		No. Of Load Applications
	kPa	psi	kPa	psi	kPa	psi	kPa	Psi	
0	103.4	15	103.4	15	93.1	13.5	10.3	1.5	500-1000
1	20.7	3	20.7	3	18.6	2.7	2.1	0.3	100
2	20.7	3	41.4	6	37.3	5.4	4.1	0.6	100
3	20.7	3	62.1	9	55.9	8.1	6.2	0.9	100
4	34.5	5	34.5	5	31.0	4.5	3.5	0.5	100
5	34.5	5	68.9	10	62.0	9.0	6.9	1.0	100
6	34.5	5	103.4	15	93.1	13.5	10.3	1.5	100
7	68.9	10	68.9	10	62.0	9.0	6.9	1.0	100
8	68.9	10	137.9	20	124.1	18.0	13.8	2.0	100
9	68.9	10	206.8	30	186.1	27.0	20.7	3.0	100
10	103.4	15	68.9	10	62.0	9.0	6.9	1.0	100
11	103.4	15	103.4	15	93.1	13.5	10.3	1.5	100
12	103.4	15	206.8	30	186.1	27.0	20.7	3.0	100
13	137.9	20	103.4	15	93.1	13.5	10.3	1.5	100
14	137.9	20	137.8	20	124.1	18.0	13.8	2.0	100
15	137.9	20	275.8	40	248.2	36.0	27.6	4.0	100

3.5 Permeability

Permeability tests were completed following the ASTM D 2434 standard (ASTM, 2008). Permeability, k, is the measure of a soil's ability to permit water to flow through its pores or voids under a unit hydraulic gradient $(i = \frac{dh}{ds})$. Tests were conducted on all materials, containing up to 10 percent substitute and non-plastic fines.

3.5.1 Test Apparatus

The apparatus consisted of a constant head permeameter that contained porous disks at the top and bottom of the sample. Each test was carried out in a modified CBR mold, which contained inlet and outlet valves on the top and bottom plates with rubber rings to seal the mold to prevent water from leaking during the test. The inlet and outlet valves were used to control the flow of water and to saturate the specimen. Saturation was completed from the bottom up.

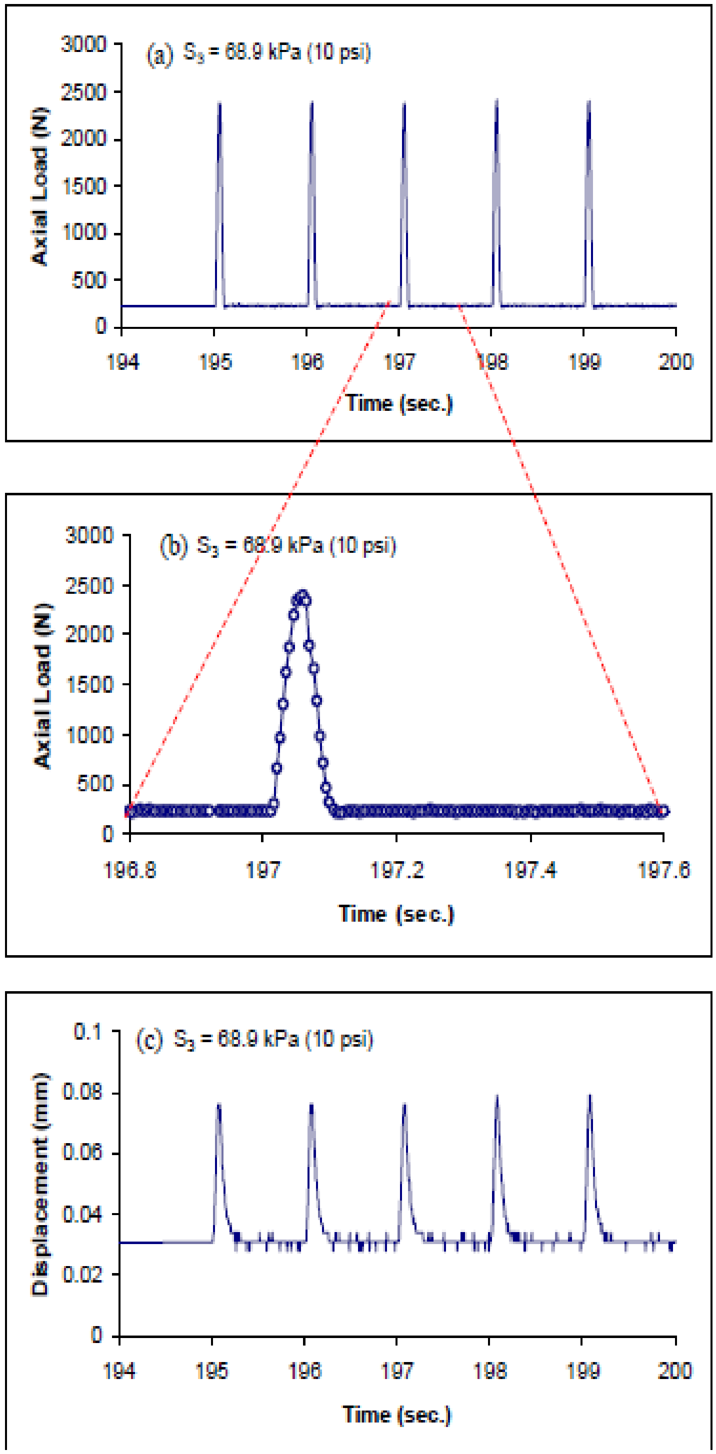

Figure 3.13 Cyclic axial load and induced displacements:
S_3 = 68.9 kPa (10 psi), S_{max} = 130 kPa

A constant-head filter tank was used to supply water to the permeameter. This was done by having a water inlet from the tap and an overflow outlet to ensure that a constant stream of water could be supplied. An outlet from the base of the water tank was attached to the inlet on the top plate of the mold. Figure 3.14 shows the apparatus used for the permeability testing.

3.5.2 Preparation and Compaction

The preparation for a permeability test began by gathering 2600 g of the desired material. A sieve analysis was performed on this material to remove any particles larger than 19 mm. Once the material was collected, the material was compacted in a 101.6 mm (4 in) mold. The compaction was completed in five layers using a hammer and a metal plate with the same diameter as the mold. Each layer was compacted with approximately 10 uniform blows until there was no visible motion of surface particles relative to the edges of the metal plate.

The top plate was then placed on the mold and a vacuum was applied through a second, empty chamber under a minimum of 20 in Hg (67.7 kPa) for 15 minutes to remove air adhering to soil particles and from the voids. Following the evacuation of the air, slow saturation of the specimen under full vacuum occurred. A second chamber was used because once the specimen was fully saturated, water from the first mold travelled into the empty chamber to prevent water from entering the vacuum pump. Upon saturation, the vacuum was removed and the outlet valve from the water supply was closed.

3.5.3 Permeability Test

To begin a test, the inlet valve to the specimen from the filter tank was turned on to allow water to flow through the specimen and out through the outlet valve on the bottom of the mold. Measurements were delayed until a steady flow rate appeared. The tests were performed at three different head distances and were repeated three times to obtain an average flow rate.

Figure 3.14 Permeability test apparatus 1-Soil specimen and mold; 2-Constant head filter tank; 3-Outlet valve; 4-Empty Chamber; 5-Vacuum; 6- Water supply; 7- Inlet valve; 8-Collection cylinder

CHAPTER 4 EXPERIMENTAL RESULTS AND ANALYSIS

The primary objective of this study was to determine the influence of fines (minus 75 μm), both type and amount, on the resilient modulus of unbound granular materials (four Granular As) as well as on the permeability. This chapter presents the results and analysis of the experimental program that was used to determine the influence of fines. The overall properties of interest were:

- Proctor (AASHTO T99) (AASHTO, 2011) - A description of the standard Proctor compaction test can be found in Chapter 3.
- CBR (AASHTO T193-99) (AASHTO, 2011) - The California Bearing Ratio (CBR) test is one of the most commonly used testing methods to evaluate the strength (stiffness) of subgrade, subbase and base materials for the design of pavements. CBR test values can also be used to estimate the resilient modulus.
- Resilient modulus (AASHTO T307-99) (AASHTO, 2011)– M_R is a fundamental material property used to characterize subgrade soils and base/subbase materials under the physical conditions and stress states of materials in flexible pavements subject to moving wheel loads. It is a measure of material stiffness.
- Permeability (ASTM D2434) (ASTM, 2008) – A description of permeability testing can be found in Chapter 3.

Tests conducted on each material and the conditions of each test are summarized in Tables 4.1, 4.2, and 4.3. It should be noted that there was a flood in the Applied Dynamics Laboratory at McMaster University that caused a significant delay in research as the compaction and CBR machines used for this study were in the building at the time. The consequence of this flood resulted in a loss of time that could have been spent conducting more tests.

Table 4.1 Proctor test summary

Proctor Compaction	
	Original Aggregates
Source 1 Fines content=7.8%	x
Source 2 Fines content=5.7%	x
Source 3 Fines content=3.4%	x
Source 4 Fines content=4.1%	x

Table 4.2 Resilient modulus and CBR test summary

Resilient Modulus and CBR Tests									
		WC* 1		**WC 2**		**WC 3**		**WC 4**	
	Original Aggregates	**FC* 1,2,3**	**Original Aggregates**	**FC 1,2,3**	**Original Aggregates**	**FC 1,2,3**	**Original Aggregates**	**FC 1,2,3**	**Types of Fines**
Source 1	x		x		x		x		
FC=7.8%		xxx		xxx		xx			F1
		xx		xx		xx		xx	F2
Source 2	x		x		x		x		
FC=5.7%		xxx		xxx		xx		x	F1
		xx		xx		xx		xx	F2
Source 3	x		x		x		x		
FC=3.4%		xxx		xxx		xxx			F1
		xx		xx		xx		xx	F2
Source 4	x		x		x		x		
FC=4.1%		xxx		xxx		x			F1
								xx	F2

Note: FC = Fines content
WC = Water content
F1 = Natural Fines
F2 = Substitute Fines

Table 4.3 Permeability test summary

Permeability Tests			
	Original Aggregates	**Fines content 1,2,3**	**Types of Fines**
Source 1	x		
		xxx	F1
		xx	F2
Source 2	x		
		xxx	F1
		xx	F2
Source 3	x		
		xxx	F1
		xx	F2
Source 4	x		
		xxx	F1
			F2

Note: See Table 4.2 notes

4.1 CBR Tests

CBR tests were carried to evaluate the strength/stiffness of four different Granular A aggregates. Referring to Table 4.2, two types of fines were used, natural fines from the corresponding aggregate (F1) and substitute fines from another source (F2). To determine the influence of fines the on CBR for each of the combinations, tests were performed at three or four water contents. Summaries of the water contents, dry densities and CBR values for all source materials can be found in Appendix B.

4.1.1. Effect of Natural (F1) Fines on CBR Values

Figures 4.1 shows the relation of water content to the CBR values at different F1 fines content corresponding to 5 mm (0.2 in) displacements. The CBR values at 5 mm were larger than those at 2.5 mm (0.1 in) displacements.

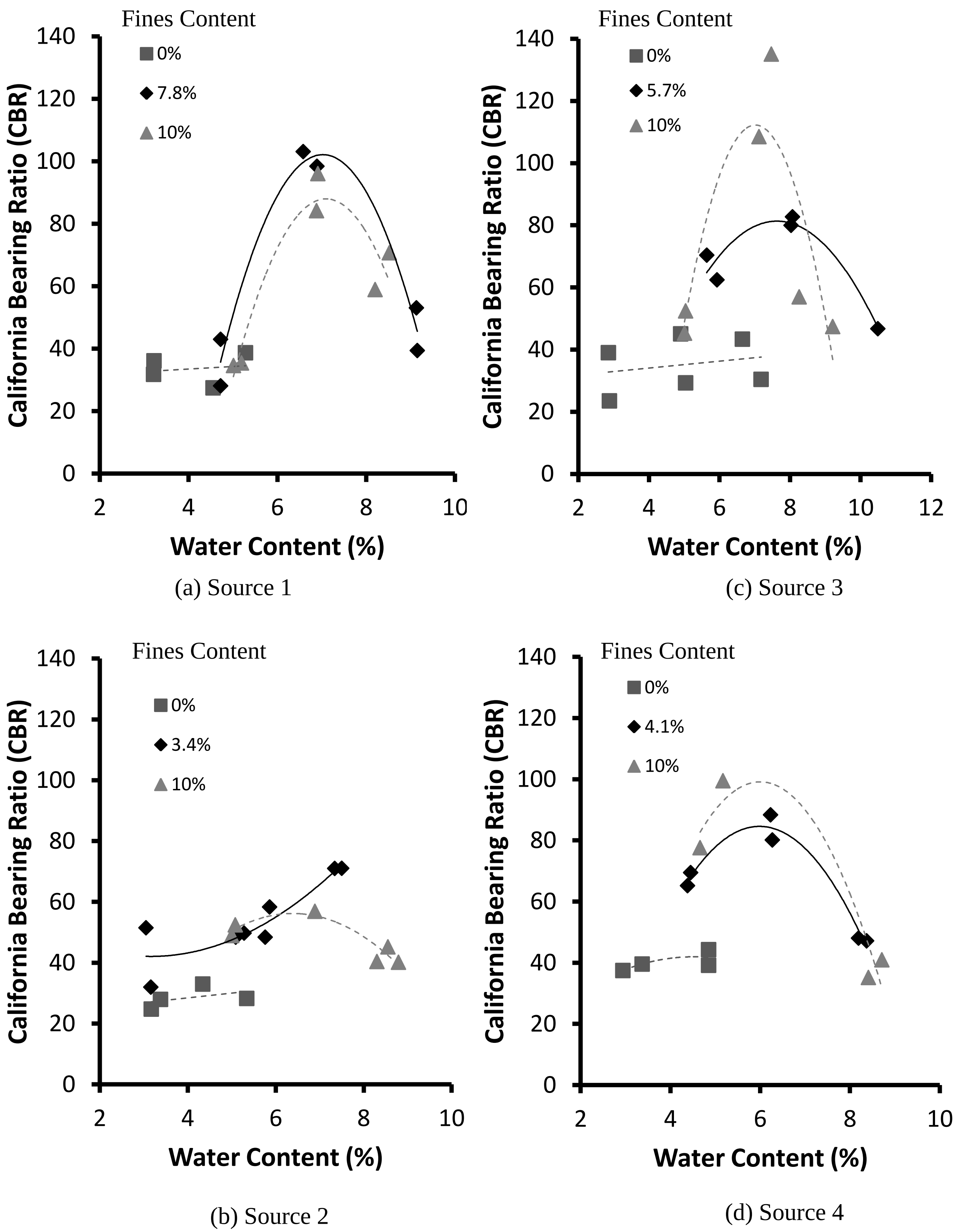

Figure 4.1 CBR (5 mm) vs. water content for various F1 fines content

Three different fines contents were tested for each of the four sources, original fines content, 0 percent fines and 10 percent fines. The optimum water content was determined for each source for the natural fines content but not for the other fines contents. For each of the figures in Chapter 4 a solid line is used to represent the tests in which the optimum water content was determined from Proctor compaction and a dashed line represents tests where the water contents were preselected.

It is evident that some fines must be present in the aggregate in order to increase the CBR value. With 0 percent fines present the CBR values were virtually independent of water content. All sources are seen to have CBR values of 40 or less, which is well below that required by AASHTO for a granular base (Guo, 2013). It is observed that the CBR of Sources 1 and 3, which have a higher fines content, display a greater sensitivity to water content, supported by the data of Table 3.3. Tests completed on specimens with fines tended to have definite peak CBR values but there is no clear recognizable trend. The CBR values were largest when the tests were conducted at optimum water content and upon conducting tests at greater than optimum water conditions the CBR values decreased as expected. This is consistent with the Hashiro's (2005) observations. The optimum water contents for Sources 1, 2 and 4 were similar for original fines and 10 percent F1 fines but for Source 3 there is a slight difference. For Source 2 F1 fines specimens the CBR can be seen to increase with increasing water content without a decrease after optimum, however 10 percent F1 fines shows an optimum. This was attributed to Source 2 at low fines content having had problems retaining water when the water content was above 7 pefrcent, causing water to run to the bottom of the mold during testing. Source 4 was found to also have some problems when the water content was above 7 percent. For both materials at water contents above optimum, water was also seen to flow out of the mold during preparation.

It can also be observed that the CBR values for Sources 1 and 2 were larger for original fines content compared to 10 percent fines, which is consistent with the data of Bennert and Maher (2005). For Sources 3 and 4 the CBR values for 10 percent fines content were larger. With regard to Source 3 this may be associated with the presence of silty fines. This material also showed the largest difference in CBR when adding fines. In general the CBR values were lower than expected for crushed rock. Had the modified Proctor compaction been used the CBR values would have been much higher.

As mentioned in Chapter 3, tests had been conducted previously at McMaster University on aggregate from various MTO regions. Source 3 was one of these regions so the results from the previous study were compared to the results of this study (Stolle et al., 2005). The optimum water contents from the eariler McMaster study was approximately 7.9 percent which is similiar to the optimum water content for this study, 8 percent. The CBR values are also similiar with this study producing a CBR value at 5 mm of 81 and the earlier study achieving a CBR value of 93. The only difference between the two studies is the value for the coefficient of uniformity, C_u. The sieve anaylsis for the earlier study had used less than half the material that was used in this study to determine the grain size distribution and also used more sieves, which which is believed to have influenced the value for D_{60} that was used in the C_u calculation. The value of D_{60} in the earlier study also did not fall within the Granular A boundaries, thus resulting in a larger coefficient of uniformity than observed in this study. It appears that with a sufficient amount of fines, ranging from 5 to 10 percent, Sources 1, 3 and 4 attain CBR values that are required by a good granular base, $CBR > 80$ (AASHTO, 2011).

Figure B.1 in Appendix B shows the water content and CBR relationship for 2.5 mm displacements and Table 4.4 summarizes the maximum CBR values for each case.

4.1.2. Effect of Density on CBR Values of Aggregates with Natural (F1) Fines

Figure 4.2 presents the variation of CBR of the four different sources as a function of the different dry densities for the case of F1 fines. The dry densities, ρ_{dry}, are separated into two figures for each source, one showing the relation with the CBR value at 5 mm displacement and the other, found in Figure B.2 of Appendix B, for CBR values at 2.5 mm.

Table 4.4 Maximum CBR values for F1 fines

List	*w* (%)	CBR (2.5 mm)	CBR (5 mm)
S1/7.9% F1	6.6	83.4	103.1
S1/0% F1	5.3	39.0	38.7
S1/10% F1	6.9	61.6	96.1
S2/3.4% F1	5.9	46.9	58.4
S2/0% F1	4.3	26.6	33.0
S2/10% F1	6.9	45.8	56.9
S3/5.7% F1	8.1	63.4	82.7
S3/0% F1	6.7	34.4	45.1
S3/10% F1	7.5	90.5	135.1
S4/4.1% F1	6.2	81.2	88.4
S4/0% F1	4.9	41.2	44.3
S4/10% F1	5.2	86.6	99.5

For the case of 0 percent fines the CBR values for all sources were not very sensitive to dry density. With no fines present in a soil sample, course aggregate interlocking is important, yielding lower densities and larger voids due to the lack of fines but provides good drainage and is less susceptible to frost heave (Haider, 2013); (Siswosoebrotho et al., 2005). For Sources 1 and 3 there is a definite trend of increasing CBR with increasing ρ_{dry}, especially for 10 percent fines. The CBR value also slightly increases as the ρ_{dry} increases for Source 2 original fines but with 10 percent F1 for Source 2 and all cases for Source 4 there is no recognizable trend between CBR and dry density.

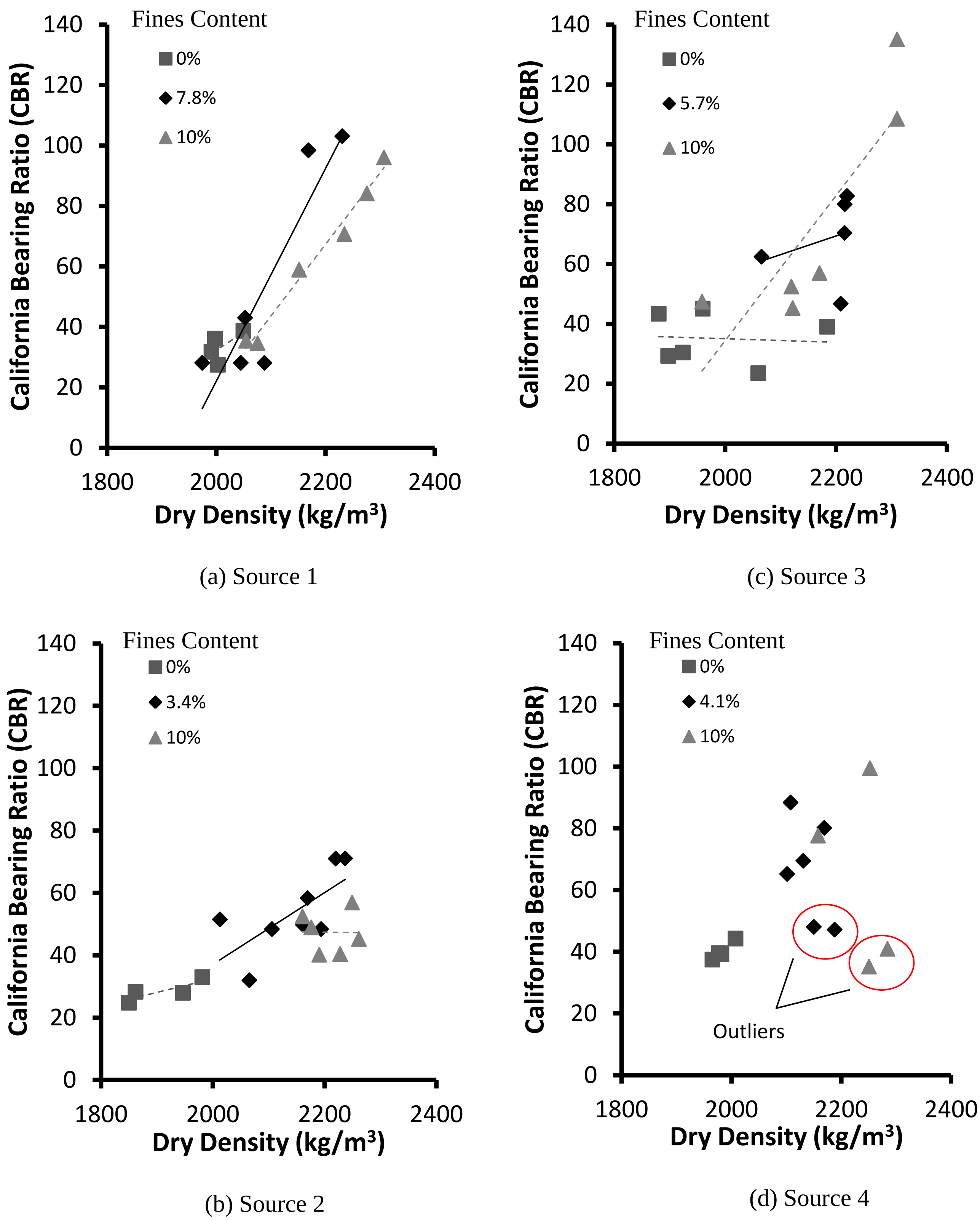

Figure 4.2 CBR (5 mm) vs. dry density for various F1 fines contents and water contents

As marked in Figure 4.2 (d) with a red circle, the data points are considered outliers because the water content appeared to be too high; the specimen looked wet during fabrication. Comparing the dry densities from the Proctor compaction to the dry densities from CBR testing, the dry densities were larger for the CBR specimens but followed similar trends, where the ρ_{dry} increases as the water content reaches optimum and decreases thereafter.

Referring to the tables in Appendix B, the maximum dry density for Source 1 to 3 occurred at the same water content for 10 percent fines as for the natural fines content, optimum water content. For Source 4 the maximum dry density occurred when the water content was approximately 8 percent, for 4.1 percent F1 and 10 percent F1 fines. The dry density increased as the fines content increased from 0 percent fines to 4.1 percent F1 fines to 10 percent F1 fines.

4.1.3. Effect of Substitute (F2) Fines on CBR Values

As indicated previously, fines must be present for the CBR values to increase at a selected compaction level. Figure 4.3 shows the relation between CBR and water content for F2 fines at 5 mm displacement with the remaining plots shown in Figure B.3 in Appendix B. As the fines content increases we see that the maximum CBR value does not change significantly. The plasticity index of the F2 fines is only moderately larger than that of the original fines for all sources. CBR tests were conducted with 5 percent and 10 percent with the substitute fines for all materials. It can be seen that at 5 percent fines the tendency is to have a larger maximum CBR value. For Source 2 the CBR values at 5 percent fines are only marginally larger.

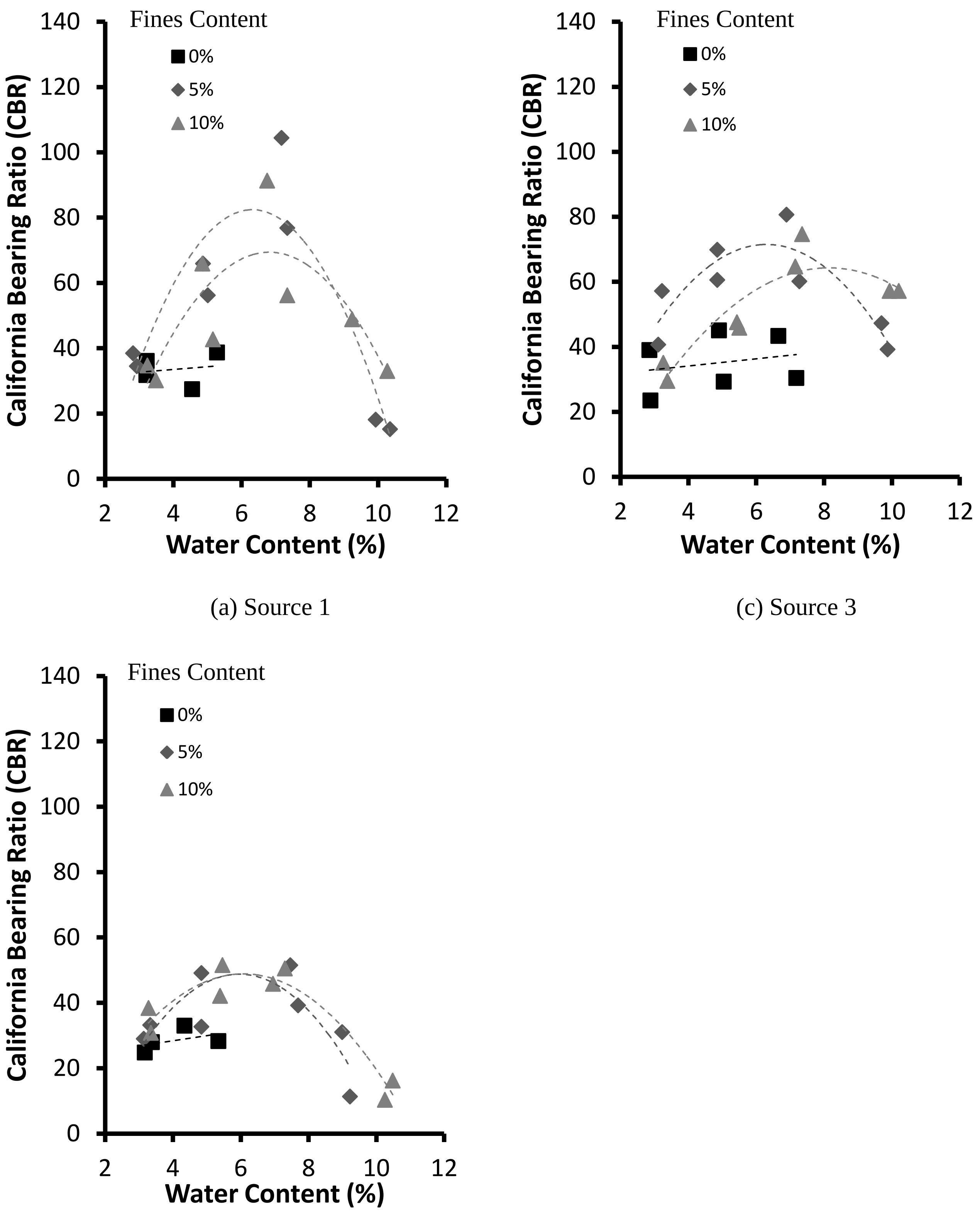

(a) Source 1

(c) Source 3

(b) Source 2

Figure 4.3 CBR (5 mm) vs. water content for various F2 fines contents

As with the tests for F1 fines, there was no significant change in CBR when comparing 5 percent and 10 percent F2 for all sources. However, the change in CBR between the data points for 5 percent F2 is large. A maximum CBR value can be seen at a certain water content for each source. For Source 1 there is scatter amongst the CBR values at approximately 7.5 percent water content. There also appears to be a slight shift in water content when compared to the results for the F1 fines.

There is no shift in water content at the maximum CBR for Source 2 but it is suspected that for water contents greater than 7 percent Source 2 had problems retaining water. There was a shift in the optimum water content for the Source 3 Fines 2 specimen containing the substitute fines.

A summary of the largest CBR values for each case is presented in Table 4.5. It is evident that there is no clear trend when comparing the CBR values from specimens containing F2 fines to those with F1 fines. Therefore a strong statement cannot be made on the effect of substitute fines.

Table 4.5 Maximum CBR values for F2 fines

List	*w* (%)	CBR (2.5mm)	CBR (5mm)
S1/5%	7.2	81.2	104.4
S1/10%	6.8	70.4	91.3
S2/5%	7.5	43.6	51.5
S2/10%	5.5	45.8	51.5
S3/5%	6.9	63.8	80.7
S3/10%	7.4	55.4	74.7

4.1.4. Effect of Dry Density on CBR Values of Aggregates with Substitute (F2) Fines

As with F1 fines the dry density vs. CBR (5 mm) relations were examined for cases where the original fines were replaced with substitute fines as shown in Figure 4.4. The 2.5 mm displacement results are found in Figure B.4 of Appendix B.

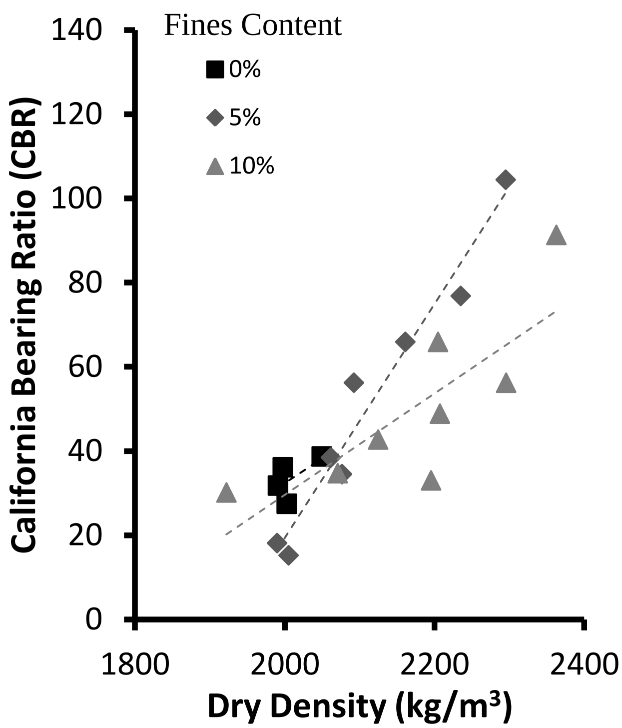

(a) Source 1

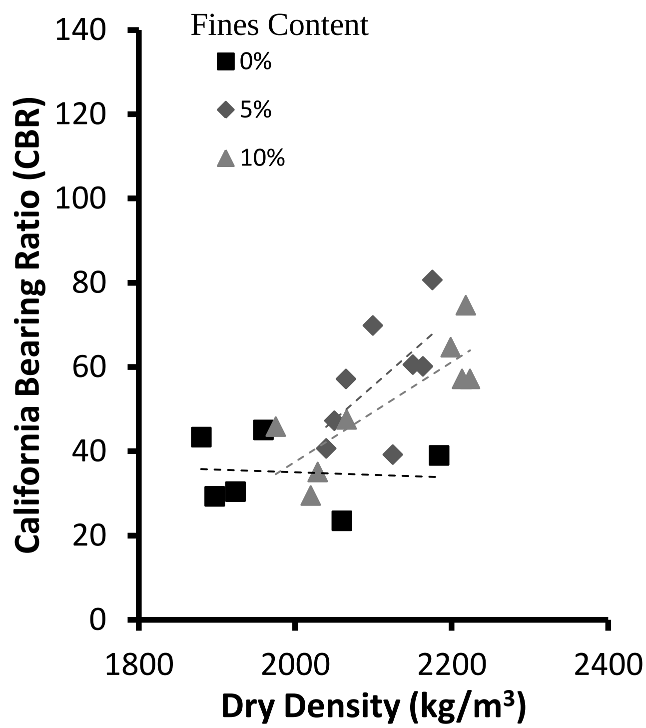

(c) Source 3

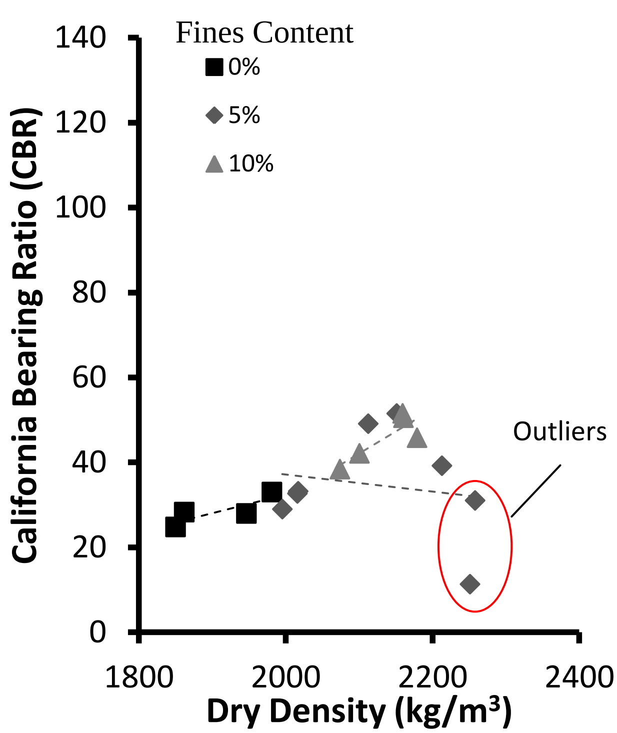

(b) Source 2

Figure 4.4 CBR (5 mm) vs. dry density for various F2 fines contents and water contents

There is a clear trend that the CBR increases as the dry density increases for Source 1 and Source 3 for both 5 percent and 10 percent F2 fines. For Source 2, there is no recognizable trend. This again is attributed to the problem of the material not being able to retain water greater than 7 percent which causes a decrease in CBR values, which can be seen from the points in the red circle.

Referring to the tables in Appendix B, the maximum dry density for each source came when the water content was approximately 7 percent. The only exception to this is for 10 percent substitute fines for Source 3 where the maximum dry density occurred at 10 percent. Comparing the dry densities of samples containing F2 fines to F1 fines it can be seen that the dry densities of the aggregates containing F2 fines were slightly higher.

Although the dry densities of the aggregates with F2 fines was slightly higher, the difference between the influence of F2 fines and F1 fines was minimal and no clear conclusion can be drawn on the effect of dry density on CBR.

4.1.5 Soaked CBR Tests

The moisture sensitivity of CBR for aggregate Sources 1, 3 and 4 were examined by carrying out soaked CBR tests on specimens with original fines, 0 percent fines and 10 percent fines contents corresponding to the optimum water content and natural fines.

Tables 4.6 to 4.8 show the results of the soaked CBR tests along with the percent swelling. The swelling measurement revealed that volume swelling induced by soaking is less than 0.05% in all tests. Such small swelling may be considered negligible in engineering practice. Source 3 shows that there is not much change in unsoaked and soaked CBR values. Figure 4.5 shows the CBR values for all sources with natural, 0 percent and 10 percent F1 fines as a function of dry density.

Table 4.6 Source 1 Soaked CBR values

List	*w* (%)	CBR (0.1)*	CBR (0.2)*	$\bar{x}$* (0.1)	$\bar{x}$ (0.2)	ρ_{dmax} (kg/m^3)	Swell (%)
S1/7.8% F1 (w=6.6)	6.58	31.9	42.6	29.95	40.05	2858.4	0.05
	6.64	28	37.5			2694.7	0.04
S1/0% F1 (w=4.9)	4.93	38.5	43.8	36	40.6	2023.1	0
	4.85	33.5	37.4			2016.9	0.04
S1/10% F1 (w=5.9)	5.82	46.7	58.8	48	58.3	2205.2	0.03
	5.94	49.3	57.8			2162.4	0.01

Table 4.7 Source 3 Soaked CBR values

List	*w* (%)	CBR (0.1)*	CBR (0.2)*	$\bar{x}$* (0.1)	$\bar{x}$ (0.2)	ρ_{dmax} (kg/m^3)	Swell (%)
S3/5.7% F1 (w=8.0)	8.08	55.9	87.8	56.5	81.95	2139.5	0.02
	8.01	57.1	76.1			2257.3	0.04
S3/0% F1 (w=4.6)	4.5	20.9	30.8	24.5	33.7	1864.7	0.01
	4.66	28.1	36.6			2017.9	0.01
S3/10% F1 (w=7.3)	7.3	61.2	85.9	60.45	82.7	2265	0
	7.27	59.7	79.5			2290.7	0

Table 4.8 Source 4 Soaked CBR values

List	*w* (%)	CBR (0.1)*	CBR (0.2)*	$\bar{x}$* (0.1)	$\bar{x}$ (0.2)	ρ_{dmax} (kg/m^3)	Swell (%)
S4/4.1% F1 (w=6.3)	6.32	39.5	48.5	38.9	44.65	2136.4	0.03
	6.38	38.3	40.8			2292.2	0.03
S4/0% F1 (w=4.8)	4.64	13.9	16.9	16.8	21.25	1801	0
	4.92	19.7	25.6			1963.8	0
S4/10% F1 (w=6.3)	6.38	30.6	37.1	35.45	40.2	2051.6	0
	6.2	40.3	43.3			2057.8	0

Figure 4.6 compares the variation of the soaked and unsoaked CBR values for clean aggregates and 10 percent F1 fines with dry density. The results show that there is no significant decrease in the CBR values for soaked conditions.

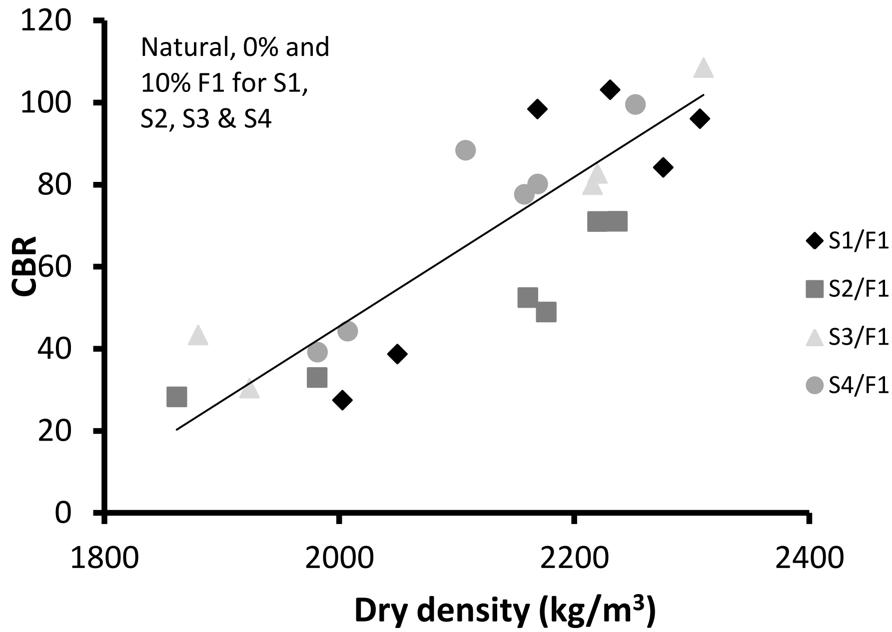

Figure 4.5 Unsoaked CBR (5 mm) vs. dry density for various F1 fines contents and water contents

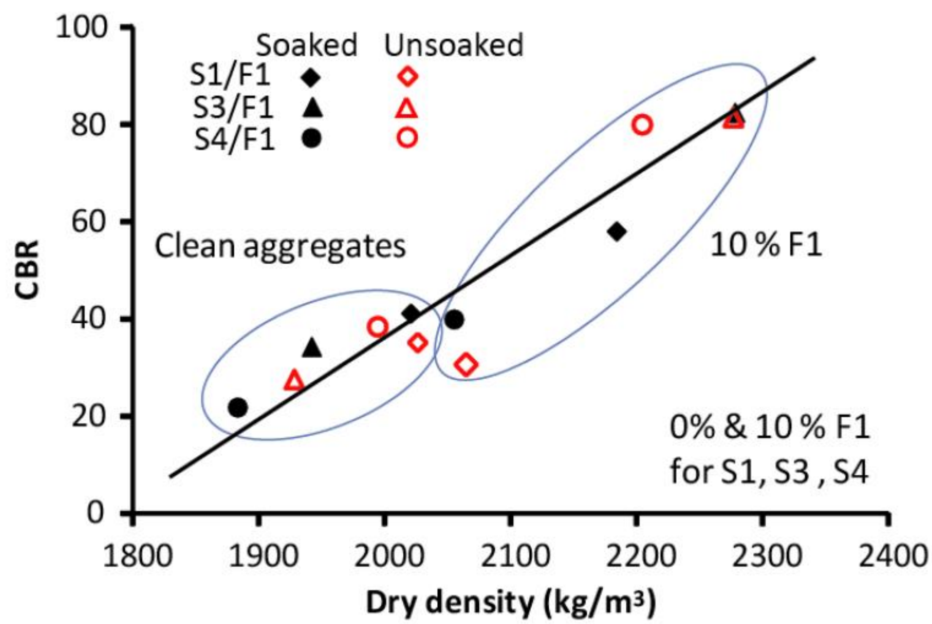

Figure 4.6 Soaked CBR (5 mm) vs. dry density for various F1 fines contents and water contents

4.2. Resilient Modulus Tests

This study investigated the moisture sensitivity of the resilient modulus along with the sensitivity to different fines content. Tests were performed at different water contents with fines removed, at two F1 fines contents and at two F2 fines contents. The optimum water contents obtained from standard Proctor test results of original aggregates were used to estimate the water contents for compacting of the resilient modulus test specimens. As previously mentioned, Stolle et al. (2005) reported that the optimum water content for an M_R test specimen is actually lower than w_{opt} from Proctor tests. Specimens compacted at the Proctor optimum water content consistently appeared to be wet of optimum when compacted by vibration.

In this study kPa was used for the unit of pressure. The cell confining pressures used in M_R tests were 20.7 kPa (3 psi), 34.5 kPa (5 psi), 38.9 kPa (10 psi), 103.4 kPa (15 psi), and 137.9 kPa (20 psi). Figures 4.7 and 4.8 illustrate representative measured resilient modulus results for 3.4 percent natural and 5 percent substitute fines, respectively. Both figures correspond to Source 2 material at 5 percent water content. Comparing the plots in these figures it can be seen that the resilient modulus results for both sets of fines are similar. The plots for all resilient modulus tests on the four sources can be found in Appendix C.

Several of the resilient modulus tests for each source failed prematurely. A list of the failed tests is provided in Table 4.9. A failed test refers to a test that was unable to be completed from start to finish. There were three main reasons for failure of these tests: high water content, development of excess permanent deformation during the pre-conditioning phase, and the failure of LVDTs to properly record displacement.

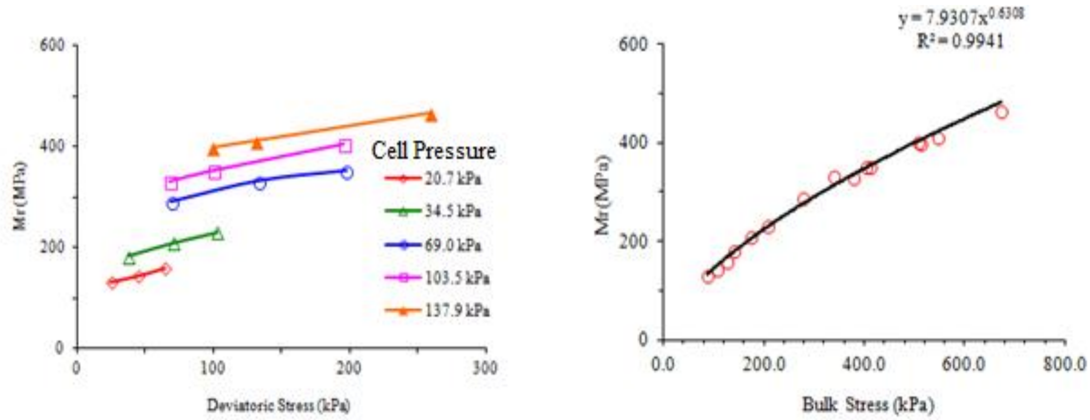

Figure 4.7 Resilient modulus vs. bulk Stress at various deviatoric stresses for natural (F1) fines, Source 2

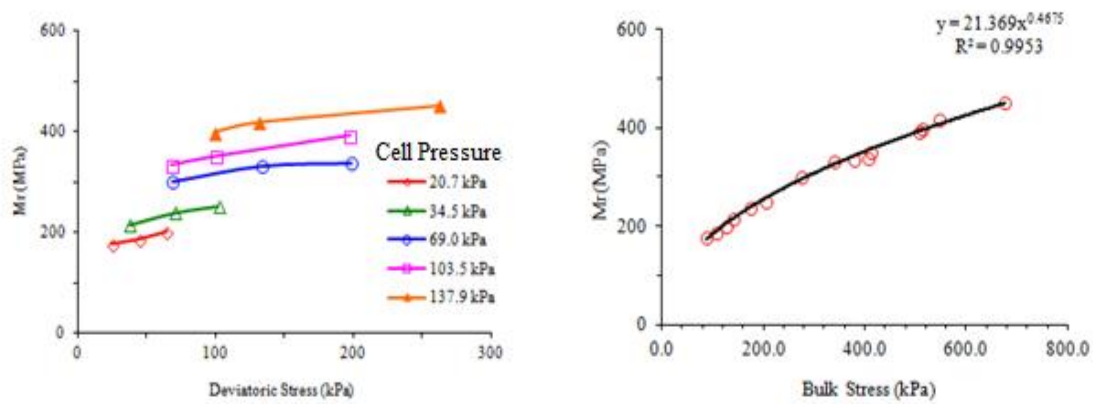

Figure 4.8 Resilient modulus vs. bulk Stress at various deviatoric stresses for substitute (F2) fines, Source 2

4.2.1. Influence of Natural and Substitute Fines on M_R

For the purpose of this study, specimens at two natural fines contents, one with 0 percent fines and two with substitute fines were investigated for each of the four Granular A sources. The influence of fines content on resilient modulus is addressed in this section where the water content is kept constant and the fines content changes. The same information is presented in Appendix D.1, except the fines content is held constant and the effect of water content is shown.

Figures 4.9 to 4.12 display the resilient modulus versus bulk stress relations for each source for different water contents. Scrutiny of the results indicates that there was no systematic influence of fines content on the relations. For example the influence of fines content on the M_R values for Source 1 at 3 percent water content have a different trend than the M_R values for Source 2 at 3 percent water content. At 3 percent and 5 percent water content only Source 1 displayed no systematic variation whereas Sources 2, 3 and 4 followed the expected sensitivity of M_R to percent fines, in which M_R decreased as the fines content increased.

Table 4.9 Resilient modulus failure tests

Source	Fines Content	*w* (%)	Reason for Failure
Source 1	10% F1	8	High Water Content
Source 1	10% F2	7	LVDT
Source 2	3.4% F1	2.9	Pre-conditioning permanent deformation
Source 2	3.4% F1	6.9	Pre-conditioning permanent deformation
Source 2	0% F1	5	High Water Content
Source 2	5% F2	7	High Water Content
Source 2	10% F1	8	High Water Content
Source 2	10% F2	7	High Water Content
Source 3	5.7% F1	5.95	Pre-conditioning permanent deformation
Source 3	10% F1	5	Pre-conditioning permanent deformation
Source 4	4.1% F1	8.3	High Water Content
Source 4	5% F2	3	LVDT
Source 4	10% F1	5	LVDT
Source 4	10% F1	8	High Water Content
Source 4	10% F2	7	LVDT

Given that the fines (natural and substitute) were of similar plasticity, the influence of fines type is seen to be not pronounced. At higher fines content, such as 7.9 percent F1 for Source 1 and 10 percent F1 for Sources 1 to 4, the resilient moduli tend to be lower. This also contradicts the findings of Richardson and Lusher (2009) and Yoder and Witczak (1975), where they stated the optimum fines content for M_R is similar to the optimum fines for maximum CBR in the range of 6 to 9 percent. The optimum fines content for M_R is found to be different than that of CBR. The optimum fines content range is seen to be lower than 6 percent as noted previously the different compaction methods for CBR and M_R. It should be noted that the results in Appendix C indicate that some of the M_R values of the specimens were sensitive to deviatoric stress, such as the Source 1 specimens with 7.9 percent F1 and 10 percent F1 fines at a 5 percent water content and Source 4 specimens with 4.1 percent F1 and 10 percent F2 fines at a 3 percent water content.

At 7 percent water content, some specimens appeared to be too wet for resilient modulus testing. Only a few tests could be completed for Sources 1 and 4, with all tests failing for Source 2 with water at the bottom of the specimen. For Source 3, all tests were completed successfully. This is a drawback of using the optimum water contents corresponding to Proctor compaction because the optimum water content for Proctor compaction is different from vibratory compaction.

The last figure for each source, i.e (d), is a collection of M_R data that were grouped according to similar trends. The similarities in M_R with natural and substitute fines for various combinations of fines and water content can be seen as well as the non-systematic variance in M_R with fines content.

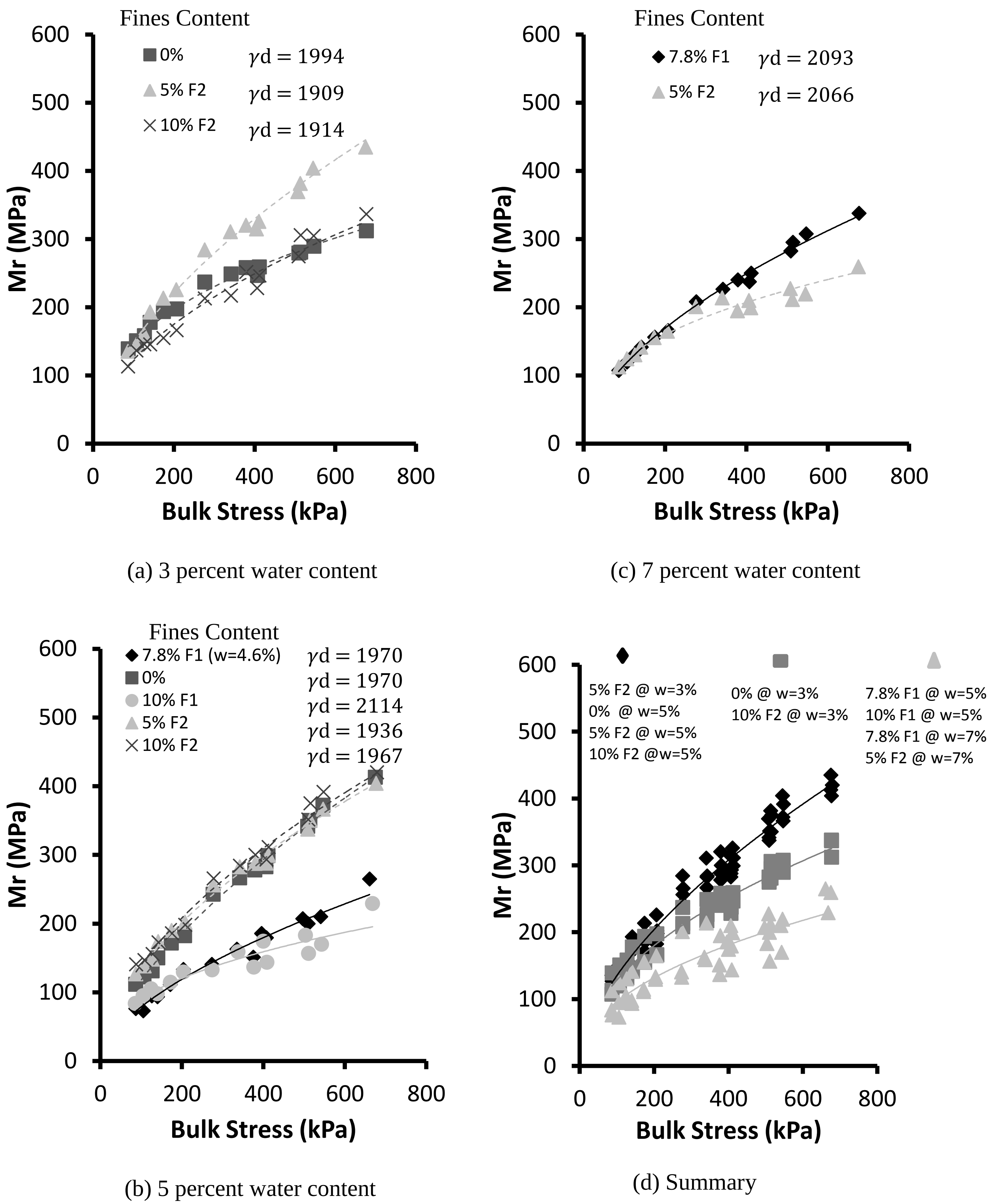

(a) 3 percent water content

(c) 7 percent water content

(b) 5 percent water content

(d) Summary

Figure 4.9 Source 1 M_R vs. bulk stress at various water contents and fines contents

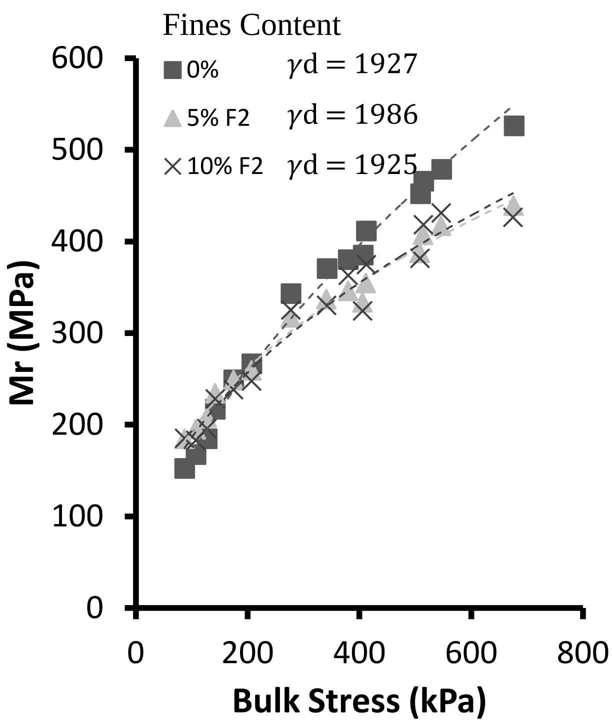

(a) 3 percent water content

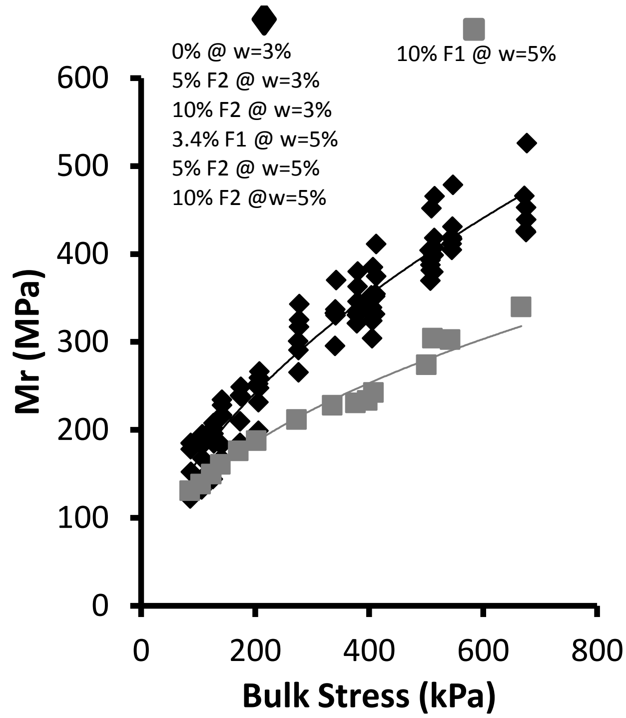

(c) Summary

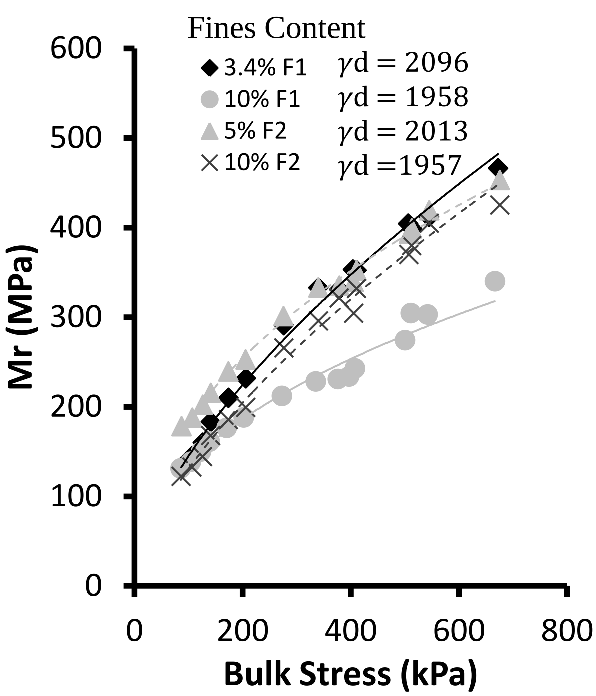

(b) 5 percent water content

Figure 4.10 Source 2 M_R vs. bulk stress at various water contents and fines contents

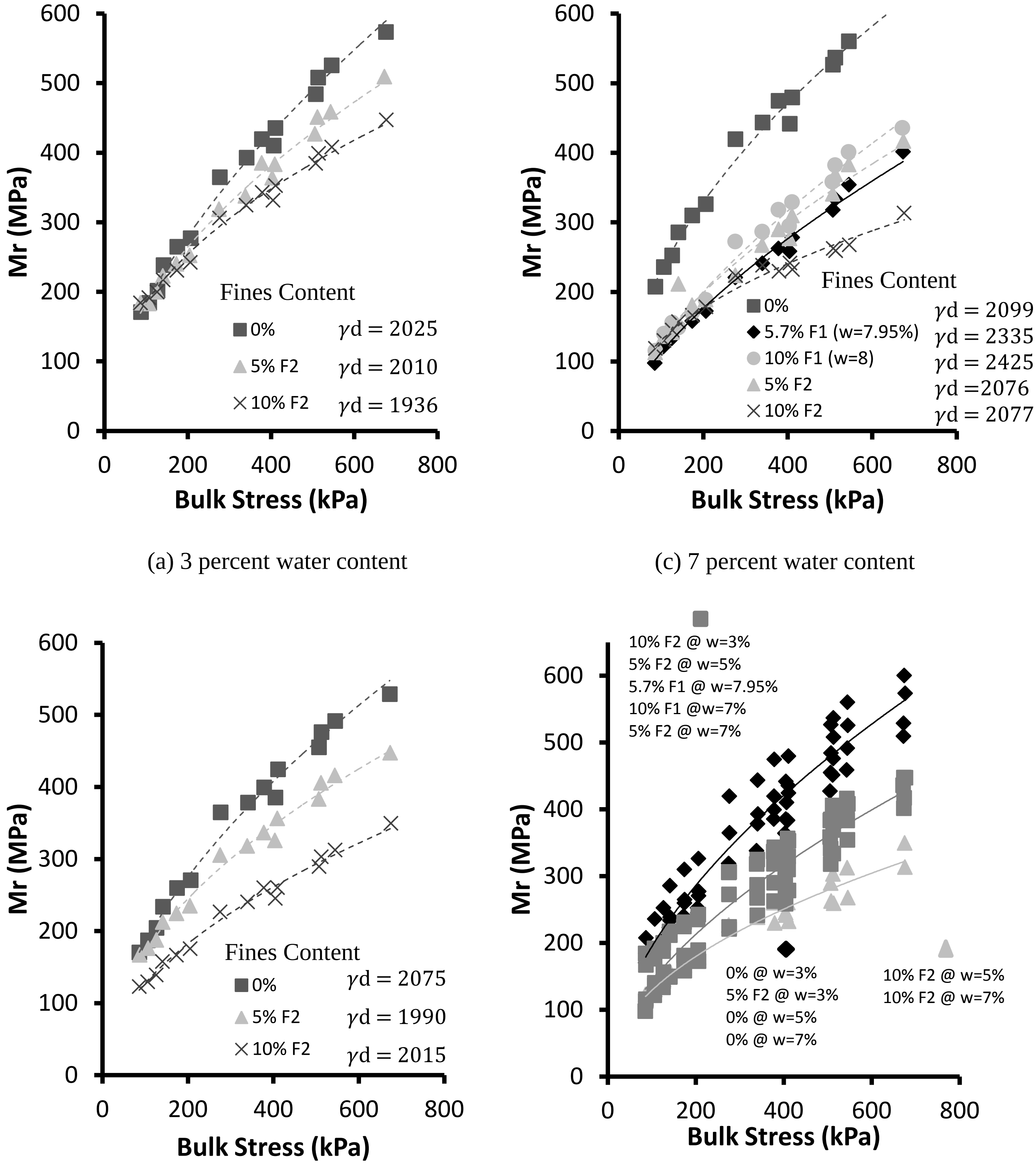

(a) 3 percent water content

(c) 7 percent water content

(b) 5 percent water content

(d) Summary

Figure 4.11 Source 3 M_R vs. bulk stress at various water contents and fines contents

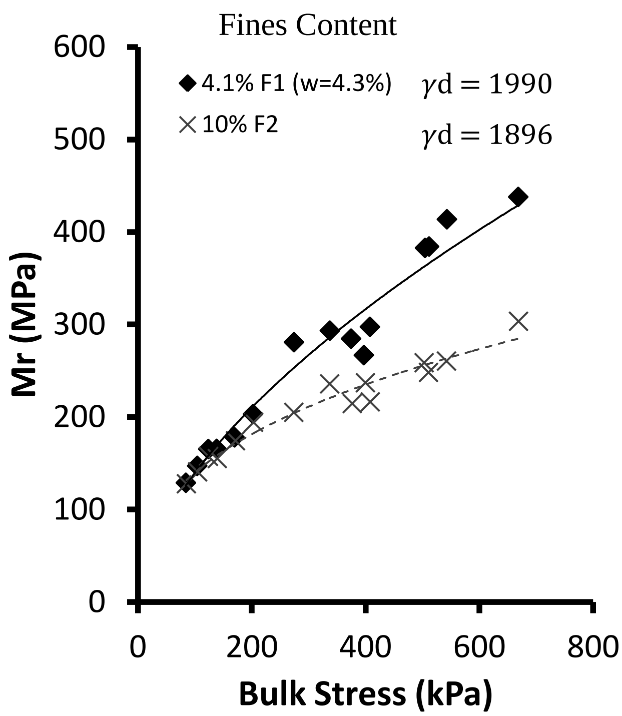

(a) 3 percent water content

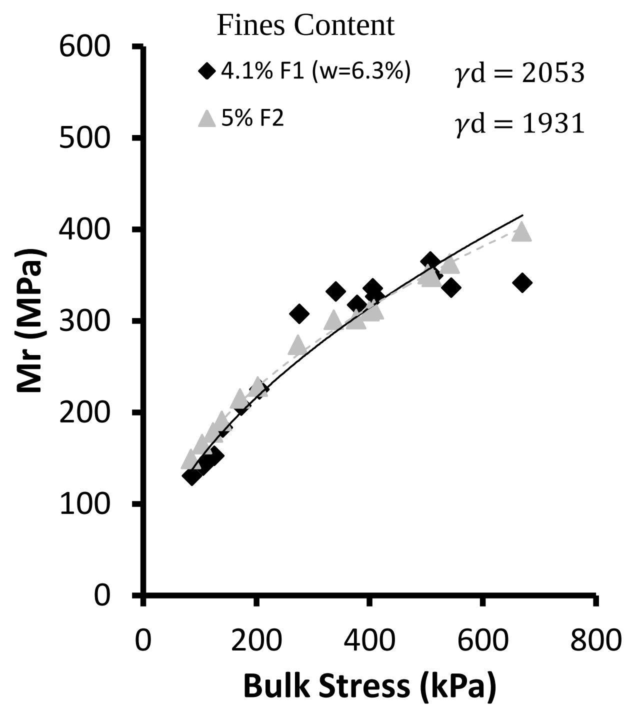

(c) 7 percent water content

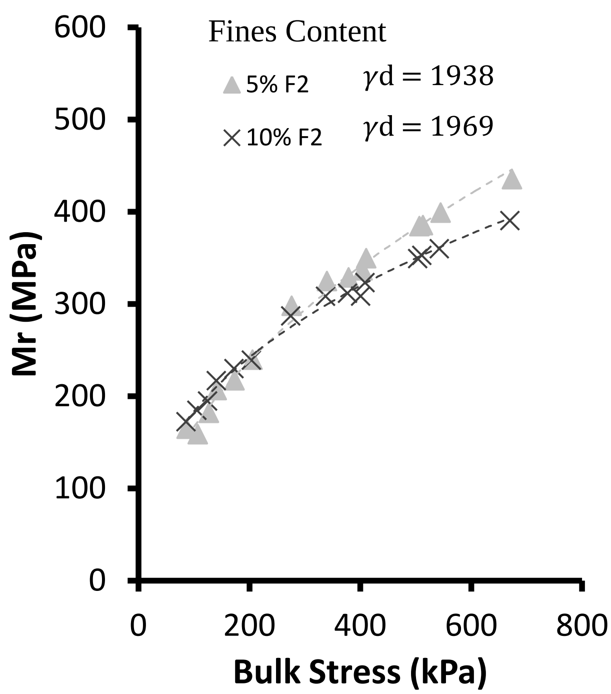

(b) 5 percent water content

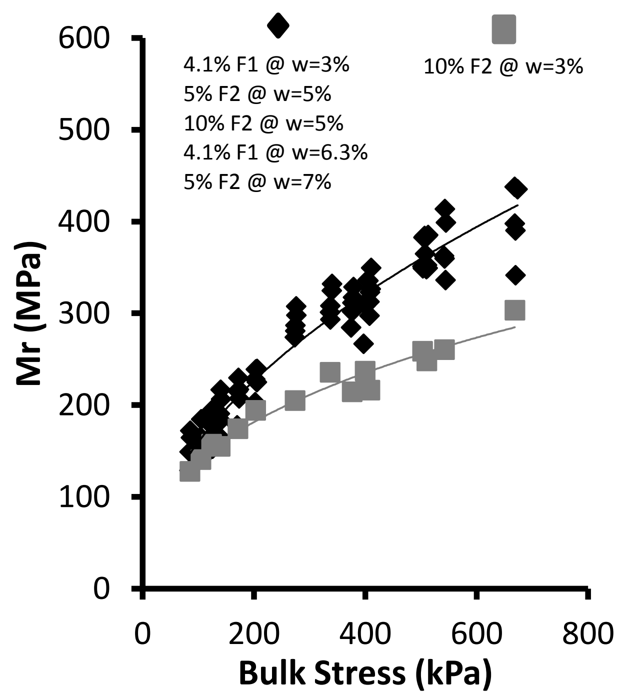

(d) Summary

Figure 4.12 Source 4 M_R vs. bulk stress at various water contents and fines contents

To summarize the results, the *PI* of the Sources 1, 2 and 4 natural fines is almost identical to the *PI* of the substitute fines, which explains the similarities in M_R values. The *PI* of Source 3 natural fines is much lower than the *PI* of the substitute fines. For Source 3, a possible explanation for the difference in M_R is that the physical properties were altered when the silt fines were replaced with clay fines. This is consistent with the results of Barksdale and Itani (1989) who report that the M_R decreased when fines from one source were added to aggregates from another source.

The variation of regression coefficients with respect to fines content for the K-θ model is presented in Figure 4.13. The regression coefficients with respect to fines for the Uzan and AASHTO models are found in Appendix D.2. The K-θ model is shown because this model had the least amount of scatter in the k values at each of the fines contents. The different k values correspond to different water contents. It is observed that as the fines content increases the value of K_1 decreases and the trend line for of K_2 is almost constant for all three models. For the Uzan and AASHTO models, the trend line for K_3, was found to increase as the fines content increased. Comparing the results to the results from Guo et al. (2006) the trends for K_1 are similar, decreasing with increasing fines but for K_2 and K_3 the trends are not similar. Given no systematic variation occurring when the water content is constant, the effect of paste content is looked at in the next section.

4.2.2 Influence of Paste

For the four sources, the resilient modulus values, at 200 and 400 kPa bulk stress, are plotted against the percent paste in Figure 4.14. The percent paste is the combination of fines content and water content at the time of ***compaction***. For example, a specimen with 5 percent passing the 75 μm sieve at 5 percent water content would contain a total of 10 percent paste.

Comparing the results at 200 and 400 kPa bulk stresses, the trends are similar, almost parallel, with the values at 200 kPa being lower as expected. Unlike the results for constant water content, the results for percent paste show a more systematic trend. As the paste content increases the resilient modulus values tend to decrease, except for Source 4. This exception, in which the M_R is almost constant as percent paste increases, is attributed to not having enough tests results.

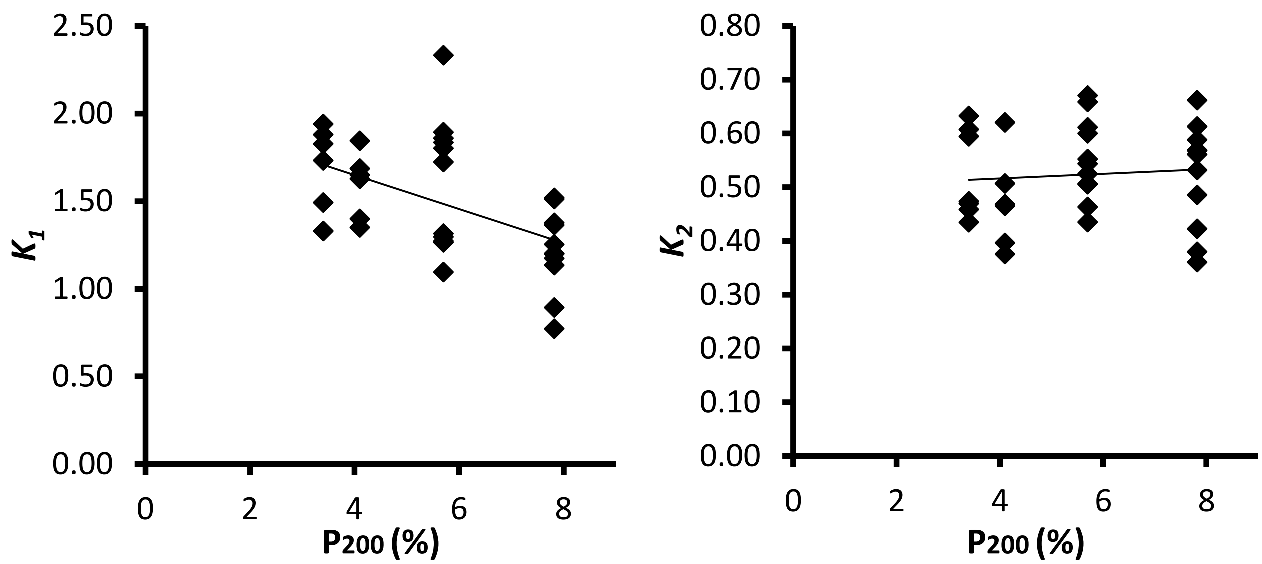

Figure 4.13 Variation of k-coefficient with fines content for *K-θ* Model

4.2.3 Influence of Water Content and Fines Content on *m* and *b*

Rather than fitting a power function to the data, linear interpolation, $M_R = b - m\theta$, is used in this section. Using the plots of resilient modulus vs. bulk stress the slopes, *m*, and 'y' intercepts, *b*, for each source were determined by using a linear regression. When calculating the slopes and intercepts for each test the resilient modulus values for 20.7 kPa (3 psi), and 34.5 kPa (5 psi) were not included because for most tests the values were similar to one another and some data points were skewed.

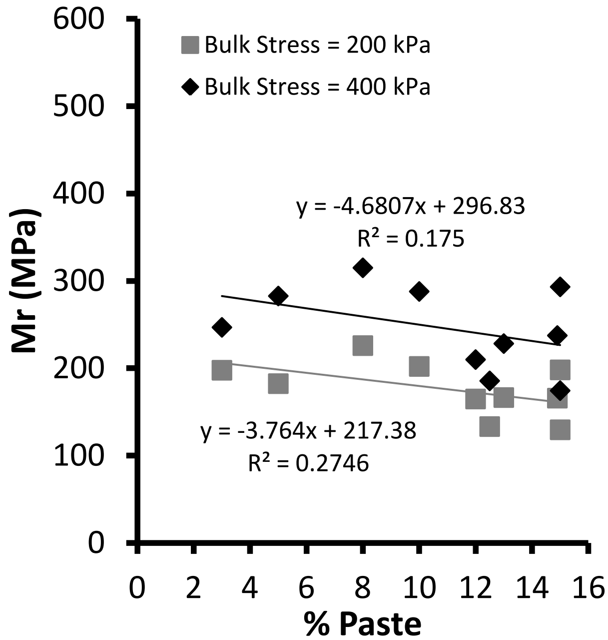

(a) Source 1

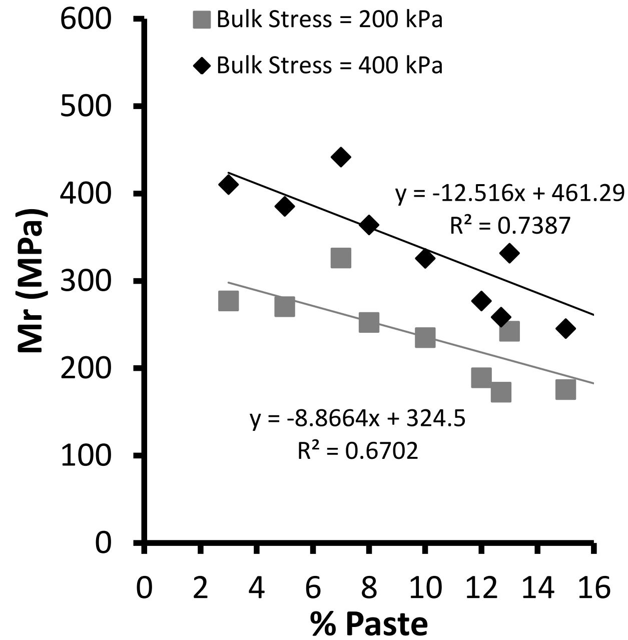

(c) Source 3

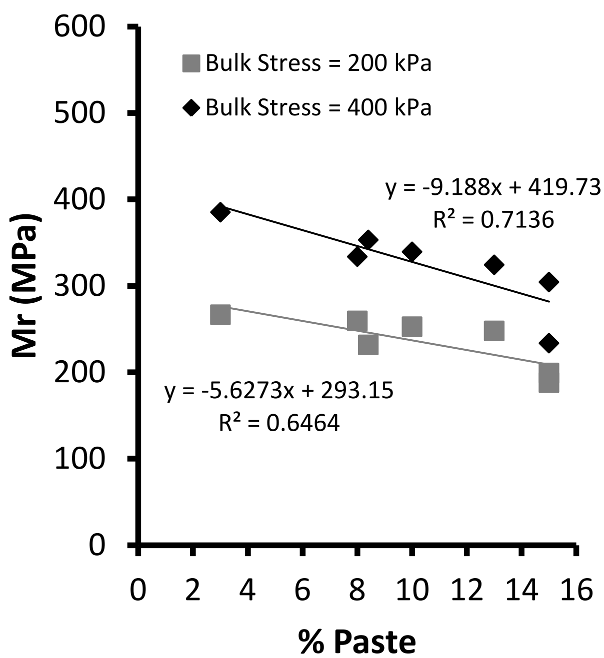

(b) Source 2

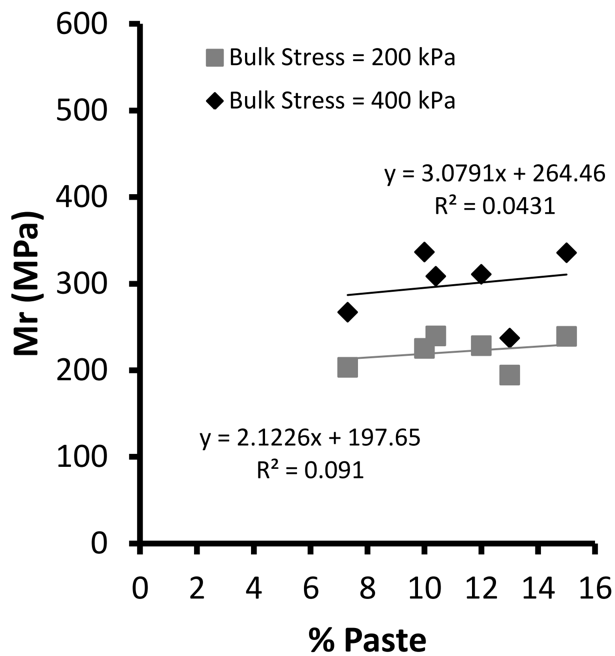

(d) Source 4

Figure 4.14 M_R vs. percent paste

With the *m* and *b* calculated, the effects of water content and fines content on both were determined. Tables summarizing the regression results for aggregates with natural and substitute fines are presented in Appendix D.3.

Figure 4.15 presents the frequency distribution for *m* and *b* for natural fines and substitute fines and Figure 4.16 presents the values of *m* and *b* versus the percent paste. It can be seen that for both natural and substitute fines *m* follows a skewed normal distribution but *b* does not. In general, it was found that as the fines content increased for specimens with natural and substitute fines the slopes decreased.The trend line for the slope versus the percent paste is negative. With a smaller *m* value the resilient modulus values does not change as fast with an increase in bulk stress. A larger *m* value tended to occur when the water content of a specimen was near the optimum water content for each source.

It is observed that as the percent paste increased the value of *b* decreased for specimens with both natural and substitute fines. The majority of *b* values were at 180 and 220 for specimens with F1 fines and 10 percent F1 fines for each source. The majority of *b* values for substitute fines were at 200, from Source 3, and greater than 280, from specimens with 5 percent substitute fines of Sources 2, 3 and 4. Focusing on water content, the value of *b* was higher for aggregates with substitute fines when the water content was below optimum and the value of *b* was higher for aggregates with natural fines when the water content was near optimum. Based on the results the value of *b* tended to be higher for aggregates with substitute fines compared to natural fines.

Figure 4.17 shows the trend line for the correlation between the slope, *m*, and "y" intercept, *b*. It ss observed that the data has a tendency for *b* to increase with an increase in *m.*

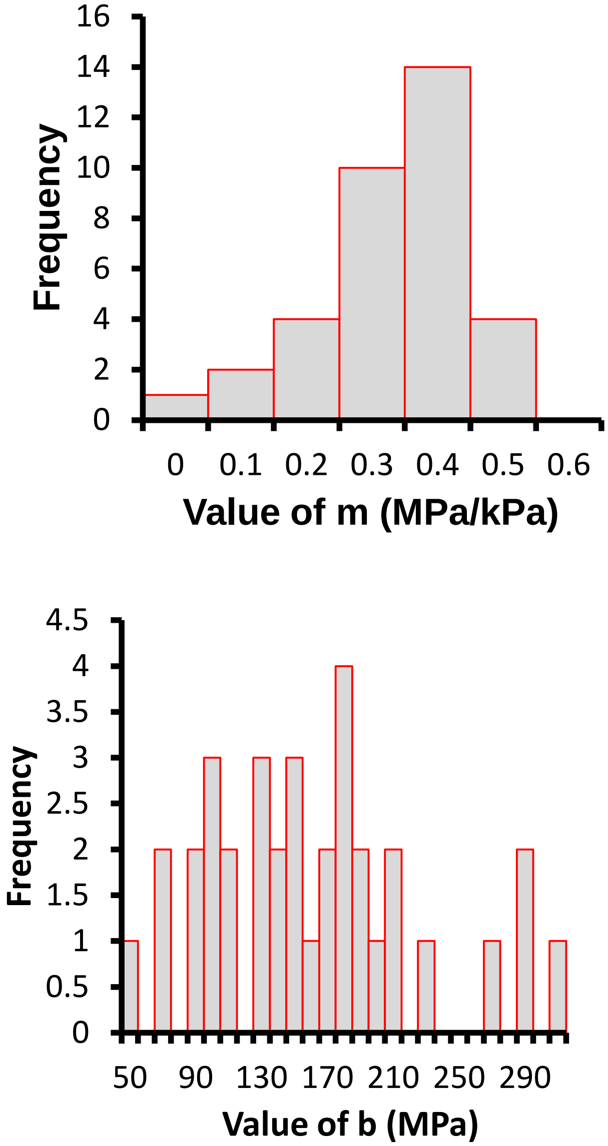

Figure 4.15 Frequency plots for *m* and *b*

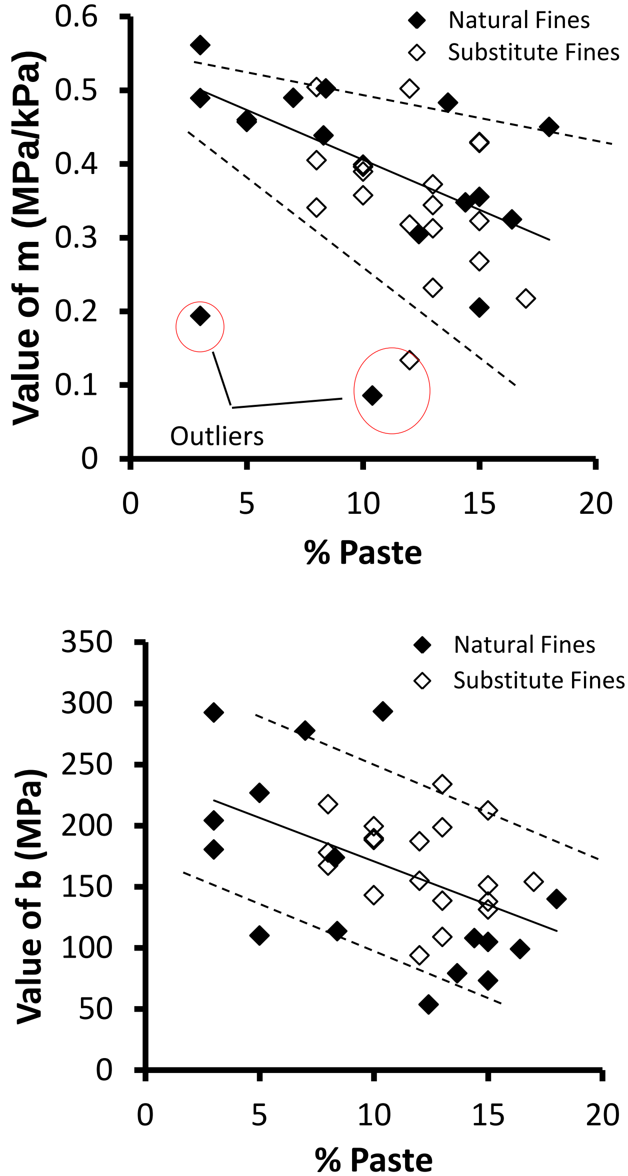

Figure 4.16 *m* and *b* vs. percent paste

4.2.4 Influence of Regression Coefficients for K_i, i = 1,2 and 3

Three models were used to determine the regression coefficients of each specimen, Uzan model, AASHTO model and K-θ model. The regression coefficients for each model and source are presented in Appendix D.4.

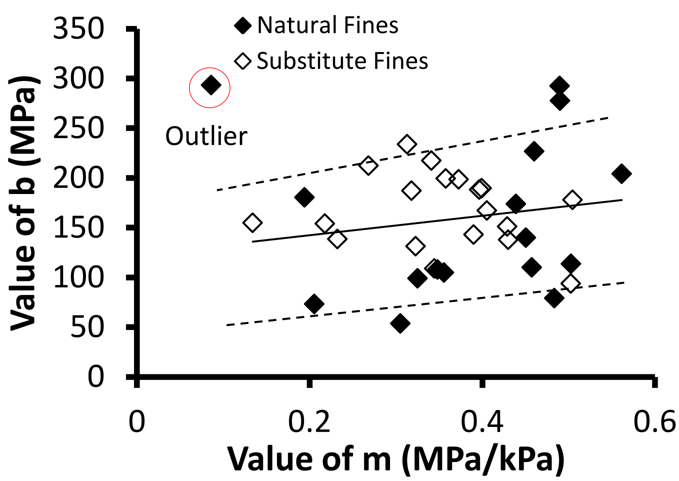

Figure 4.17 *m* vs. *b*

Figure 4.18 summarizes the distribution of regression coefficients from this study for the Uzan model. It was found that K_1 tended to be in the interval 1.1< $|K_1|$ < 1.6. The materials in which the first peak of values, K_1 = 1.1, occurred were for specimens containing Source 1 and Source 3 natural fines with fines greater than 8 percent and water content ranging from 5 percent to 8 percent.

The second peak of values at K_1 = 1.6 occurred for specimens containing substitute fines of Sources 2, 3 and 4 with water contents ranging from 3 percent to 5 percent. The majority of values for K_2 were in the interval 0.4< $|K_2|$ < 0.6. The majority of 0 values for K_3 occurred for specimens of Source 3 natural fines and Sources 2 and 4 substitute fines. The values which were not 0 occurred when the fines content was greater than 8 percent. It was also observed the materials with a larger K_2 value tended to have a negative value for K_3.

Figure 4.19 shows the distribution of regression coefficients for the AASHTO model. For this model the values of k_1 tended to fall between 1.1 and 1.9 which was a slightly larger range than for the Uzan model. The majority of the k_1 values at 1.3 and 1.8 came when substitute fines were used. The k_1 values at 0.7 and 0.8 come from Source 1 at 8 percent or higher fines content and 5 percent water content. The values for k_2 were generally the same for the AASHTO model as for the Uzan model. For the k_3, the AASHTO model produced more negative values, which the majority being between -0.1 and 0. The values which fell between this range came from all sources but the majority of -0.1 values came from Source 3 samples. Similar to the Uzan model, the values of k_2 tend to increase as k_3 decreases, seen in Figure 4.20, which coincides with the findings of Stolle et al. (2005).

The distributions of regression coefficients for the K-θ model are summarized in Figure 4.21. The K_1 values were similar to those from the AASHTO model. Regarding K_2, because K_3 was neglected the lower K_2 values from the AASHTO and Uzan models increased and the higher K_2 values decreased slightly.

The regression coefficients versus the percent paste are presented in Appendix D.4. For the Uzan and AASHTO models, when the percent paste increased the trend lines for K_1 decreased Iand K_3 increased. For the K-θ model as the paste increased the trend line for K_1 also decreased. For all three models the trend line for K_2 did not appear to change as the percent paste increased.

A regression analysis on the experimental data was also performed based on Equation (8) from Guo et al. (2006). The regression constants for the Uzan, AASHTO and K-θ models are presented in Table 4.7 to 4.9. Figure 4.22 compares the experimental results with those calculated from the regression model for the K-θ model. The comparisons for the Uzan and AASHTO models are provided in Appendix D.4. The K-θ results obtained most closely match the experimental data. It should be noted that Guo (Guo et al. 2006) use percentages for P_4, P_{200} and the water contents, but for this study fractions were used for P_4, P_{200}, and w, and as well the dry density terms were divided by 1000. Comparing the results from Table 2.4 to Tables 4.7 to 4.9, the terms which are negative are different. For example, from Table 2.4 constants b, d, and *e* are negative for K_1 but from Tables 4.7 through 4.9 constants *a*, *c*, and *f* are negative. In other words we see that regression is sensitive to the model used to describe the dependencies.

Table 4.10 Regression constants from Equation (8) (Guo et al. 2006) for Uzan Model

UZAN Model				
Variable	Coefficient	K_1	K_2	K_3
P_4	a	-0.136	0.1046	-0.0545
P_{200}	b	0.1192	-0.152	0.0857
w/w_{opt}	c	-0.2506	-0.1281	-0.0252
ρ_{dry}/ρ_{opt}	d	27.0129	-22.186	11.8228
W	e	0.017	0.0367	-0.003
ρ_{dry}	f	-0.013	0.0101	-0.0052
w_{opt}	g	1.4879	-1.1073	0.5658
	h	-0.9033	3.7241	-1.9741

Table 4.11 Regression constants from Equation (8) (Guo et al. 2006) for AASHTO Model

AASHTO Model				
Variable	Coefficient	k_1	k_2	k_3
P_4	a	-0.0683	0.0951	-0.1359
P_{200}	b	0.0068	-0.1384	0.2181
w/w_{opt}	c	-0.3021	-0.1354	-0.0544
ρ_{dry}/ρ_{opt}	d	13.15	-20.269	29.9666
W	e	0.0317	0.0369	-0.0099
ρ_{dry}	f	-0.007	0.0092	-0.0133
w_{opt}	g	0.8509	-1.0206	1.4527
	h	1.3423	3.4477	-5.1717

Table 4.12 Regression constants from Equation (8) (Guo et al. 2006) for *K-θ* Model

k-θ Model			
Variable	Coefficient	K_1	K_2
P_4	a	-0.0792	0.057
P_{200}	b	0.0261	-0.0775
w/w_{opt}	c	-0.2903	-0.1474
ρ_{dry}/ρ_{opt}	d	15.2912	-11.8596
w	e	0.0288	0.0336
ρ_{dry}	f	-0.0079	0.0055
w_{opt}	g	0.946	-0.612
	h	0.9919	2.0014

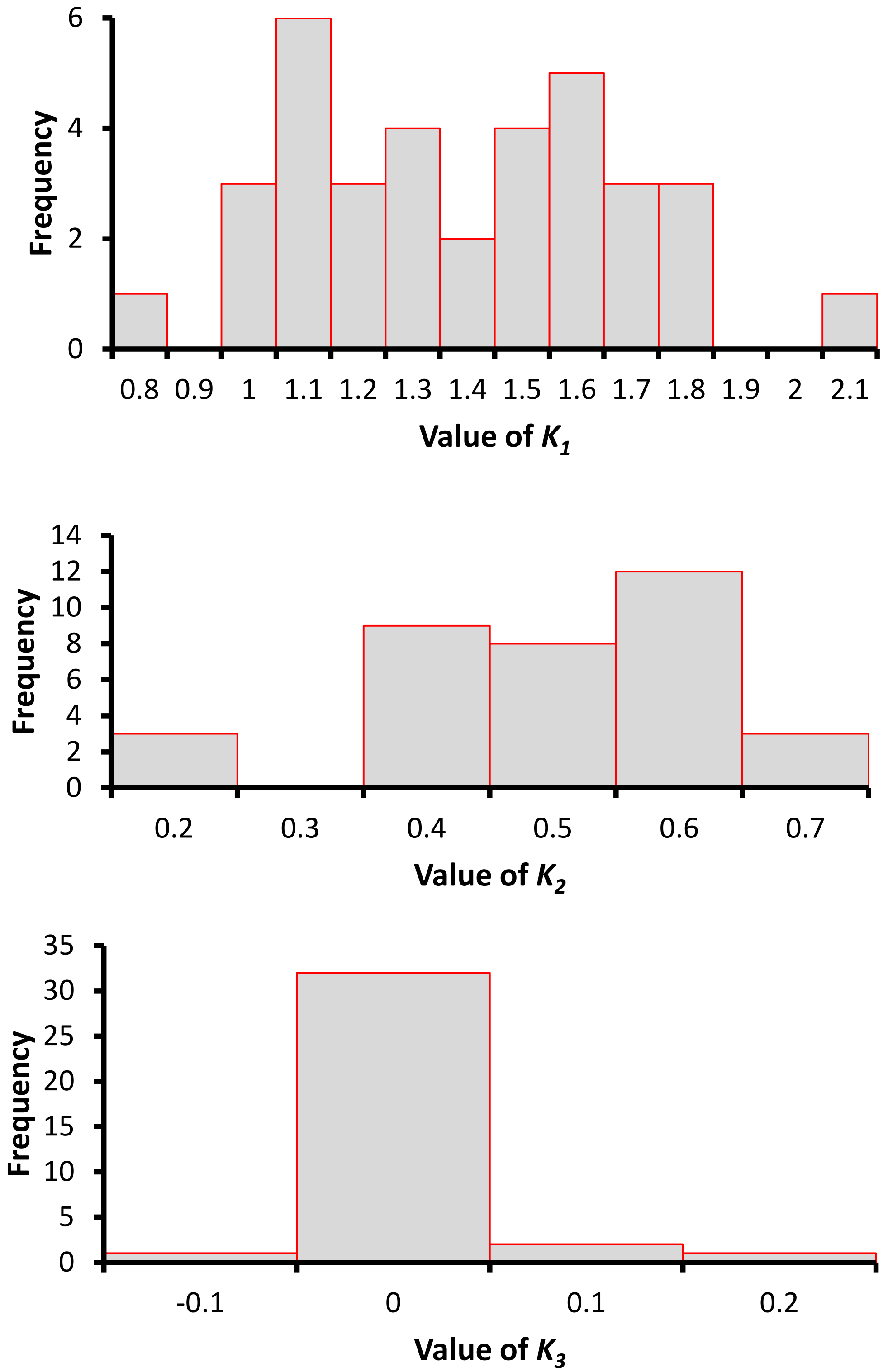

Figure 4.18 Frequency plots for regression coefficients K_1, K_2, and K_3 from Uzan model

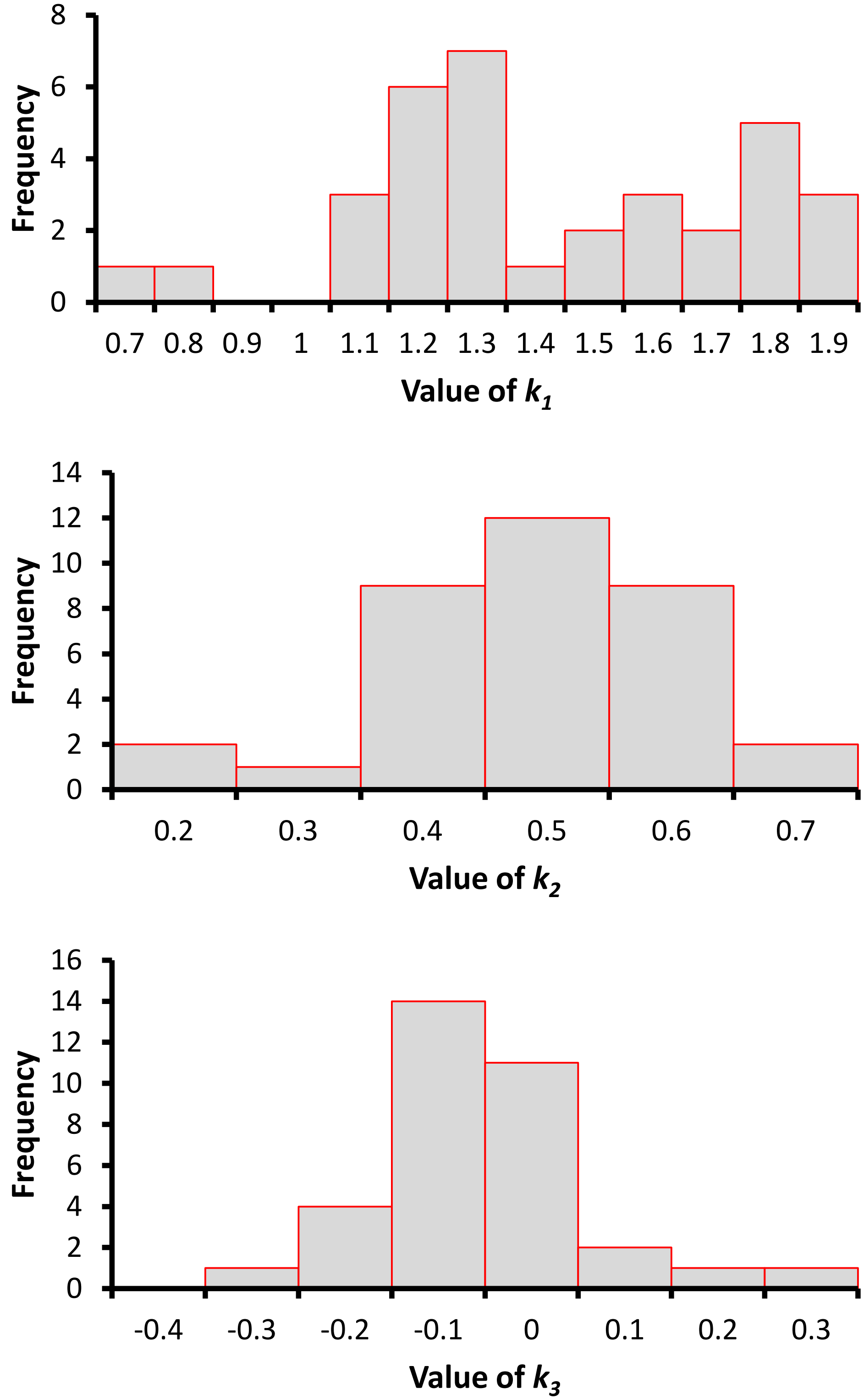

Figure 4.19 Frequency plots for regression coefficients k_1, k_2, and k_3 from AASHTO model

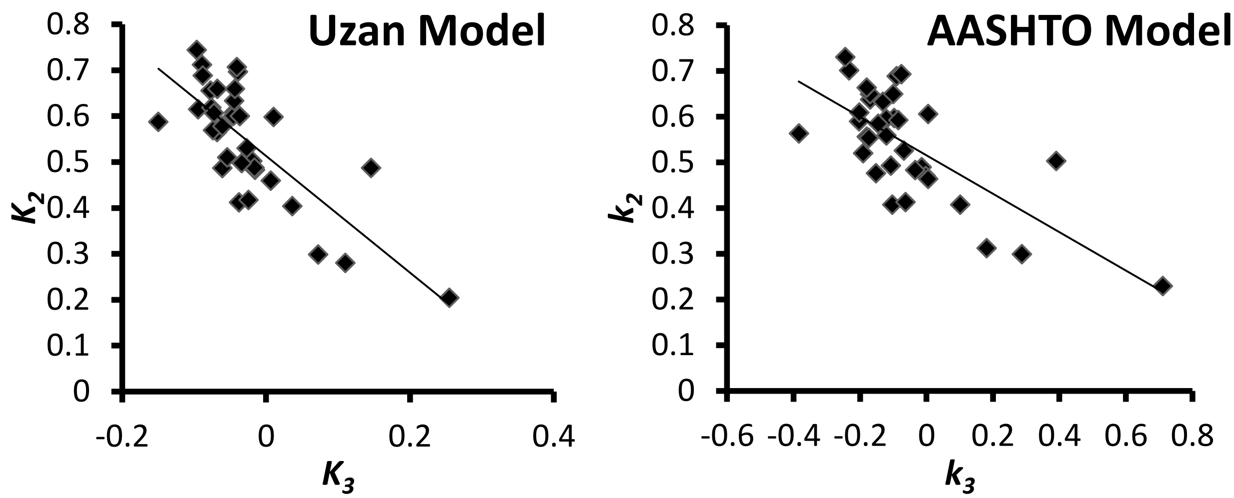

Figure 4.20 Relation between Regression Coefficients K_2 and K_3

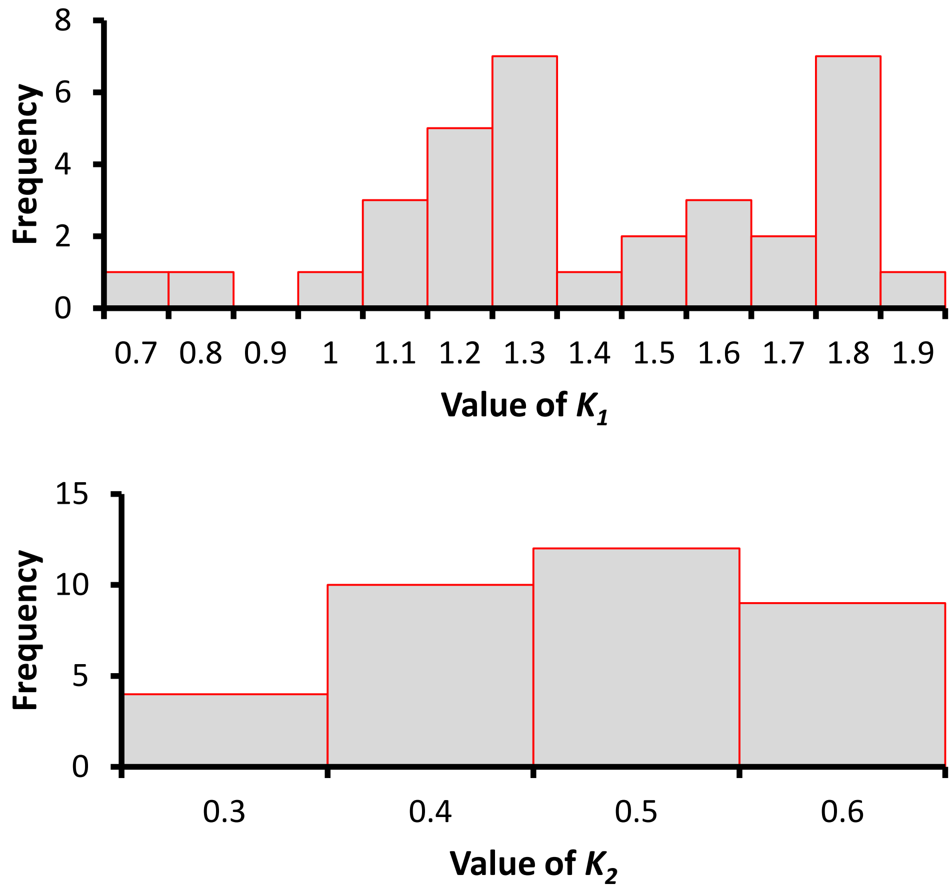

Figure 4.21 Frequency plots for regression coefficients K_1 and K_2 from K-θ model

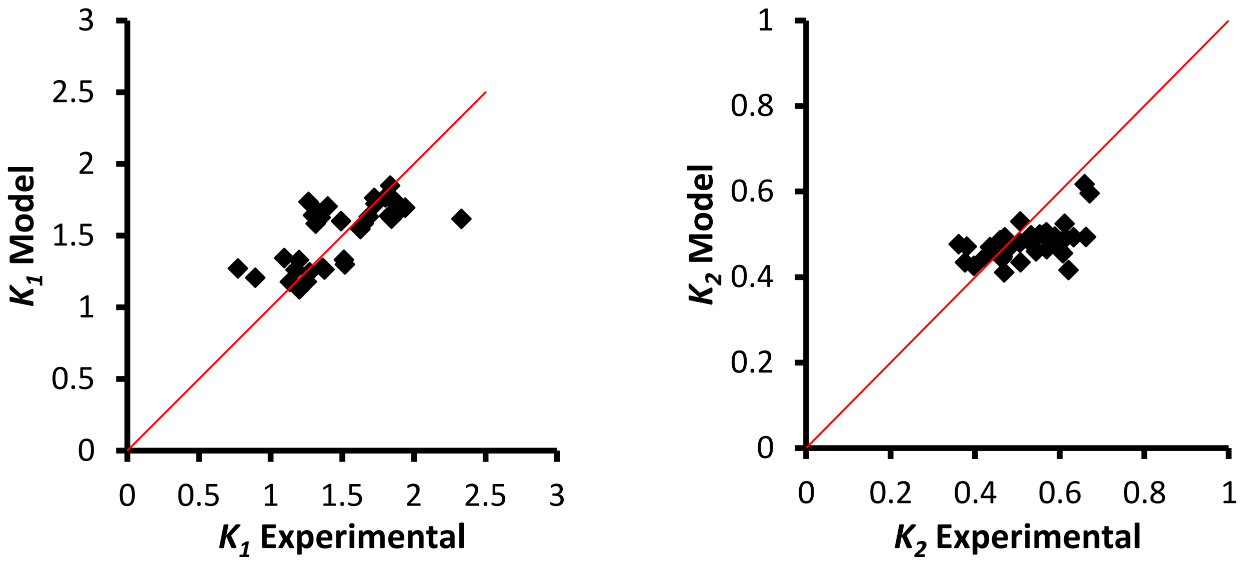

Figure 4.22 K-θ model K-coefficients from Equation (8)

4.2.5 Damping Ratio Considerations

Another source of information, which can be gathered from the resilient modulus tests is the damping ratio associated with each material for each of the pressure, moisture content and fine content conditions. The damping ratio, D, a measure of the energy dissipation, has been calculated for Source 1 through 4 at 20.7 kPa, 34.5 kPa, 68.9 kPa, 103.4 kPa, and 137.9 kPa confining pressures, using the following equation

$$D = \frac{1}{4\pi}\frac{\Delta W}{W} \tag{11}$$

where ΔW is the energy dissipated in a closed loop and W is the elastic energy, as shown in Figure 4.23.

Figure 4.24 displays a representative measured energy stress-strain loop. This figure is from Source 3 with natural fines content.

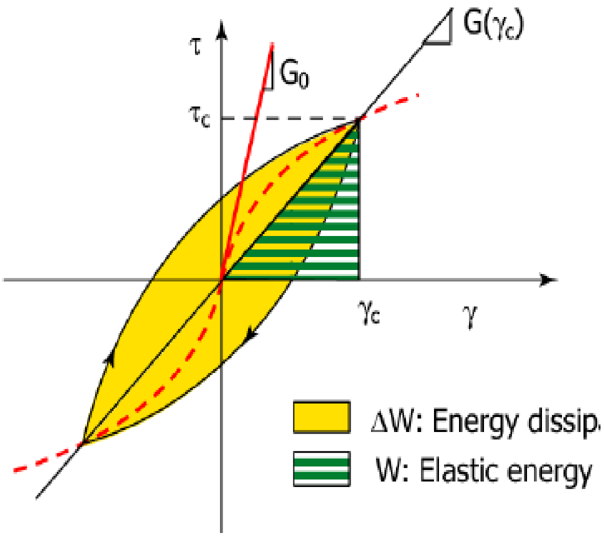

Figure 4.23 Elastic energy and energy dissipation during cyclic loading (Guo, 2014)

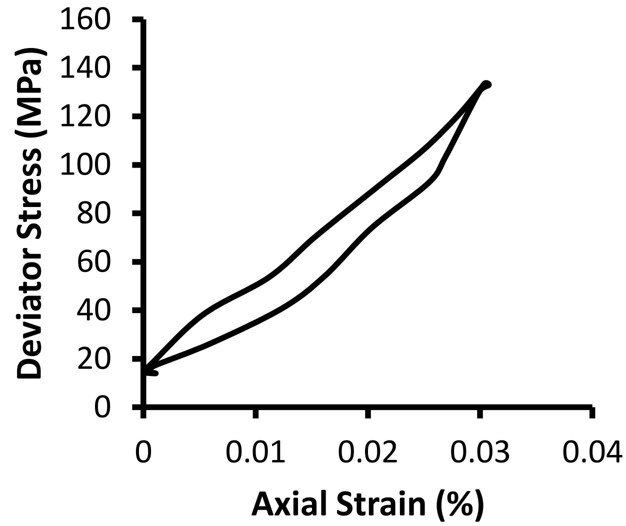

Figure 4.24 Energy dissipated for natural F1 fines, Source 3

Three load sequences were carried out at each confining pressure, resulting in three different damping ratios. For each of the figures presented in this section the average of the three damping ratios is used. All the tests that failed were again excluded from the analysis. Figure 4.25 shows that the damping ratios for all samples with natural fines decrease with an increase in confining pressure. The damping ratios that are highest correspond to the samples where the resilient modulus values were lowest. For example from Figure 4.25 (a) *D* values were highest for 10 percent F1 fines at 5 percent water content. The resilient modulus values at 10 percent F1 were lower (Figure D.1). As well, the damping ratios were lower when the water content was close to optimum.

Similar to the specimens with natural fines, the damping ratios decreased as the confining pressure increased for specimens containing substitute fines with the exception of the damping ratios of specimens containing 5 percent F2 at 7 percent water content. For this test *D* increased as the confining pressure increased at 137.9 kPa and the sample was found to be sensitive to deviatoric stress. Once again, higher damping ratios correspond to the lower resilient modulus values as anticipated. Comparing the natural fines, specimens to substitute fines specimens, the damping ratios were similar, which was largely attributed to the *PI* of the natural fines and substitute fines being similar.

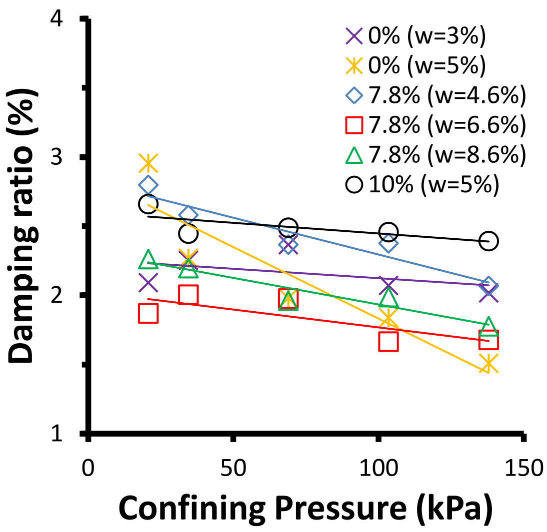

(a) Natural (F1) fines

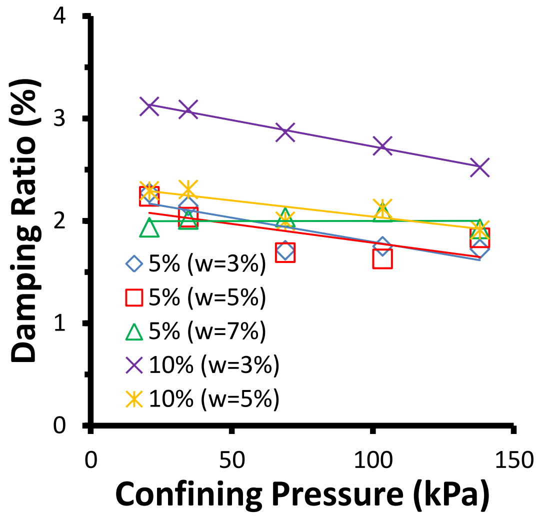

(b) Substitute (F2) fines

Figure 4.25 Damping ratio for Source 1

As with Source 1, the damping ratios for Source 2 with natural fines and substitute fines decrease as the confining pressure increases. It can be seen for both F1 and F2 fines in Figure 4.26, as the fines content increases the damping ratios increase. The damping ratios were also lowest at optimum water content, corresponding to the higher M_R values. The damping ratios of F1 fines specimens were lower than those containing F2 fines indicating higher resilient modulus values.

The damping ratios of Source 3 decrease as the confining pressure increases for all specimens. Similar to Sources 1 and 2, the lower damping ratios corresponded to higher resilient modulus as 0 percent F1 fines specimens produced the largest resilient modulus values for Source 3. In Figure 4.27, the results for Source 3 with substitute fines show clearly that as the fines content increases the damping ratio decreases. Specimens with 3 percent water content produced the lowest damping ratio with 10 percent F2 fines and 7 percent water content producing the highest damping ratio, which corresponds to the M_R being highest at 3 percent and lowest at 7 percent. Comparing the damping ratios of material containing natural fines to those with substitute fines, the damping ratios were similar as anticipated.

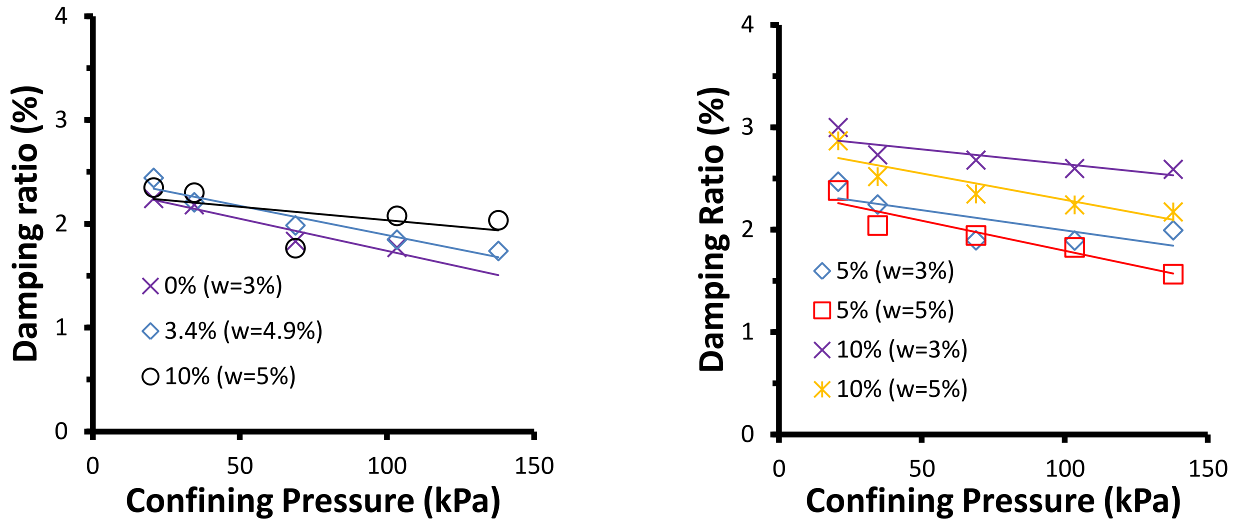

(a) Natural (F1) fines (b) Substitute (F2) fines

Figure 4.26 Damping ratio for Source 2

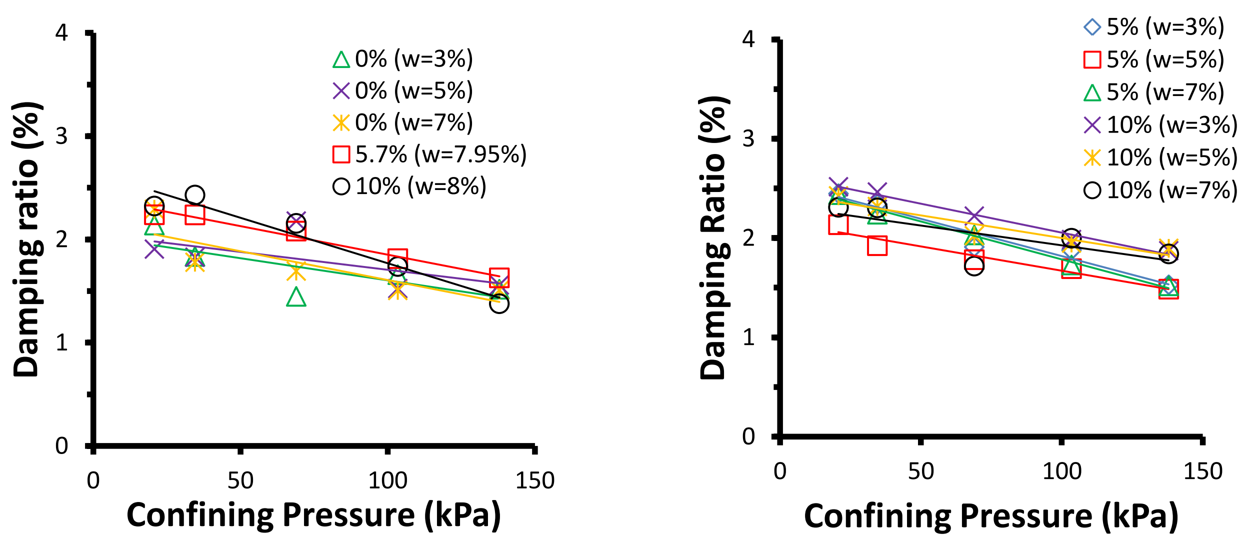

(a) Natural (F1) fines (b) Substitute (F2) fines

Figure 4.27 Damping ratio for Source 3

Following with the same trend as the previous three sources, the damping ratios decrease as the confining pressure increases for Source 4. The damping ratio was lowest for specimens compacted at the optimum water content that was determined from standard Proctor compaction.

The damping ratios for substitute fines in Figure 4.28 (b) also decreased as the confining pressure increased. *D* was higher for aggregate with 10 percent F2 fines than for aggregate with 5 percent F2 fines, at 5 percent water content in particular. Overall the damping ratios were similar for specimens containing natural and substitute fines. Comparing the damping ratios of all four sources, Source 3 damping ratios of specimens with natural fines were the lowest. Source 4 damping ratios for specimens containing natural fines were similar to Source 2, which is to be expected as the gradations for both sources were similar. The damping ratios for specimens with substitute fines were similar.

The damping ratios for each source were compared to the percent paste as shown in Figure 4.29. For Sources 1, 2 and 3, the damping ratios increased slightly as the percent paste increased. For Source 4 no trend can be observed for specimens with natural fines because there were only two successful tests.

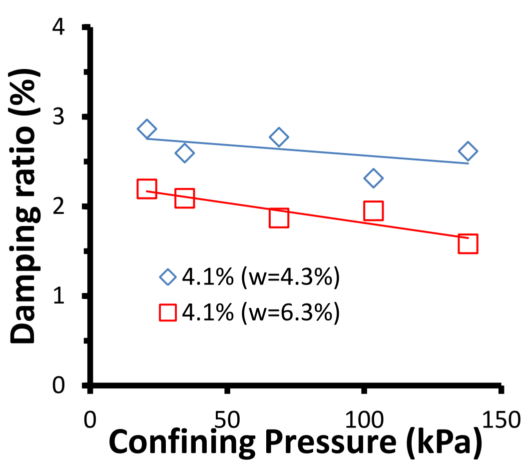

(a) Natural (F1) fines

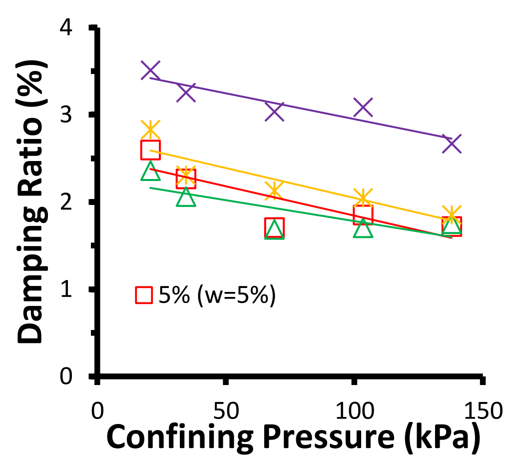

(b) Substitute (F2) fines

Figure 4.28 Damping ratio for Source 4

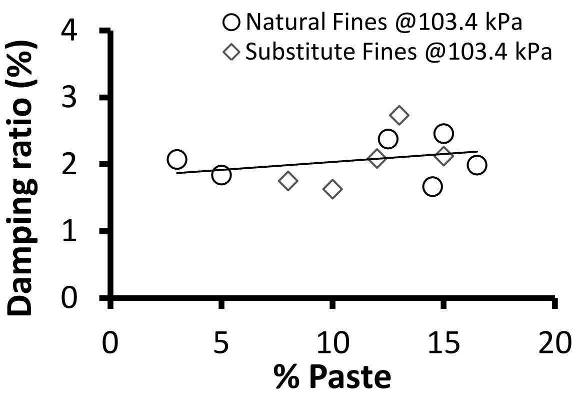

(a) Source 1

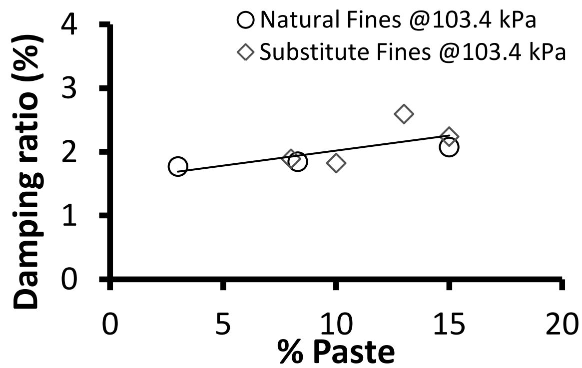

(b) Source 2

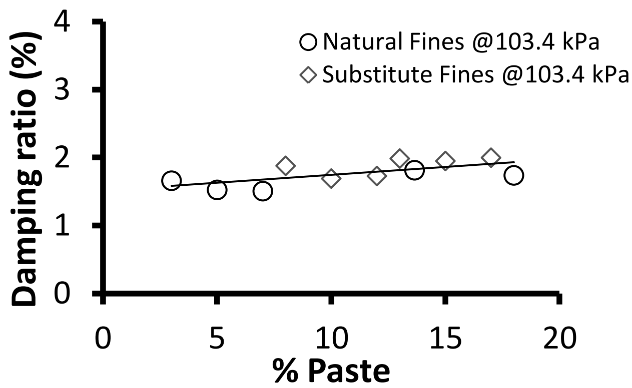

(c) Source 3

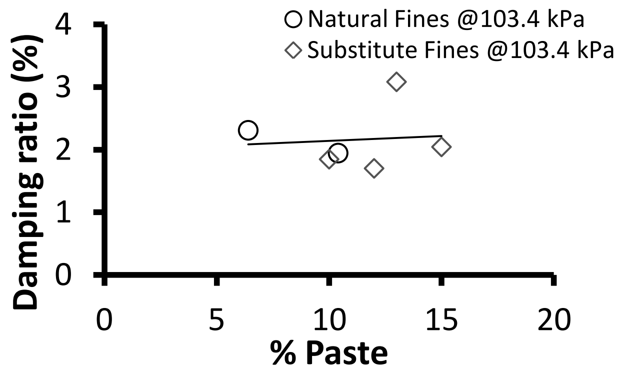

(d) Source 4

Figure 4.29 Damping ratio vs. percent paste

4.2.6 *CBR* vs. M_R

A final parameter to which resilient modulus is compared is *CBR*. Figure 4.30 presents the *CBR* values for specimens containing both natural and substitute fines and the corresponding M_R values. According to the trend lines, the *CBR* value increased as the M_R value decreased, corresponding to the bulk stresses of 200 kPa and 400 kPa, for Sources 1, 2 and 3. For Source 4 not enough tests were conducted to determine a trend. Comparing the results at 200 kPa and 400 kPa bulk stresses, the trend lines are almost parallel with the values at 200 kPa being lower as expected, similar to the results found in Chapter 4.2.2.

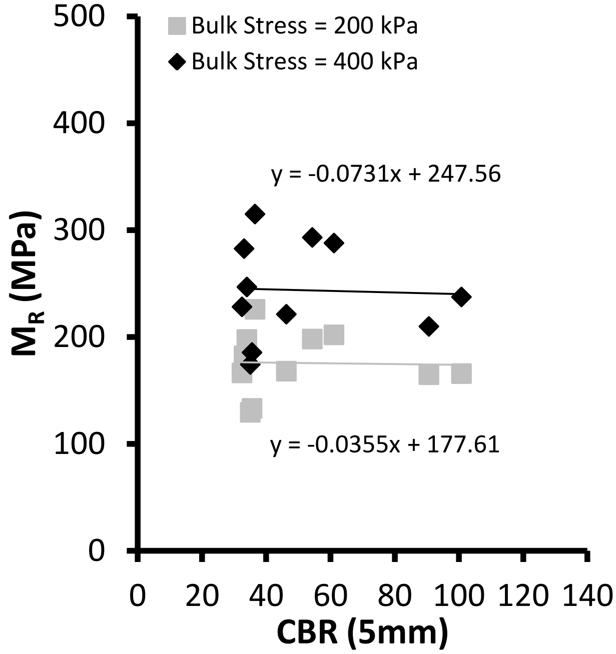

(a) Source 1

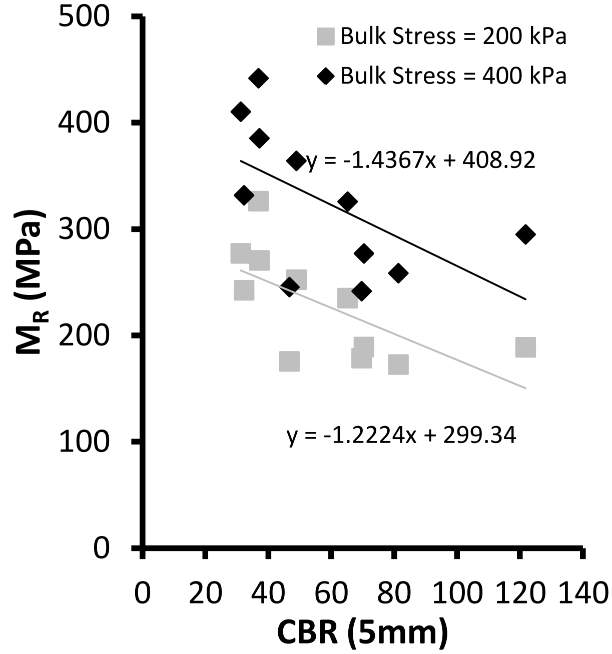

(c) Source 3

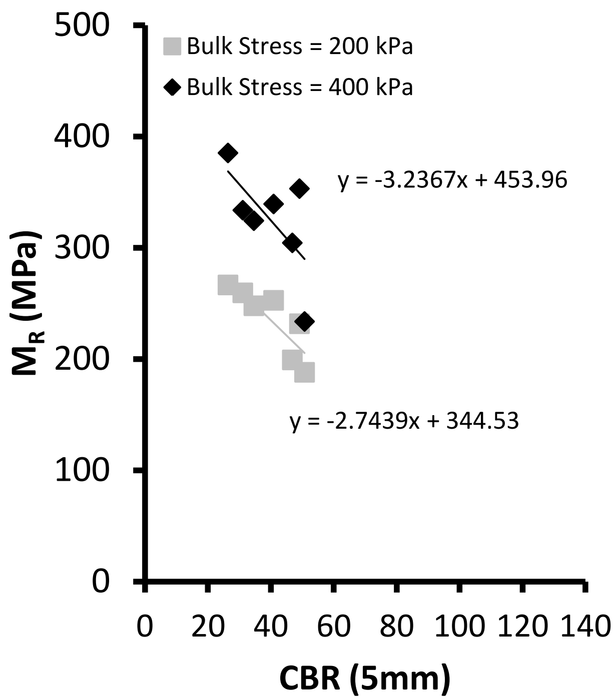

(b) Source 2

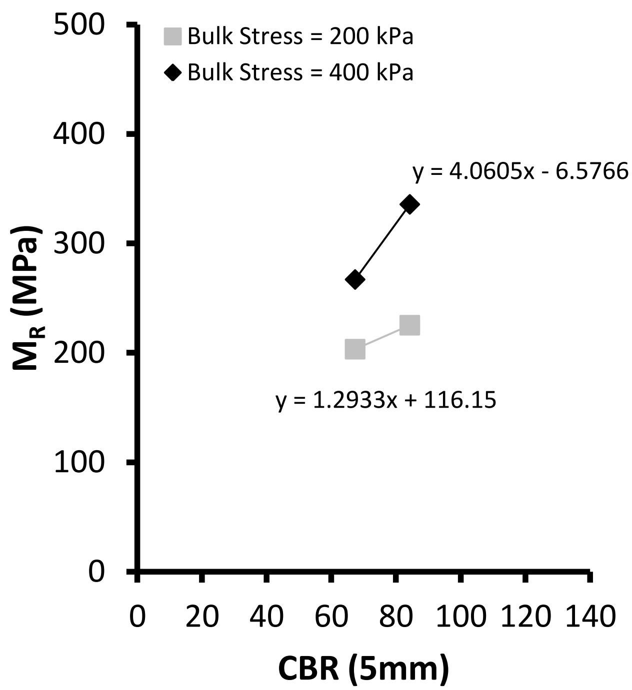

(d) Source 4

Figure 4.30 *CBR* vs. M_R

The trends observed in the figures are inconsistent with respect to what is presented the literature. Based on correlation equations found in literature, Table 2.3 in particular, the M_R should increase as the CBR values increase. Guo et al. (2006) also found that M_R, which is stress-state dependent, cannot be uniquely related to CBR, which is an index property of a material.

4.2.6 Permanent Deformation

The development of permanent deformation for the four sources was examined, the results of which are presented in Figure 4.31. Figure 4.31 plots the accumulated strain at the end of each confining pressure following the loading program given in Table 3.6. The first term in the legend refers to the type of fines, natural (F1) or substitute (F2), the second term represents the fines content (%), and the third term represents the water content (%). For Source 1 the permanent deformation was larger for specimens containing natural F1 fines, but for Sources 2, 3 and 4, the permanent deformations for natural and substitute fines were similar.

Figure 4.32 presents the accumulated strain versus the percent paste for each source. The trend lines clearly show that the accumulated strain at the end of a test increases as the percent paste increase.

4.3 Permeability Tests

One of the three factors, which is important for the design of pavement structures, is the ability of the granular base or subbase to drain rapidly. In order to calculate the drainage of a base layer, the permeability must be calculated. The constant head test method was used in this thesis to determine the permeability at three different constant heads, 71.4 cm, 61 cm and 53.7 cm.

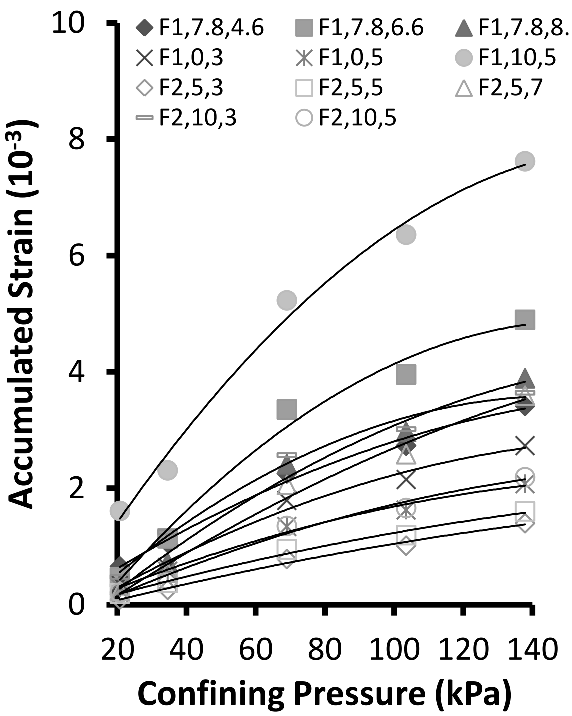

(a) Source 1

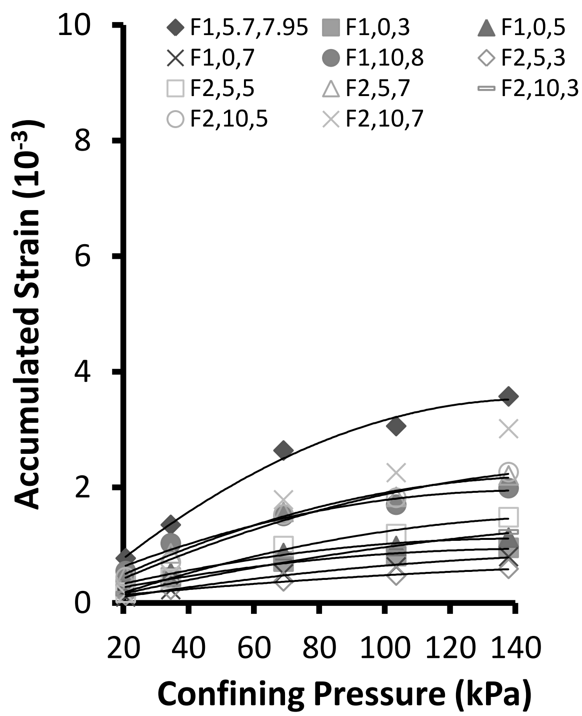

(c) Source 3

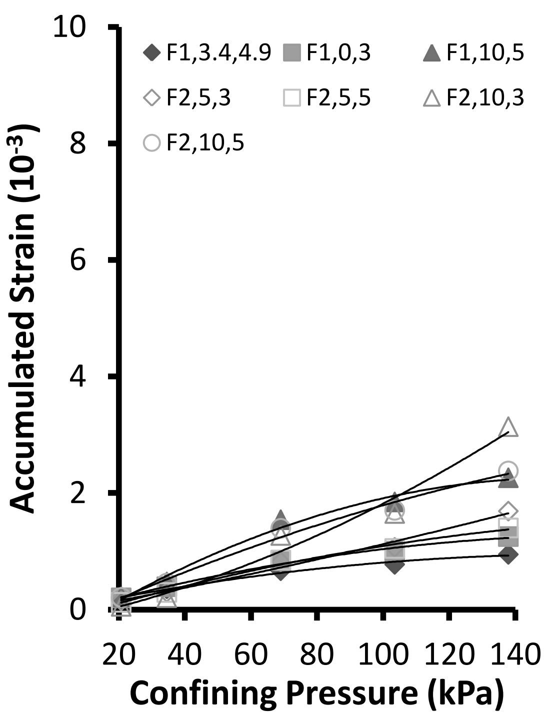

(b) Source 2

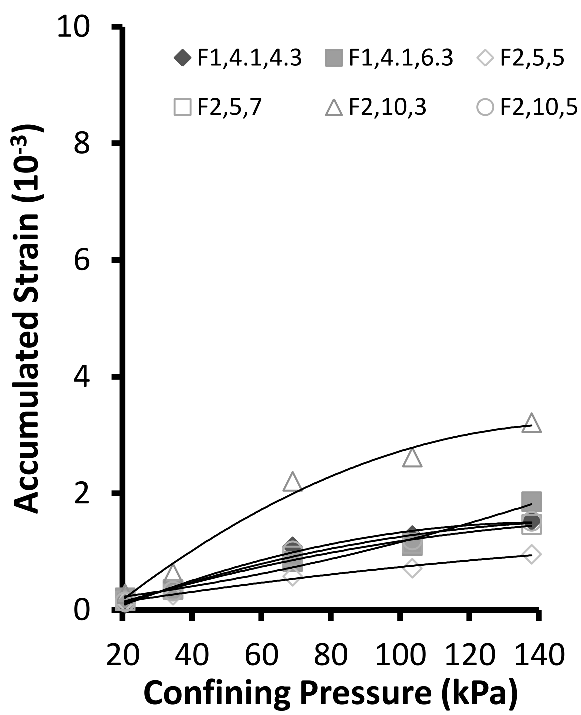

(d) Source 4

Figure 4.31 Accumulated strain for each Source

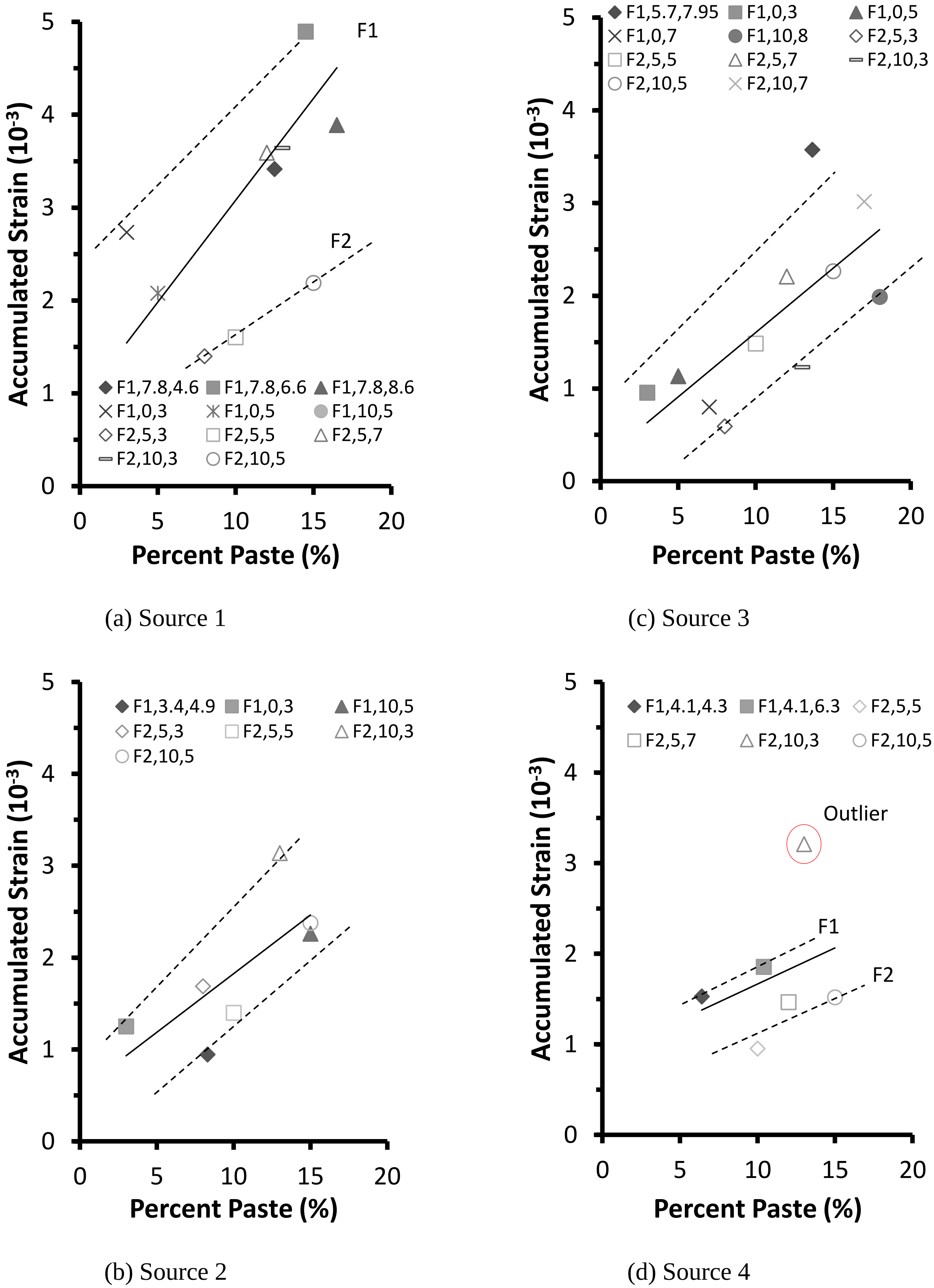

Figure 4.32 Percent paste vs. accumulated strain at the end of the test

Table 4.10 summarizes the results of the tests conducted on each of the sources. The equation used to calculate the permeability is given as

$$k = \frac{QL}{Aht} \tag{12}$$

where Q is the volume of discharge in cm^3, L is the length of specimen in cm, A is the cross-sectional area of the permeameter, h is the hydraulic head difference (constant head) in cm and t is the time for discharge in seconds.

Table 4.13 Permeability results

Material \ Hydraulic Gradient	Permeability (cm/sec)		
	6.14	5.25	4.62
Source 1/0%	0.0224	0.0229	0.0230
Source 1/7.8% F1	0.0109	0.0137	0.0163
Source 1/10% F1	0.0046	0.0052	0.0093
Source 1/5% F2	0.0032	0.0032	0.0037
Source 1/10% F2	0.0028	0.0039	0.0045
Source 2/0%	0.0123	0.0145	0.0153
Source 2/3.4% F1	0.0072	0.0075	0.0080
Source 2/10% F1	0.0059	0.0077	0.0079
Source 2/5% F2	0.0033	0.0046	0.0054
Source 2/10% F2	0.0041	0.0048	0.0049
Source 3/0%	0.0140	0.0146	0.0152
Source 3/5.7% F1	0.0058	0.0063	0.0065
Source 3/10% F1	0.0057	0.0062	0.0056
Source 3/5% F2	0.0046	0.0045	0.0043
Source 3/10% F2	0.0039	0.0024	0.0022
Source 4/0%	0.0112	0.0101	0.0074
Source 4/4.1% F1	0.0065	0.0039	0.0037
Source 4/10% F1	0.0058	0.0038	0.0037

The results for each source are separated in Figure 4.33 showing the effect of fines content on the permeability. For each of the sources the permeability when no fines were present was significantly larger than for those specimens with fines, which was to be expected as the voids in the aggregate structure are empty at zero fines content and the water can flow through more easily. When fines were present the results were similar but the permeability slightly decreased as the fines content increased for both natural and substitute fines cases. The results support the findings of Emery and Lee (1977) where the hydraulic conductivity decreases for Granular A crushed limestone when 10 percent fines were included. Also the permeability did not change much as the gradient varied in a certain range.

The grain size is an important factor in determining the permeability. Haider (2013) found that permeability is more sensitive to smaller grain sizes (D_{10} and D_{30}) compared to larger sizes (D_{50} and D_{60}). As the percent passing the smaller grain sizes increases the permeability increases. Onur (2014) found that with a high coefficient of uniformity the permeability is lower. Source 1 had the smallest D_{10} and D_{30} values and largest C_u value compared to the other sources but the permeability was higher for Source 1. Emery and Lee (1977) report that the hydraulic conductivity of a Granular A crushed limestone decreases from 3.41×10^{-2} cm/s to 1.26×10^{-4} cm/s when 10 percent fines are included.

Again it should be noted that the *PI* of the substitute fines were similar to the *PI* of the natural fines for Sources 1, 2 and 4. For Source 1 the permeability decreased further with the addition of substitute fines, which was unexpected because with the similarity in *PI* the values were expected to be similar. The *PI* of Source 3 natural, silt fines was lower than the *PI* of the clay fines of the substitute material which explains the decrease in permeability for Source 3 as silt is expected to produce a slightly higher k (Dawson A. , 2008)

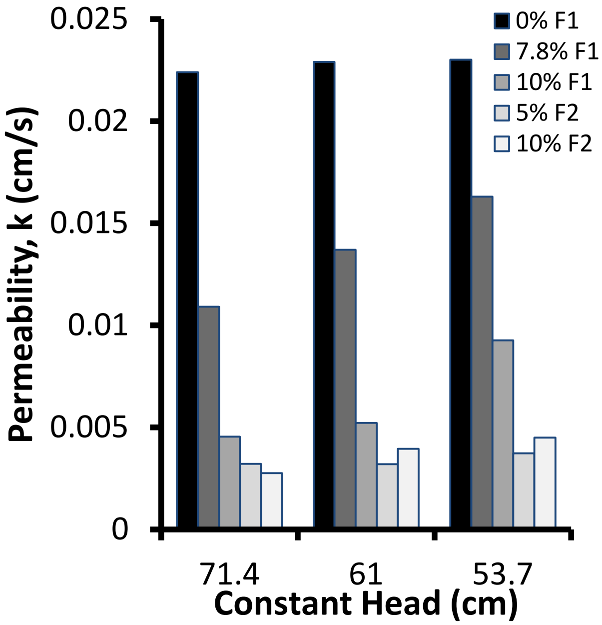

(a) Source 1

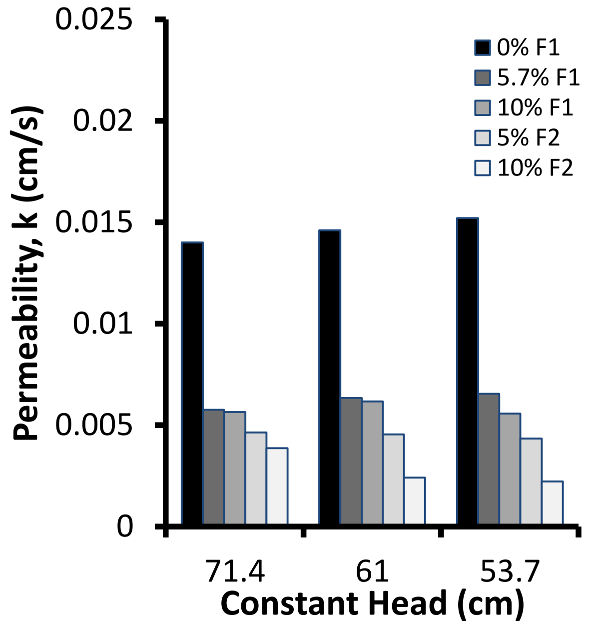

(c) Source 3

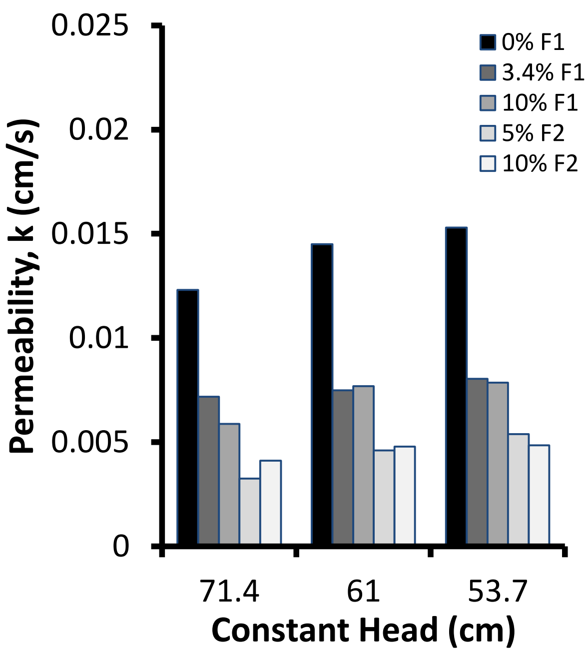

(b) Source 2

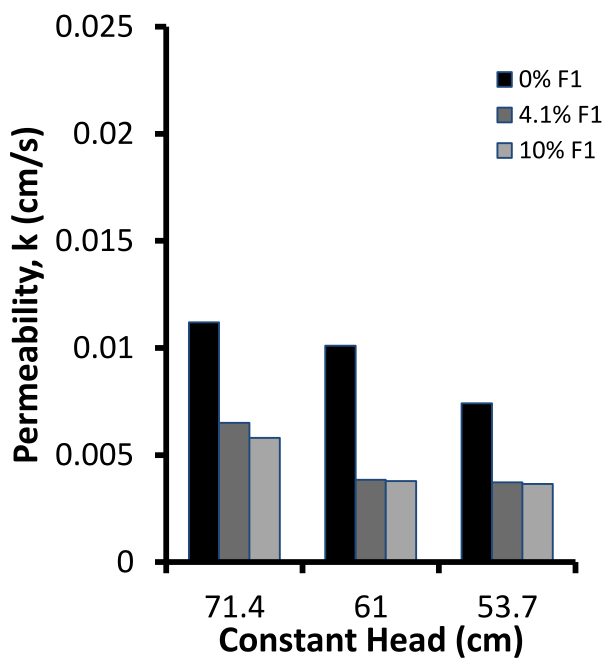

(d) Source 4

Figure 4.33 Permeability of Sources 1 through 4

4.4 Influence on Design of Pavement Structures

To evaluate the influence of fines in the granular base/subbase layers on flexible pavement performance, we examine the variation of the structural number of granular base layers at different fines content, with the clean aggregates as the reference. To achieve this goal, information from AASHTO 1993 method was used in the following analysis.

According to AASHTO 1993, the structural number of the granular base layer of a flexible pavement is determined as $SN = a_2 m_2 h_2$, in which h_2 is the base layer thickness, with a_2 and m_2 being the structural coefficient and the drainage coefficient of the base layer, respectively. Referring to AASHTO 1993, the value of a_2 depends on the CBR value or the resilient modulus of the aggregates in the granular base layer. Referring to Tables 4.4 and B.1, for Source 1 aggregate with approximately the same water content, the CBR values are not affected by the fines content (natural to 10 percent). This implies that the structural number a_2 is not sensitive to the fines content as far as *the same compaction level is achieved.*

On the other hand, the drainage coefficient m_2 depends on the quality of drainage and how long the pavement structure is exposed to moisture levels approaching saturation, as shown in Tables 4.14 and 4.15. It is clearly shown that the permeability has significant influence on the quality of drainage and hence the drainage coefficient. Therefore, one can expect that the variation of fines contents tends to have direct impact on the drainage coefficient m_2 and hence the structural number of the granular base given that the coefficient of permeability varies with fines content. For simplicity, we use the following quantity to quantify the influence of fines content on the structural number of the granular base layer:

$$R = \frac{SN_{(FC)}}{SN_{ref}} = \frac{(a_2 m_2 h_2)_{FC}}{(a_2 m_2 h_2)_{ref}} \approx \frac{(m_2)_{FC}}{(m_2)_{ref}} \tag{13}$$

in which $(m_2)_{FC}$ and $(m_2)_{ref}$ are the drainage coefficients of the aggregate with fines content FC and the reference aggregate, respectively.

Table 4.14 Quality of drainage (AASHTO, 1993)

(AASHTO Guide for Design of Pavement Structures, 1993)

Quality of Drainage	Minimum Permeability	Time to Drain
Excellent	1000 ft/day	2 hours
Good	85 ft/day	1 day
Fair	11 ft/day	1 week
Poor	0.5 ft/day	1 month
Very Poor	0.02 ft/day	Water will not drain

Table 4.15 Layer drainage coefficients m_i (AASHTO, 1993)

	Percent of time pavement structure is exposed to moisture levels approaching saturation			
Quality of drainage	Less than 1%	1–5%	5–25%	Greater than 25%
Excellent	1.40–1.35	1.35–1.30	1.30–1.20	1.20
Good	1.35–1.25	1.25–1.15	1.15–1.00	1.00
Fair	1.25–1.15	1.15–1.05	1.00–0.80	0.80
Poor	1.15–1.05	1.05–0.80	0.80–0.60	0.60
Very poor	1.05–0.95	0.95–0.75	0.75–0.40	0.40

Since this study focuses on the granular base layer, only the layer structural coefficient for granular base, a_2, and the drainage coefficient for granular base, m_2 were used. Table 4.16 summarizes the results of the calculations to determine the design of the granular base for all sources including the average permeability the layer structural coefficient of each source, the quality of drainage and the corresponding drainage coefficient, and the normalized structural coefficient, a_2m_2. It was assumed that the percent of time the pavement structure is exposed to moisture levels approaching saturation was between 5 percent and 25 percent, which was used to determine m_2. For Sources 1 and 3 the quality of drainage begins as fair but decreases to poor as the fines content increases and for Sources 2 and 4 the drainage remains fair. The excellent condition in Table 4.16 refers to a pavement with excellent drainage at less than 1 percent of time approaching saturation, where m_2 is 1.4 as well as a layer structural coefficient of 1.4. Comparing the structural number of each source to the structural number of an excellent aggregate, Source 1 was the closest to a perfect aggregate at 64 percent. When the fines content increased to 10 percent and the drainage quality was low, the ratio decreased to as low as 47 percent for Source 3 and 50 percent for Source 1.

Table 4.16 Drainage coefficients and structural numbers

Material	Average Permeability (cm/sec)	ft/day	Quality of Drainage	Drainage Coefficient, m_2	a_2m_2 (SN2)	a_2m_2 (SN2 Excellent Condition)	SN2/SN2-Excellent Condition
Source 1/0%	0.0228	64.6	fair	0.9	0.126	0.196	0.64
Source 1/7.8% F1	0.0136	38.5	fair	0.9	0.126	0.196	0.64
Source 1/10% F1	0.0063	17.8	fair	0.9	0.126	0.196	0.64
Source 1/5% F2	0.0034	9.6	poor	0.7	0.098	0.196	0.5
Source 1/10% F2	0.0037	10.5	poor	0.7	0.098	0.196	0.5
Source 2/0%	0.014	39.7	fair	0.9	0.117	0.196	0.6
Source 2/3.4% F1	0.0076	21.5	fair	0.9	0.117	0.196	0.6
Source 2/10% F1	0.0071	20.1	fair	0.9	0.117	0.196	0.6
Source 2/5% F2	0.0044	12.5	fair	0.9	0.117	0.196	0.6
Source 2/10% F2	0.0046	13.0	fair	0.9	0.117	0.196	0.6
Source 3/0%	0.0146	41.4	fair	0.9	0.119	0.196	0.61
Source 3/5.7% F1	0.0062	17.6	fair	0.9	0.119	0.196	0.61
Source 3/10% F1	0.0058	16.4	fair	0.9	0.119	0.196	0.61
Source 3/5% F2	0.0045	12.7	fair	0.9	0.119	0.196	0.61
Source 3/10% F2	0.0028	7.9	poor	0.7	0.092	0.196	0.47
Source 4/0%	0.0096	27.2	fair	0.9	0.119	0.196	0.61
Source 4/4.1% F1	0.0047	13.3	fair	0.9	0.119	0.196	0.61
Source 4/10% F1	0.0044	12.5	fair	0.9	0.119	0.196	0.61

CHAPTER 5 CONCLUSION AND RECOMMENDATIONS

5.1. Conclusions

This study presents the results and analysis of the experimental tests that were completed to determine the effect of fines content and type on unbound granular base materials. Four different source crushed rock Granular A granular base materials were investigated. For each source, tests were conducted with no fines, natural fines and 10 percent fines along with two substitute fines contents of 5 percent and 10 percent. Physical property tests including standard Proctor, sieve analysis and Atterberg limit tests were performed along with CBR, M_R and permeability tests for the four Granular A aggregates. Based on the results the following conclusions can be drawn:

1. Fines must be present for the CBR values to increase. When no fines were present in the specimens for all sources, the CBR values remained constant as the water content increased.
2. CBR values decreased for Sources 1 and 2 as the fines content increased from 0 percent to 10 percent natural fines but the CBR value increased with increasing fines content for Sources 3 and 4. Source 3 is considered to be a high quality Granular A. The CBR value also decreased as the water content increased beyond the optimum water content. As seen in Figures 4.5 and 4.6, as the density increases so does the CBR.
3. With the plasticity index of the substitute fines being similar to the plasticity index of the natural fines content for each source the CBR values were similar for specimens with substitute and natural fines resulting in no clear trend of CBR values when comparing specimens with natural and substitute fines.

4. There was no general systematic influence of fines content on M_R, with varying water content. For example, for sources with similar gradations and water contents the M_R values were different.

5. Similar to the results for CBR the M_R values were similar for natural and substitute fines specimens.

6. In general, it can be seen that there was an optimum water content, between 5 and 6 percent, and optimum fines content, between 4 and 5 percent, where the M_R was greatest.

7. As no systematic trends could be determined for M_R with respect to water content and fines content, a combination of water and fines content, percent paste during compaction, was used. It is assumed that the percent paste during compaction influences density, which has an impact on M_R.

8. Regression coefficients were calculated for each source at different combinations of water and fines content for three different models; Uzan, AASHTO and K-θ model. With increasing paste content, K_1 tended to decrease, K_2 values remained constant and K_3 increased for all models. Physical properties were also used to estimate resilient modulus using an equation from Guo et al. (2006). Based on the regression analysis results the parameters, $\rho_{dry/}\ \rho_{opt}$, appeared to influence the K values the most.

9. Another source of information retrieved from M_R tests was the damping ratio. The damping ratios were determined at different confining pressures using the energy dissipated and elastic energy. Higher damping ratios corresponded to low M_R values for all sources and the damping ratios decreased as the confining pressure increased. The damping ratios also were lowest when the water content was near the optimum.

10. The development of permanent deformation was examined and it was determined that Source 1 had the highest accumulated strain values and Sources 2, 3 and 4 had similar accumulated strain values. As the percent paste tends to increase the accumulated strain also increased for all sources.

11. The permeability was largest when no fines were present. In general there was little change in k for 5 percent to 10 percent fines but large change from 0 percent to 5 percent fines. Source 1 was observed to have the highest permeability compared to the other three sources however this was not expected as Source 1 had the highest fines content.

12. Comparing the normalized structural coefficient, a_2m_2, to a pavement structure considered to be in excellent condition, Source 1 was shown to have the highest percentage at 64 percent. As the fines content increased to 10 percent the ratio decreased to as low as 47 percent for Source 3 and 50 percent for Source 2.

5.2. Recommendations

1. A component of this study was to determine the affect of the plasticity index of fines on granular material behaviour however the plasticity index of the plastic fines used was only slightly higher than that of the original fines content. Future work should include testing of substitute fines with higher a plasticity index (clearly plastic) and higher fines levels (between 12 and 14 percent). Future work should also include different combinations of substitute fines and natural fines, such as 5 percent substitute fines and 5 percent natural fines.

2. With some aggregates sensitive to water content, more focus should be placed on the compaction methods used. Further research should be conducted on the influence of the compaction method on M_R. This also includes the use of modified Proctor compaction as

many agencies prefer the use of modified Proctor compaction compared to standard Proctor compaction

3. Soaked CBR tests should also be conducted on all test specimens to determine how the specimens are affected after the samples have been submerged in water.

4. Dynamic cone penetrometers (DCP) testing provides a in-situ index of strength and estimate of subgrade modulus. Tests results can be correlated to CBR, and resilient modulus. It is recommended that dynamic cone penetrometer testing be completed on all sources and to correlate the results to the CBR and M_R results already obtained.

REFERENCES

AASHTO. (1993). *AASHTO guide for the design of pavement structures*, Washington, D.C: American Association of State Highways and Transportation Officials.

AASHTO. (2011). *AASHTO guide for the design of pavement structures*, Washington, D.C: American Association of State Highways and Transportation Officials.

Abu-Farsakh, M. Y., Alshibli, K., Nazzal, M. D., & Seyman, E. (2004). *Assessment of In-Situ Testing Technology for Construction Control of Base Course and Embankments.* Louisiana Department of Transportation and Development.

Adu-Osei, A. (2001). *Characterization of Unbound Granular Layers in Flexible Pavements.* College Station, Texas: Texas Transportation Institute.

Allen, J. J., & Thompson, M. R. (1974). *Resilient Response of Granular Materials Subjected to Time-Dependent Lateral Stresses. Transportation Research Record 510, TRB, National Research Council Board*, Washington, D.C., pp. 1-13.

Arnold, G. K. (2004). *Rutting of Granular Pavements.* Nottingham: University of Nottingham.

ASTM Standard. (2008). West Conshohocken, PA: ASTM International.

Austin, A. (2009). *Fundamental Characterization of Unbound Base Course Materials under Cyclic Loading.* Louisiana State University.

Ayodele, A. L., Falade, F. A., & Ogedengbe, M. O. (2009). *Effect of Fines content on some Engineering Properties of Lateritic Soil in Ile-Ife.* Ile-Ife: Department of Civil Engineering, Obafemi Awolowo University.

Barksdale, R. D. (1991). *The Aggregate Handbook.* Washington, DC: National Stone Association.

Barksdale, R., & Itani, S. Y. (1989). *Influence of Aggregate Shape on Base Behaviour. Transportation Research Record 1227, TRB, National Research Council Board,* Washington D.C., pp. 173-182

Belt, J., Ryynanen, T., & Ehrola, E. (1997). Mechanical Properties of Unbound Base Course. *8th International Conference on Asphalt Pavements, 1,* pp. 771-781. Seattle.

Bennert, T., & Maher, A. (2005). *The Development of a Performance Specification for Granular Base and Subbase Material.* New Jersey Department of Transportation Bureau of Research and Technology and U.S Department of Transportation Federal Highway Administration.

Caicedo, B., Coronnado, O., Fleureau, J. M., & Correia, A. G. (2009). Resilient Behaviour of Non Standard Unbound Granular Material. *Road Materials and Pavement Design , 10(2),* 287-312.

Carmichael, R. F., & Stuart, E. (1978). Predicting Resilient Modulus: A Study to Determine the Mechanical Properties of Subgrade Soils. *Transportation Research Record 1043, TRB, National Research Council Board*, Washington, D.C., pp. 20-28

Cedergren, R. H., & Godfrey, A. K. (1974). *Water: Key Cause of Pavement Failure?* Sacramento, California: Civil Engineering-ASCE.

Chai, G., & Roslie, N. (1998). The Structural Response and Behaviour Prediction of Subgrade Soils using Falling Weight Deflectometer in Pavement Construction. *3rd Internation Conference on Road and Airfield Pavement Technology,* Beijing, China, April.

Cole, D. M., Irwin, L. H., & Johnson, T. C. (1981). Effect of Freezing and Thawing on Resilient Modulus. *Transportation Research Record 801, TRB, National Research Council Board*, Washington, D.C., pp.51.

Cost 337 Final Report (2000), *Unbound granular materials for road pavement.* European Commission, Brussels, Luxembourg.

Dawson, A. R., Thom, N. H., & Paute, J. L. (1996). Mechanical Characteristics of Unbound Granular Materials as a Function of Condition. *Flexible Pavements, Proc., Eur. Symp. Euroflex*. A. G. Correia, ed., Balkema, Rotterdam, The Netherlands, pp. 35-44.

Dawson, A. (2008). *Water in Road Structures: Movement, Drainage and Effects.* Nottingham, UK: Nottingham Transportation Engineering Centre.

Dodds, A., Logan T., McLachlan, M., & Patrick, J. (1999). *Dynamic Load Properties of New Zealand Base Course*. Transfund New Zealand Report 151

Emery, J. J. (2012). Asphalt Technology. Shiloh Canconstruct Limited.

Emery, J. J., & Lee, M. A. (1977). *Layer Coefficients based on Resilient Modulus Tests, OJT and CRP Project.*

Frost- Susceptible Soils. (2008). Retrieved from American Concrete Pavement Association.

George, K. P. (2004). *Prediction of Resilient Modulus from Soil Index Properties.* Final report. The University of Mississippi. U.S Department of Transportation Federal Highway Adminstration.

George, K. P., & Uddin, W. (2000). *Subgrade Characterization For Highway Pavement Design* Final report. Mississippi Department of Transportation.

Gudishala, R. (2004). *Development of Resilient Modulus Prediction Models for Base and Subgrade Pavement Layers from In Situ Devices Test Results.* Andhra Pradesh, India: Sri Krishna Devaraya University.

Guo, P. (2014, January). Soil Dynamics: Dynamic Soil Properties.

Guo, P. (2013). Characterization of Soil Properties

Guo, P., Stolle, D. F., & Liu, Y. (2006). *Unbound Resilient Modulus Testing of Typical Base, Subbase Materials in Ontario.* Minsitry of Transportation Ontario.

Haider, I. (2013). *Geomechanical and Hydraulic Behaviour of Maryland Graded Aggregate Base Materials.* University of Maryland.

Han, Y. P. (2005). *Resilient Modulus Estimation System.* University of Missouri-Rolla.

Hashiro, R. S. (2005). *Correlation of Resistance Value (R-Value) with California Bearing Ratio (CBR) for Use in the Design of Flexible Pavements.* University of Hawaii.

Haynes, J. H., & Yoder, E. J. (1963). *Effects of Repeated Loading on Gravel and Crushed Stone Base Course Materials used in the AASHO Road Test.* Highway Research Board, No. 39, pp.82-96.

Heukelom, W., & Klomp, A. J. (1962). *Dynamic Testing as a Means of Controlling Pavements During and After Construction.* Michigan: Proceedings of the First International Conference on Structural Design of Asphalt Pavements, Ann Arbor, Michigan, August 20th.

Heydinger, A. G., Xie, Q. L., Randolph, B. W., & Gupta, J. D. (1996). *Analysis of Resilient Modulus of Dense and Open-Graded Aggregates. Transportation Research Record 1547, TRB, National Research Council Board*, Washington, D.C., pp. 1-6

Hicks, L. D. (1956). *Design and Construction of Base Courses.* Washington, D.C: 35th Annual Meeting, Highway Research Board Bulletin.

Hicks, R. G., & Monismith, C. L. (1971). *Factors Influencing the Resilient Response of Granular Material. Transportation Research Record 345, HRB, National Research Council Board*, Washington, D.C., pp. 15-31

Huang, Y. H. (1993). *Pavement Analysis and Design.* Englewood Cliffs, New Jersey: Prentice-Hall, Inc.

Institute, T. A. (1982). *Research and Development of the Asphalt Institute's Thickness Design Manual, 9th Edition.*

Instruction Rep. GL-92-3. Vicksburg, Mississippi: Waterways Experiment Station.

Jorenby, B. N., & Hicks, R. G. (1987). *Base Course Contamination Limits. Transportation Research Record 1095, TRB, National Research Council Board,* Washington, D.C., pp. 86-101

Kolisoja, P. (1994). Large Scale Dynamic Triaxial Test with Coarse Grained Aggregates. *Proceedings for the 4th International Conference on Bearing Capacity of Roads and Airfields, Volume 2.* Minneapolis, Minnesota.

Kolisoja, P. (1997). *Resilient Deformation Characteristics of Granular Materials.* Tampere, Finland: Thesis, Tampere University of Technology.

Lam, A. (1982). *Resilient Moduli of Flexible Pavement Materials.* McMaster University.

Lekarp, F. (1997). *Permanent Deformation Behaviour of Unbound Granular Materials.* Stockholm: Royal Institute of Technology.

Lekarp, F., & Dawson, A. (2000). *Modelling permanent deformation behaviour of unbound granular materials.* Construction and Building Materials, *in press*, 12(1), pp. 9-18.

Maher, A., & Bennert, T. (2000). *Resilient Modulus Properties of New Jersey Subgrade Soils.* New Jersey: New Jersey Department of Transporation.

Maree, J. H. (1982). *Aspects of the Design and Behaviour of Road Pavements with Granular Base Layers.* University of Pretoria.

Mishra, D., & Tutumluer, E. (2012). *Aggregate Physical Properties affecting Modulus and Deformation Characteristics of Unsurfaced Pavments*. J. Mater. Civ. Eng, *24*(9), 1144-1152.

Nazzal, M. (2003). *Field Evaluation of In Situ Test Techniology for QC/QA During Construction of Pavement Layers and Embankments.* Louisianna State University.

Ohiduzzaman, M., Lo, S. C., & Craciun, O. (2011). *Effect of Plasticity of Fines on the Deformation Behaviour of Unbound Granular Base Material.* Geo-Frontiers.

Onur, E. M. (2014). *Predicting the Permeability of Sandy Soils from Grain Size Distributions.* Kent State University.

OPSS PROV 1010. (2013). *Material specification for Aggregates - Base, Subbase, Select Subgrade, and Backfill material*. Ontario Provincial Standard Specification.

Phang, W. A. (1971). *The Effects of Seasonal Strength Variation on the Performance of Selected Base Materials.* Department of Highways, Ontario.

Rahim, A. M., & George, K. P. (2004). *Subgrade Soil Index properties to Estimate Resilient Modulus. Proc. 83rd Annual meeting of the Transportation Research Board,* Washington, D.C.,

Reeves, M. (2006). *Particle Shape*. Saskatoon, Saskatchewan, Canada: Department of Civil and Geological Engineering, University of Saskatchewan.

Richardson, D., & Lusher, S. M. (2009). *Resilient Moduli of granular base materials using a modified Type 5 gradation.* Missouri Department of Transportation.

Ring, W. R. (1974). Seasonal Strength of Pavements. *Public Roads , 38*(2), pp.107-118

Sawangsuriya, A., & Edil, T. B. (2005). Evaluting stiffness and Strength of Pavement Materials. *Geotechincal Engineering*, 58(4), pp. 217-230.

Seed, H. B., Chan, C. K., & Lee, C. E. (1962). Resilience characteristics of subgrade soils and their relation to fatigue failure in asphalt pavements.. *Proc. 1st Int. Conf. On the Struct. Design of Asphalt Pavements*, Berkeley, California,: Institute of Transportation and Traffic Engieering August 8.

Senior, S. A., Gorman, B., & Szoke, S. I. (2008). Recycling Road Building Materials and Experience with Full Depth Reclamation in the Ontario Provincial Highway System. *Transportation Association of Canada.* Toronto, Canada.

Siswosoebrotho, B. I., Widodo, P., & Augusta, E. (2005). The Influence of Fines Content and Plasticity on the Strength and Permeability of Aggregate for Base Course Material. *Proceedings of the Eastern Asia Society for Transportation Studies , 5,* 845-856.

Stolle, D. F., Guo, P., & Liu, Y. (2005). *Unbound Resilient Modulus testing of Typical Base, Subbase Materials in Ontario.* MTO.

Stolle, D.F.E., Guo, P., & Emery, J.J., (2014) "Use of reclaimed asphalt pavement for granular bases", Canadian Journal of Civil Engineering, 41, 493-499.

Thompson, M. R., & Robnett, Q. L. (1976). Resilient properties of Subgrade soils. *Journal of Transportation Engineering* , 71-89.

Uthus, L. (2007). *Deformation Properties of Unbound Granular Aggregates.* Trondheim: Norwegian University of Sciene and Technology.

Uzan, J. (1985). *Characterization of Granular Material. TRB,* Washington, D.C.

Webb, W. M., & Campbell, B. E. (1986). *Preliminary Investigation into Resilient Modulus Testing for new AASHTO pavement Design Guide.* Office of Materials and Research, Georgia Department of Transportation.

Werkmeister, S., Dawson, A. R., & Wellner, F. (2004). Pavement Design Model for Unbound Granular Material. *Journal of Transportation Engineering*, *130* (5), 665-674.

Yau, A., & Von Qu, H. L. (2002). *Study of LTPP Laboratory Resilient Modulus Test Data and Response Characteristics: Final Report.* Federal Highway Administration, Publication No. FHWA-RD-02-051.

Yeh, S. T., & Su, C. K. (1989). *Resilient Properties of Colorado Soils.* Colorado Department of Highways, Report No. CDOH-DH-SM-89-9.

Yoder, E. J., & Witczak, M. W. (1975). *Principles of Pavement Design, 2nd Edition.* John Wiley and Sons.

Appendix A

Table A.1 Summary of Granular A sieve analysis results

Sieve Analysis Percent Passing		Source 1	Source 2	Source 3	Source 4
Sieve Sizes					
1 in.	25 mm	100	100	100	100
¾ in.	19 mm	96.5	98.2	95.7	96.7
½ in.	12.5 mm	81.4	77.4	75.7	78.9
No. 4	4.75 mm	55.0	47.8	46.6	43.7
No. 8	2.36 mm	41.4	32.6	34.9	25.9
No. 16	1.18 mm	30.8	21.1	25.3	15.6
No. 50	300 µm	18.2	8.9	13.2	8.1
No. 200	75 µm	7.8	3.4	5.7	4.1
D_{10} (mm)		0.10	0.37	0.20	0.40
D_{30} (mm)		1.20	2.10	1.80	2.90
D_{60} (mm)		5.00	7.80	7.90	8.00
C_u		50.00	21.08	39.50	20.00
C_c		2.88	1.52	2.05	2.63

Appendix B

Table B.1 Source 1 CBR and dry density results

List	***w (%)***	**CBR (0.1)***	**CBR (0.2)***	**$\bar{x}$* (0.1)**	**$\bar{x}$ (0.2)**	**ρ_{dmax} (kg/m^3)**
S1/7.8% F1 (w=4.7)	4.72	39.5	43.0			2052.5
	4.45	24.6	28.1	32.0	35.6	1974.0
S1/7.8% F1 (w=6.7)	6.58	83.4	103.1			2230.5
	6.89	81.5	98.4	82.4	100.8	2168.7
S1/7.8% F1 (w=9.1)	9.15	40.0	39.4			2044.8
	9.13	52.8	53.1	46.4	46.3	2088.1
S1/0% (w=3.2)	3.21	26.5	31.8			1991.0
	3.22	28.1	36.1	27.3	34.0	1997.5
S1/0% (w=4.9)	4.55	29.8	27.5			2002.7
	5.28	39.0	38.7	34.4	33.09	2049.5
S1/10% F1 (w=5.1)	5.01	32.6	34.6			2075.5
	5.19	28.7	35.4	30.7	35.03	2054.4
S1/10% F1 (w=6.9)	6.91	61.6	96.1			2306.9
	6.88	57.0	84.2	59.3	90.135	2275.7
S1/10% F1 (w=8.4)	8.52	54.2	70.7			2234.5
	8.2	46.6	58.9	50.4	64.8	2151.6
S1/5% F2 (w=2.9)	2.82	35.5	38.5			2061.6
	2.93	32.6	34.5	34.0	36.5	2076.5
S1/5% F2 (w=4.9)	5.01	49.3	56.2			2092.3
	4.87	56.7	65.9	53.0	61.1	2161.0
S1/5% F2 (w=7.3)	7.34	61.6	76.8			2235.0
	7.17	81.2	104.4	71.4	90.6	2295.1
S1/5% F2 (w=10.1)	9.93	9.90	18.1			1989.8
	10.35	10.4	15.2	10.2	16.7	2005.2
S1/10% F2 (w=3.4)	3.24	29.8	34.7			2070.7
	3.49	27.0	30.2	28.4	32.4	1922.1
S1/10% F2 (w=5)	5.16	40.9	42.7			2124.7
	4.85	56.7	65.9	48.8	54.3	2204.7
S1/10% F2 (w=7.1)	7.34	42.2	56.2			2295.7
	6.75	70.4	91.3	56.3	73.8	2362.7
S1/10% F2 (w=9.8)	9.24	37.7	48.9			2207.2
	10.27	22.8	33.0	30.2	40.9	2195.4

* 0.1 inch = 2.5 mm; $\bar{x}$ = Average
0.2 inch = 5 mm

Table B.2 Source 2 CBR and dry density results

List	*w (%)*	CBR (0.1)*	CBR (0.2)*	$\bar{x}$* (0.1)	$\bar{x}$* (0.2)	ρ_{dmax} (kg/m^3)
S2/3.4% F1 (w=3.1)	3.16	28.8	32.0			2065.3
	3.05	44.0	51.5	36.4	41.8	2012.6
S2/3.4% F1 (w=5.2)	5.28	43.5	49.7			2161.3
	5.09	38.1	48.4	40.8	49.1	2105.8
S2/3.4% F1 (w=5.8)	5.76	36.3	48.4			2193.7
	5.86	46.9	58.4	41.6	53.4	2169.4
S2/3.4% F1 (w=7.4)	7.34	57.0	71.0			2219.8
	7.5	55.3	71.1	56.2	71.0	2236.6
S2/0% (w=3.3)	3.17	18.4	24.8			1849.9
	3.38	21.2	28.0	19.8	26.4	1946.4
S2/0% (w=4.8)	4.34	26.6	33.0			1981.2
	5.34	22.7	28.3	24.7	30.6	1861.8
S2/10% F1 (w=5.0)	5	34.5	49.0			2176.1
	5.08	43.5	52.5	39.0	50.7	2160.5
S2/10% F1 (w= 7.6)	6.89	45.8	56.9			2249.1
	8.3	28.8	40.4	37.3	48.7	2227.8
S2/10% F1 (w=8.7)	8.55	34.8	45.2			2261.4
	8.79	27.6	40.2	31.2	42.7	2190.4
S2/5% F2 (w=3.2)	3.33	30.9	33.2			2017.0
	3.14	28.2	29.0	29.6	31.1	1995.4
S2/5% F2 (4.9)	4.84	29.7	32.7			2015.9
	5.02	43.4	49.1	36.5	40.9	2112.4
S2/5% F2 (w=7.6)	7.46	43.6	51.5			2151.2
	7.69	24.8	39.2	34.2	45.3	2212.8
S2/5% F2 (w=9.1)	8.99	20.5	31.0			2258.0
	9.22	8.5	11.3	14.5	21.2	2251.1
S2/10% F2 (w=3.3)	3.35	30.9	30.8			2073.8
	3.28	35.5	38.4	33.2	34.6	2100.4
S2/10% F2 (w=5.4)	5.39	35.3	42.1			2159.3
	5.46	45.8	51.5	40.6	46.8	2160.4
S2/10% F2 (w=7.1)	7.3	37.9	50.5			2178.9
	6.95	34.3	45.8	36.1	48.1	1993.5
S2/10% F2 (w=10.4)	10.48	12.2	16.2			2206.4
	10.25	7.8	10.3	10.0	13.3	2154.0

* 0.1 inch = 2.5 mm; $\bar{x}$ = Average
0.2 inch = 5 mm

Table B.3 Source 3 CBR and dry density results

List	*w (%)*	CBR (0.1)*	CBR (0.2)*	$\bar{x}$* (0.1)	$\bar{x}$* (0.2)	ρ_{dmax} (kg/m^3)
S3/5.7% F1 (w=5.8)	5.93	45.8	62.5			2065.4
	5.64	40.1	70.4	43.0	66.4	2215.2
S3/5.7% F1 (w=8.1)	8.07	63.4	82.7			2219.7
	8.03	47.3	80.0	55.3	81.4	2215.5
S3/5.7% F1 (w=10.5)	10.49	31.0	46.7			2208.3
				31.0	46.7	
S3/0% (w=2.9)	2.85	32.1	39.0			2183.9
	2.88	17.1	23.5	24.6	31.3	2059.6
S3/0% (w=5.0)	5.04	22.0	29.3			1897.0
	4.9	31.6	45.1	26.8	37.2	1959.3
S3/0% (w=6.9)	6.65	34.4	43.4			1879.9
	7.18	23.3	30.4	28.8	36.9	1923.6
S3/10% F1 (w=5.0)	5.01	33.7	45.3			2121.7
	5.04	38.2	52.5	36.0	48.9	2119.3
S3/10% F1 (w=7.3)	7.12	72.6	108.5			2310.0
	7.47	90.5	135.1	81.6	121.8	2244.4
S3/10% F1 (w=8.7)	9.21	27.7	47.4			1958.2
	8.26	27.2	57.0	27.5	52.2	2170.1
S3/5% F2 (w=3.2)	3.22	51.8	57.2			2064.8
	3.11	33.9	40.7	42.9	48.9	2039.6
S3/5% F2 (w=4.9)	4.85	59.2	69.9			2099.2
	4.85	46.4	60.6	52.8	65.2	2150.3
S3/5% F2 (w=7.1)	6.89	63.8	80.7			2175.3
	7.27	44.5	60.2	54.2	70.4	2163.2
S3/5% F2 (w=9.8)	9.69	33.7	47.3			2050.0
	9.87	29.2	39.2	31.4	43.2	2124.7
S3/10% F2 (w=3.3)	3.38	24.5	29.5			2019.8
	3.26	30.2	35.1	27.3	32.3	2028.7
S3/10% F2 (w=5.5)	5.43	37.8	47.6			2065.7
	5.5	34.0	45.9	35.9	46.7	1975.1
S3/10% F2 (w=7.3)	7.15	48.5	64.7			2198.7
	7.35	55.4	74.7	52.0	69.7	2218.0
S3/10% F2 (w=10.1)	9.93	43.4	57.2			2213.2
	10.2	32.2	46.8	37.8	52.0	2223.4

* 0.1 inch = 2.5 mm; $\bar{x}$ = Average
0.2 inch = 5 mm

Table B.4 Source 4 CBR and dry density results

List	*w (%)*	CBR (0.1)*	CBR (0.2)*	$\bar{x}$* (0.1)	$\bar{x}$* (0.2)	ρ_{dmax} (kg/m^3)
S4/4.1% F1 (w=4.4)	4.38	65.0	65.2			2101.1
	4.45	68.3	69.5	66.7	67.4	2130.6
S4/4.1% F1 (w=6.3)	6.23	81.2	88.4			2107.5
	6.27	70.6	80.2	75.9	84.3	2168.9
S4/4.1% F1 (w=8.3)	8.19	39.7	48.1			2149.8
	8.37	35.1	47.2	37.4	47.6	2187.7
S4/0% (w=3.2)	2.94	34.6	37.5			1965.2
	3.37	35.9	39.6	35.3	38.5	1977.0
S4/0% (w=4.9)	4.85	34.2	39.2			1981.5
	4.85	41.2	44.3	37.7	41.7	2007.2
S4/10% F1 (w=4.9)	4.66	73.6	77.6			2157.5
	5.17	86.6	99.5	80.1	88.6	2252.0
S4/10% F1 (w=8.6)	8.41	22.4	35.2			2250.3
	8.71	30.7	41.0	26.6	38.1	2284.0

* 0.1 inch = 2.5 mm; $\bar{x}$ = Average
0.2 inch = 5 mm

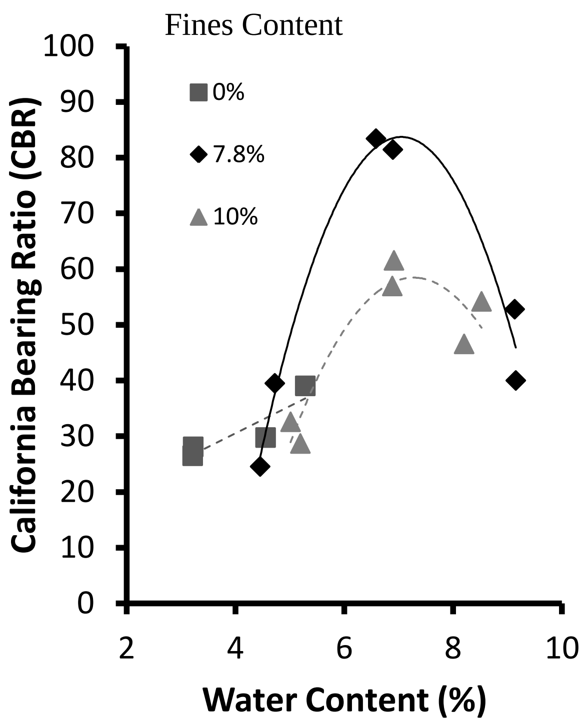

(a) Source 1

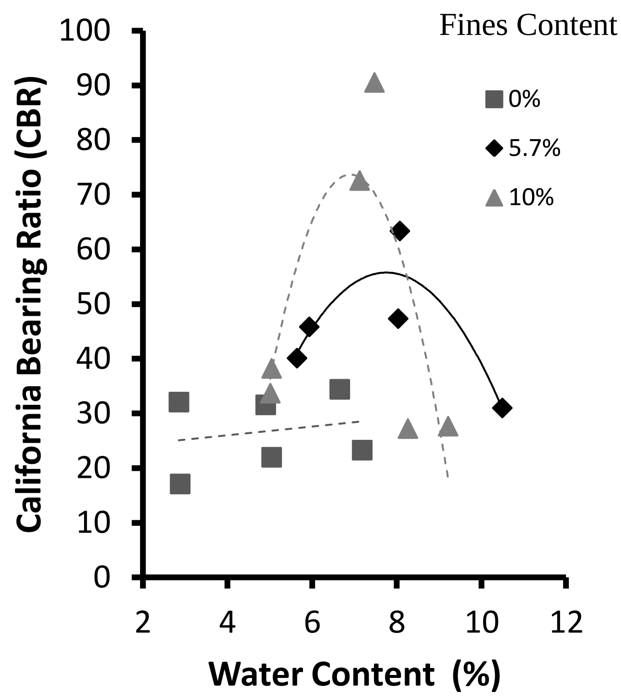

(c) Source 3

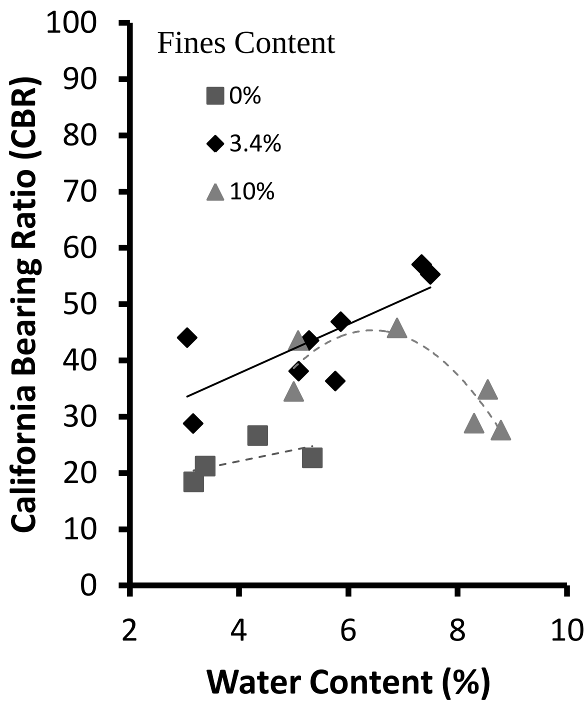

(b) Source 2

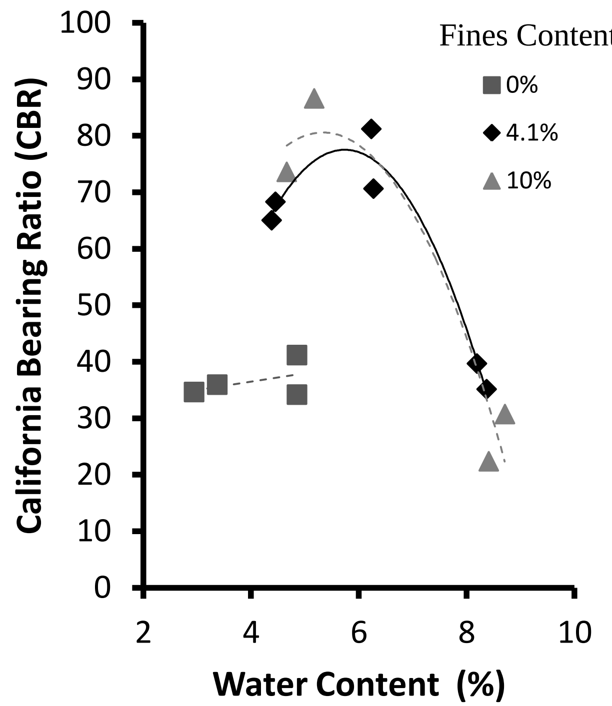

(d) Source 4

Figure B.1 CBR (2.5 mm) vs. water content for various F1 fines

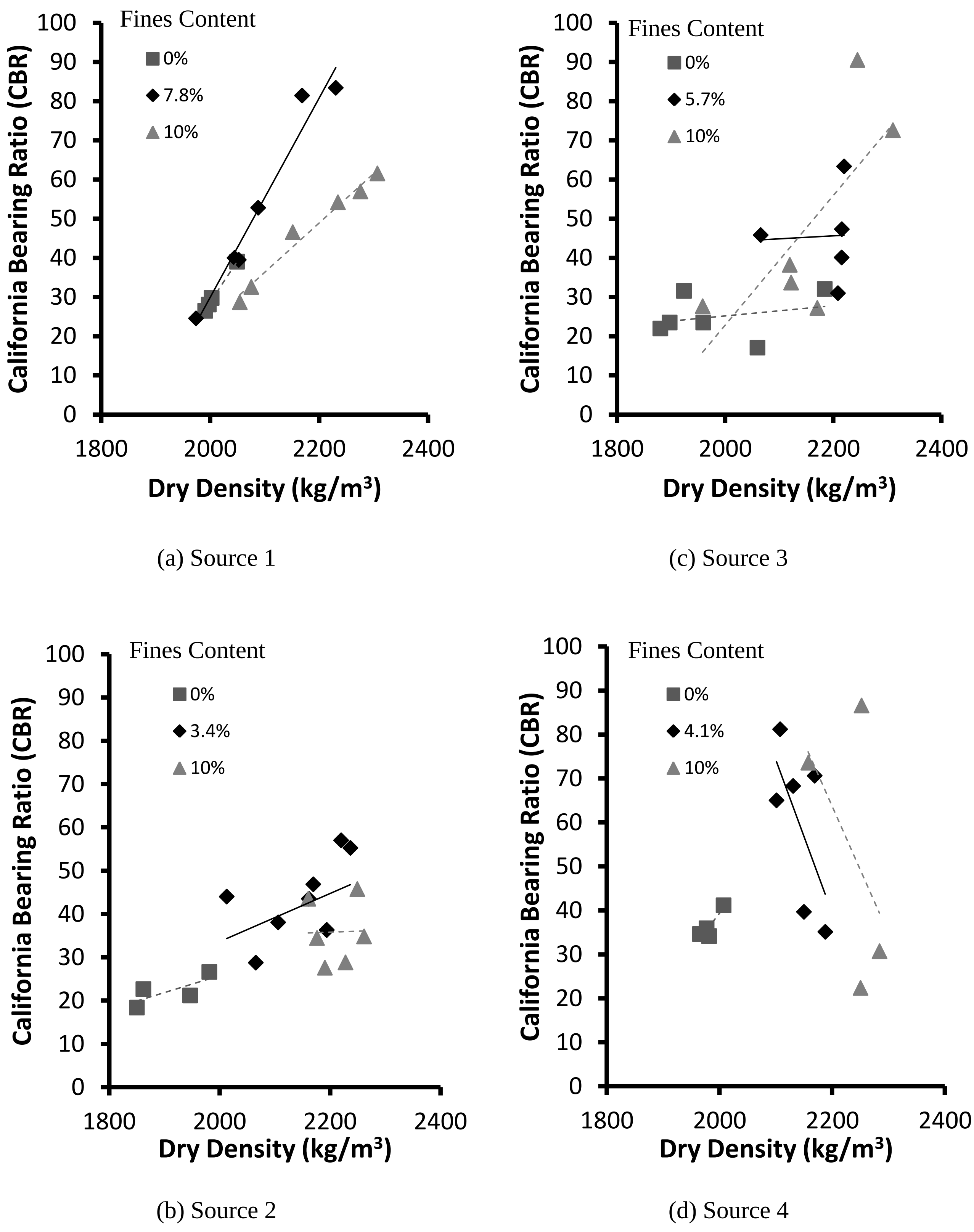

(a) Source 1

(c) Source 3

(b) Source 2

(d) Source 4

Figure B.2 CBR (2.5 mm) vs. dry density for various F1 fines contents and water contents

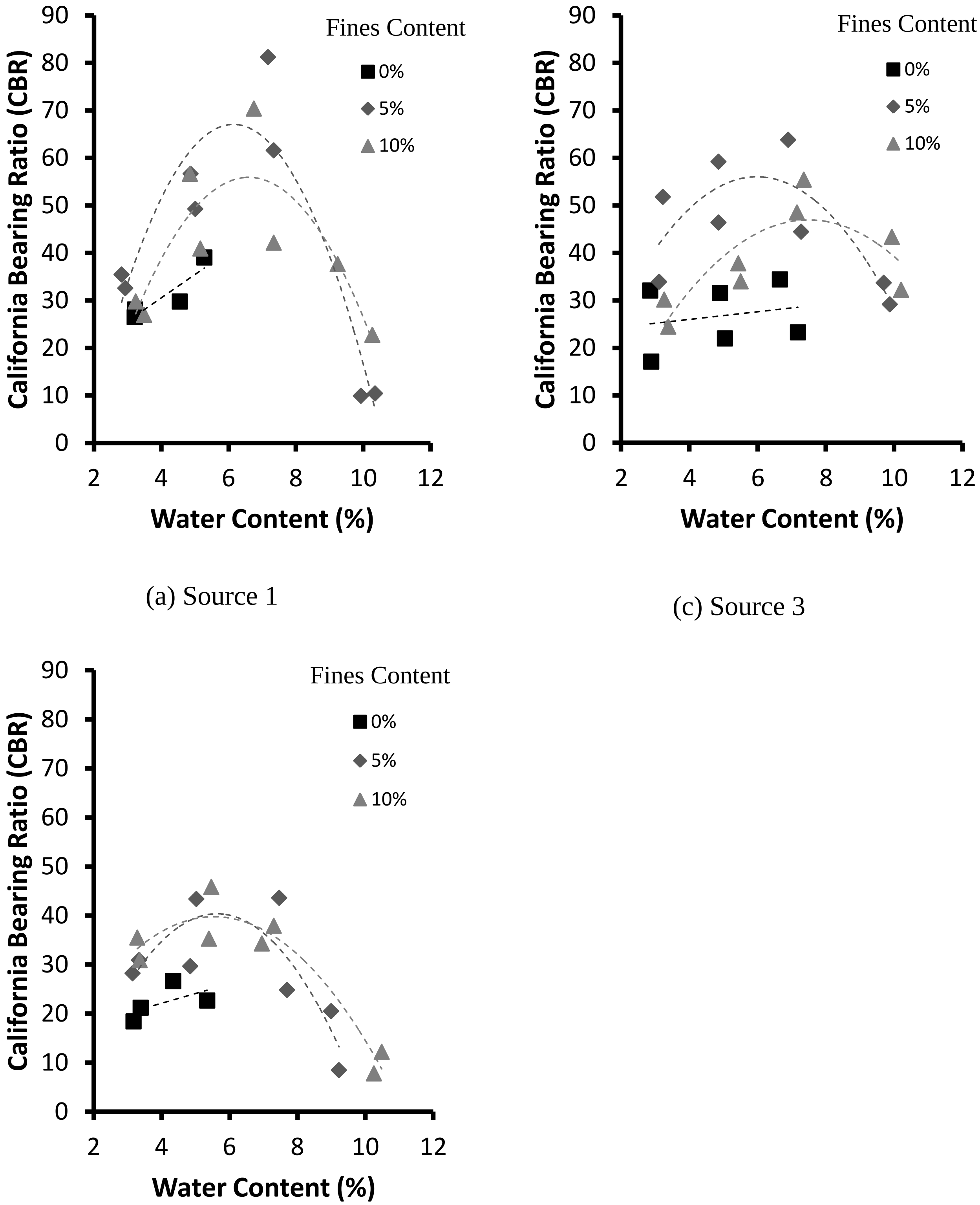

(a) Source 1

(c) Source 3

(b) Source 2

Figure B.3 CBR (2.5 mm) vs. water content for various F2 fines

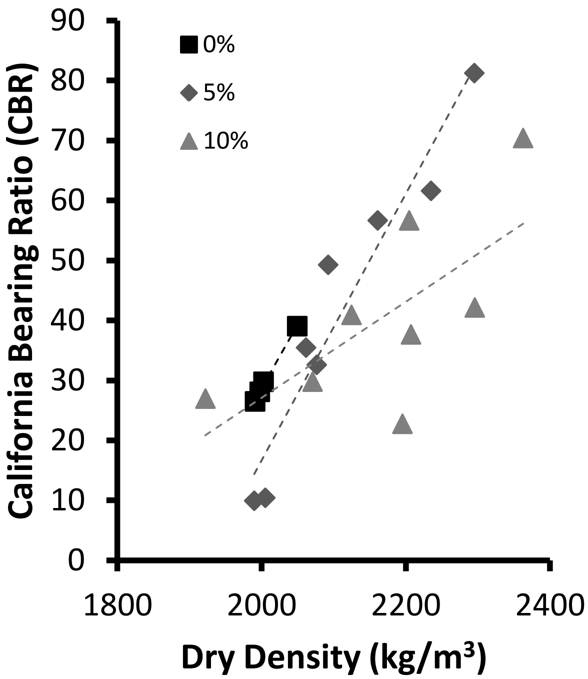

(a) Source 1

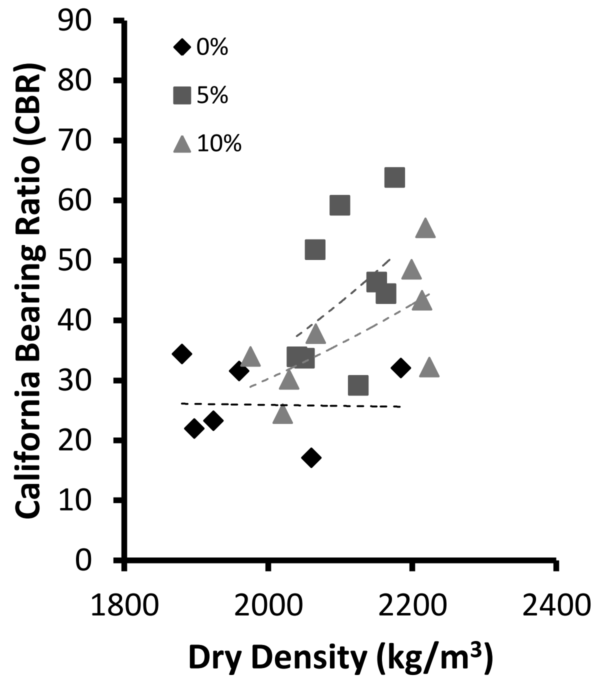

(c) Source 3

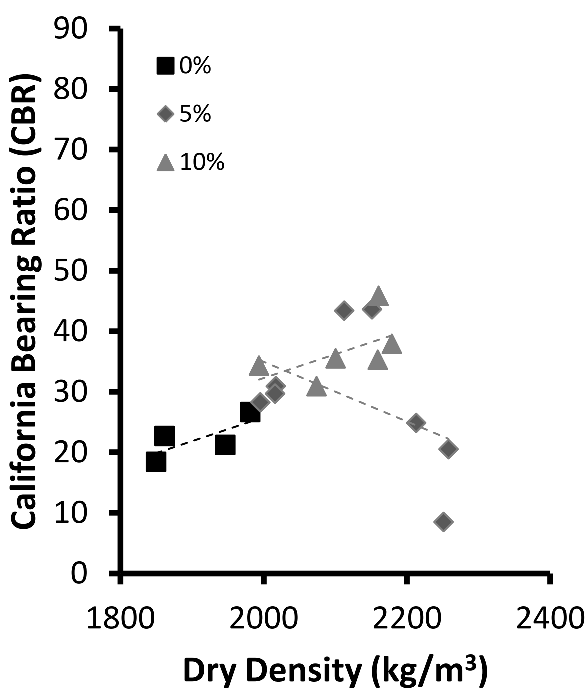

(b) Source 2

Figure B.4 CBR (2.5 mm) vs. dry density various F2 fines contents and water contents

Appendix C

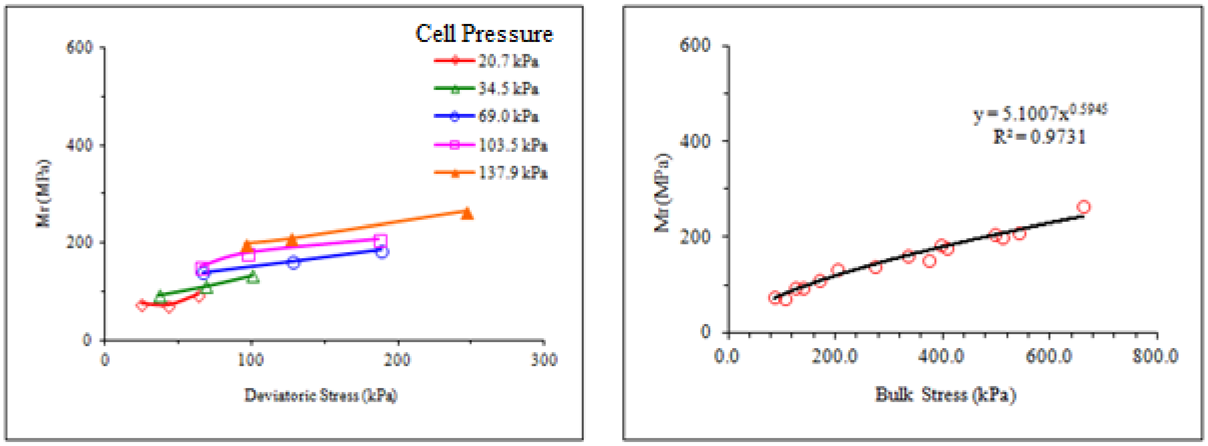

(1) Source 1 Natural Fines @ 4.6% moisture content

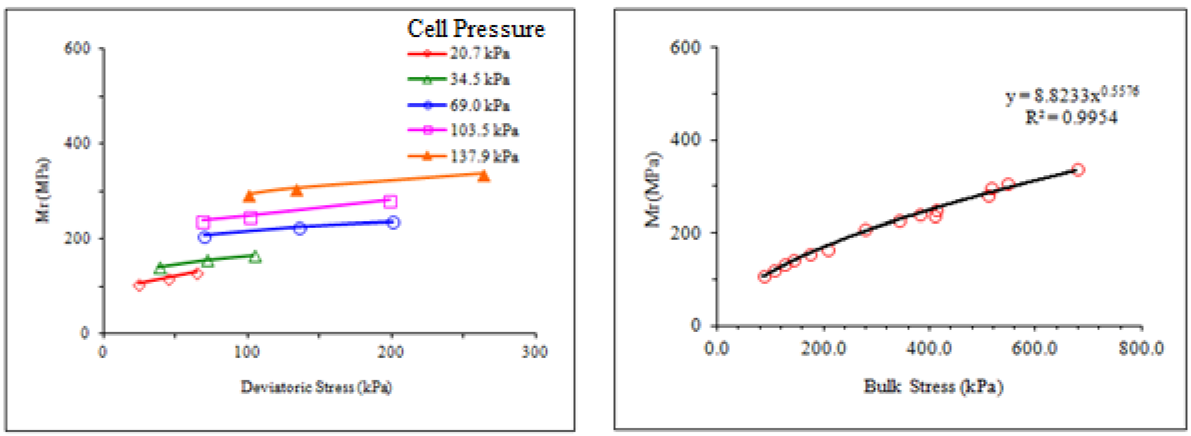

(2) Source 1 Natural Fines @ 6.6% moisture content

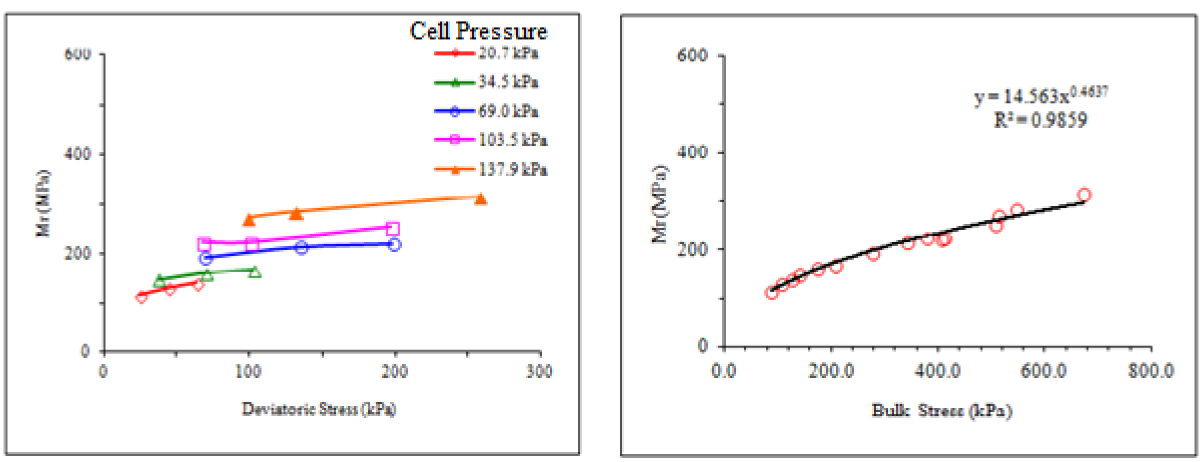

(3) Source 1 Natural Fines @ 8.6% moisture content

Figure C.1 Relationship of resilient modulus with deviatoric and bulk stresses

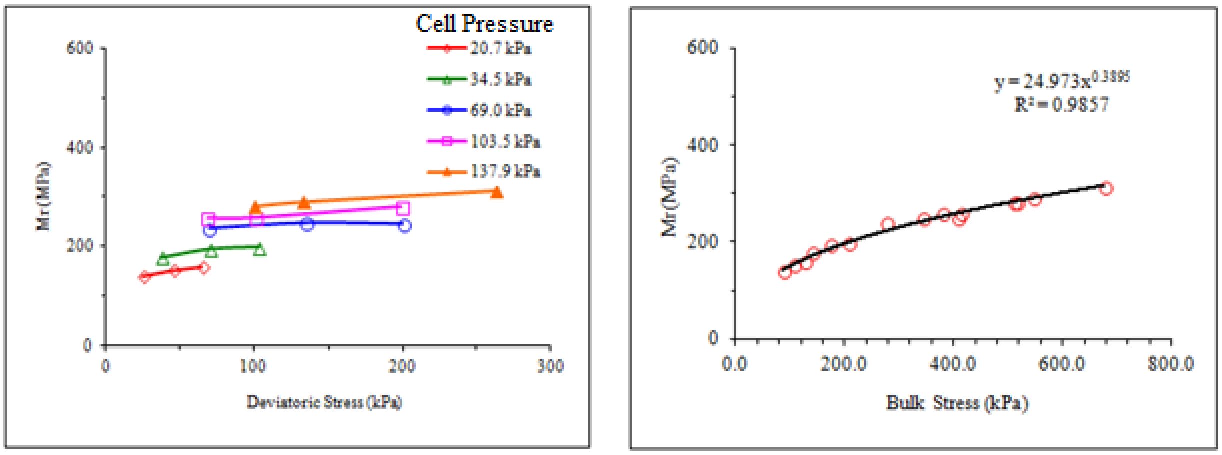

(4) Source 1 0% Fines @ 3% moisture content

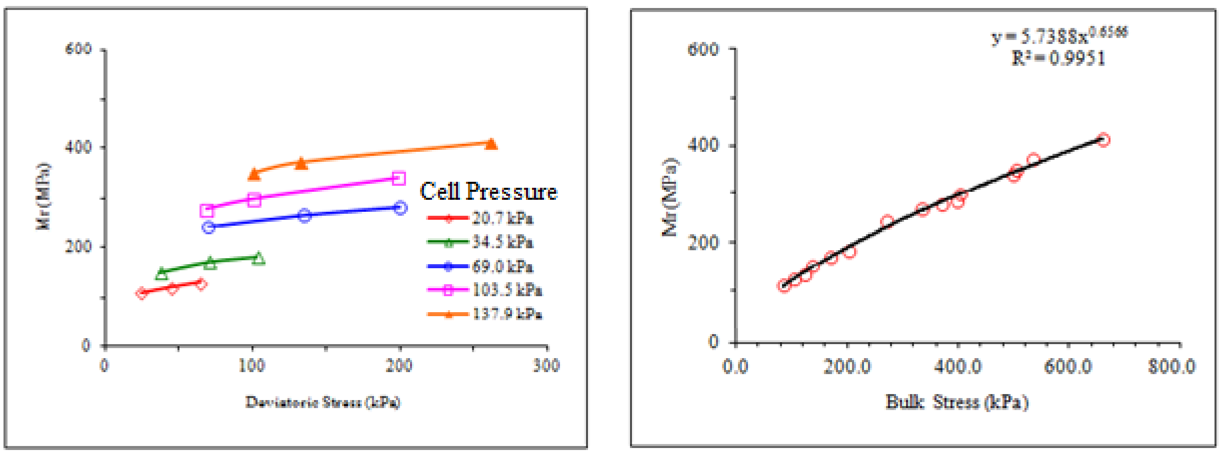

(5) Source 1 0% Fines @ 5% moisture content

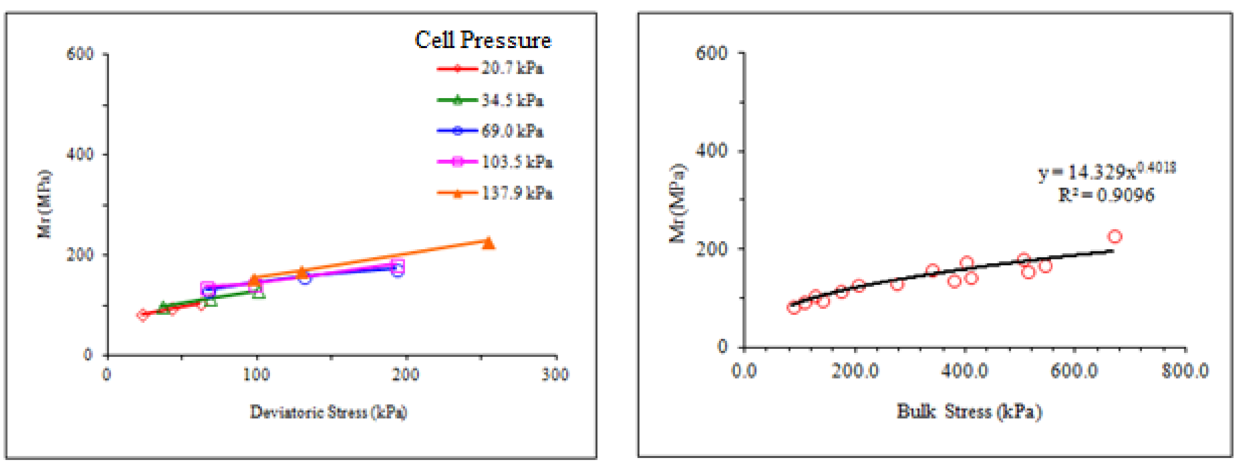

(6) Source 1 10% Natural Fines @ 5% moisture content

Figure C.1 Relationship of resilient modulus with deviatoric and bulk stresses (Cont'd)

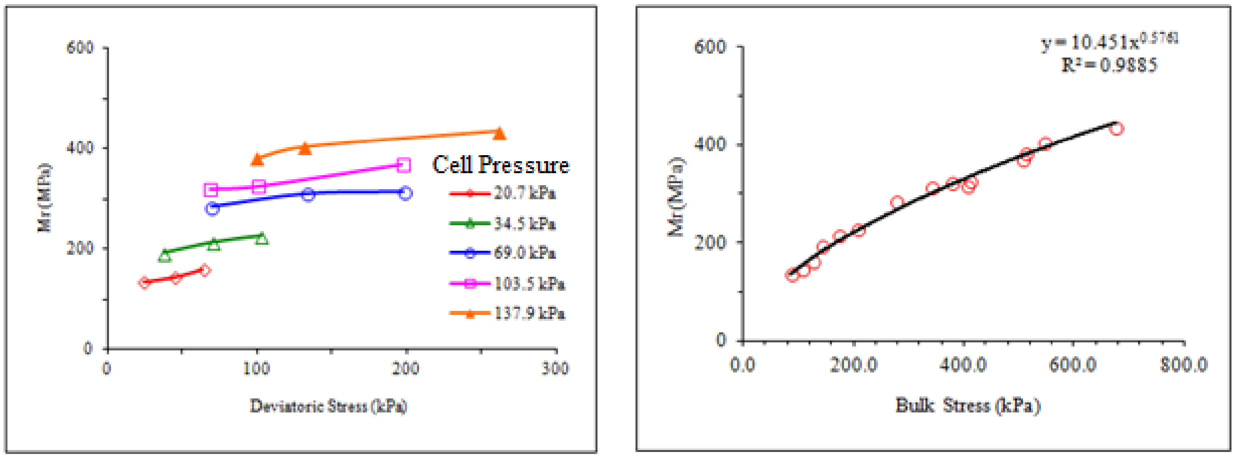

(7) Source 1 5% Substitute Fines @ 3% moisture content

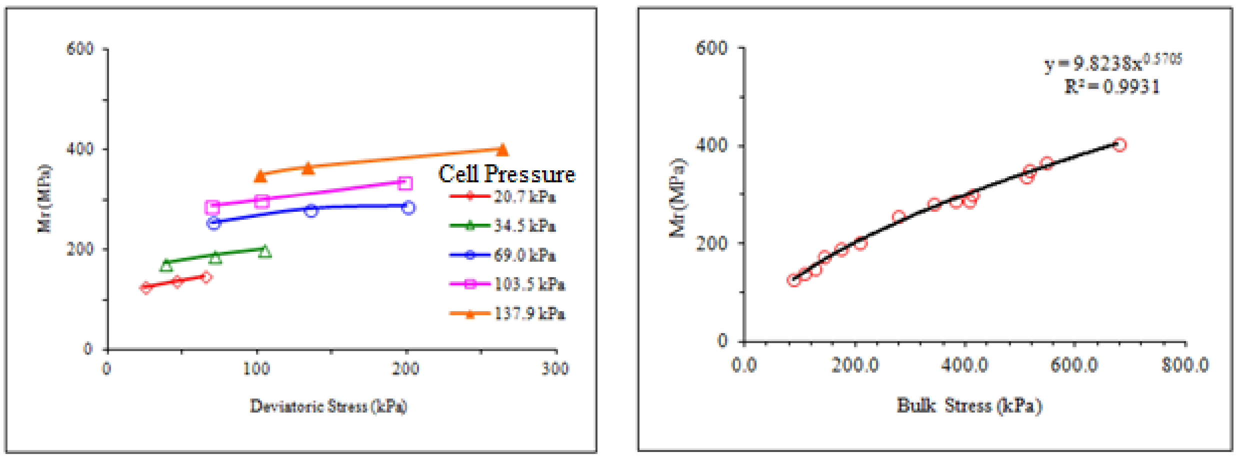

(8) Source 1 5% Substitute Fines @ 5% moisture content

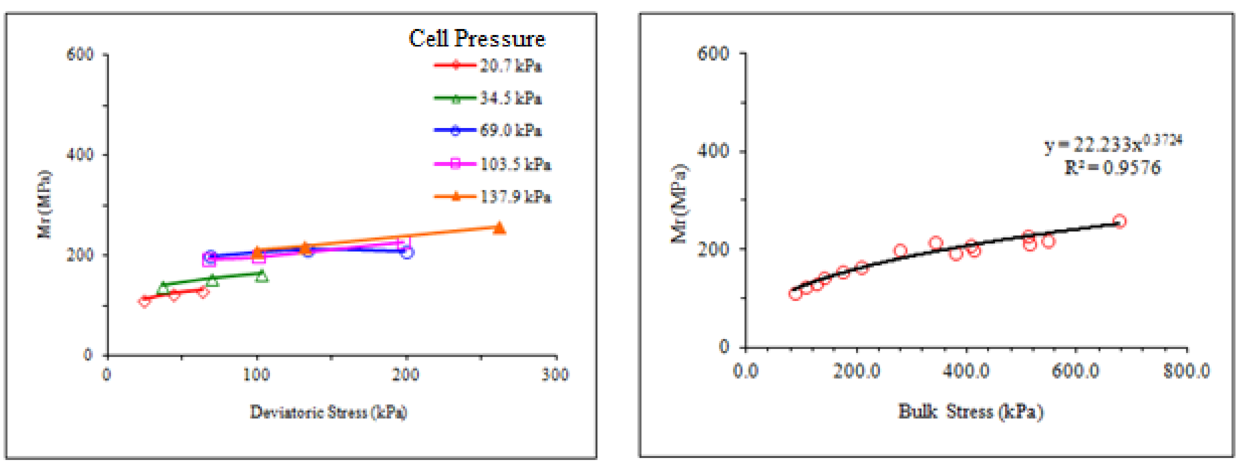

(9) Source 1 5% Substitute Fines @ 7% moisture content

Figure C.1 Relationship of resilient modulus with deviatoric and bulk stresses (Cont'd)

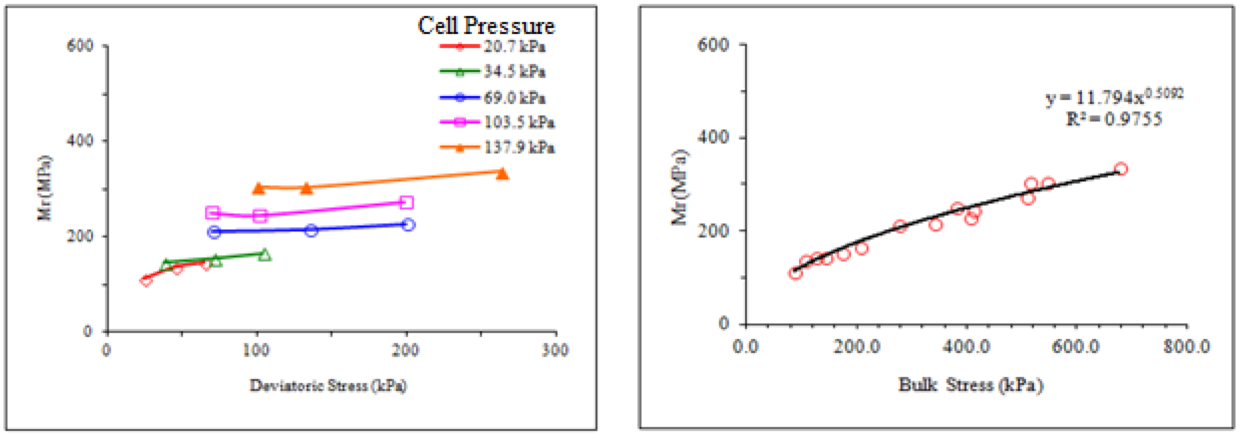

(10) Source 1 10% Substitute Fines @ 3% moisture content

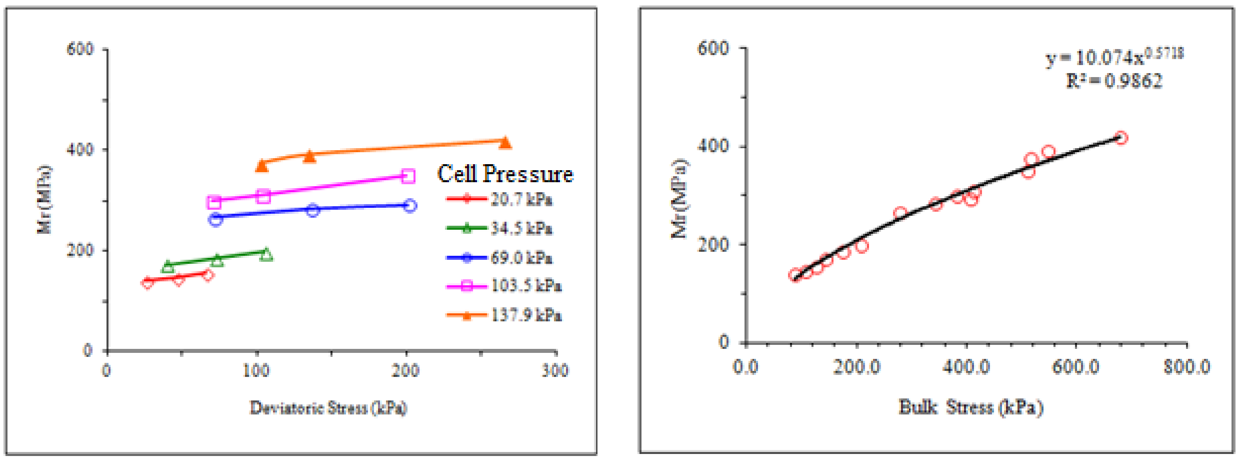

(11) Source 1 10% Substitute Fines @ 5% moisture content

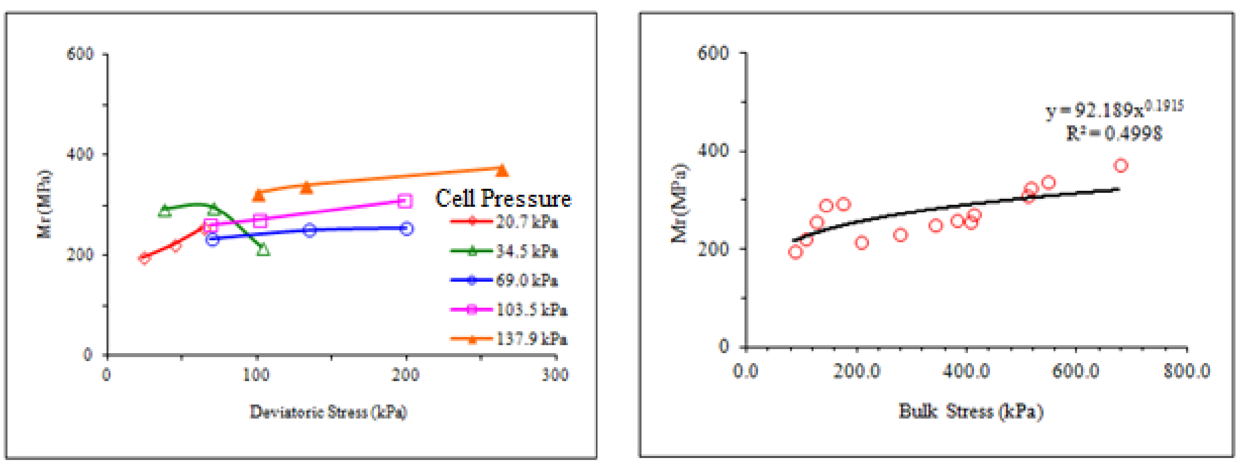

(12) Source 1 10% Substitute Fines @ 7% moisture content

Figure C.1 Relationship of resilient modulus with deviatoric and bulk stresses (Cont’d)

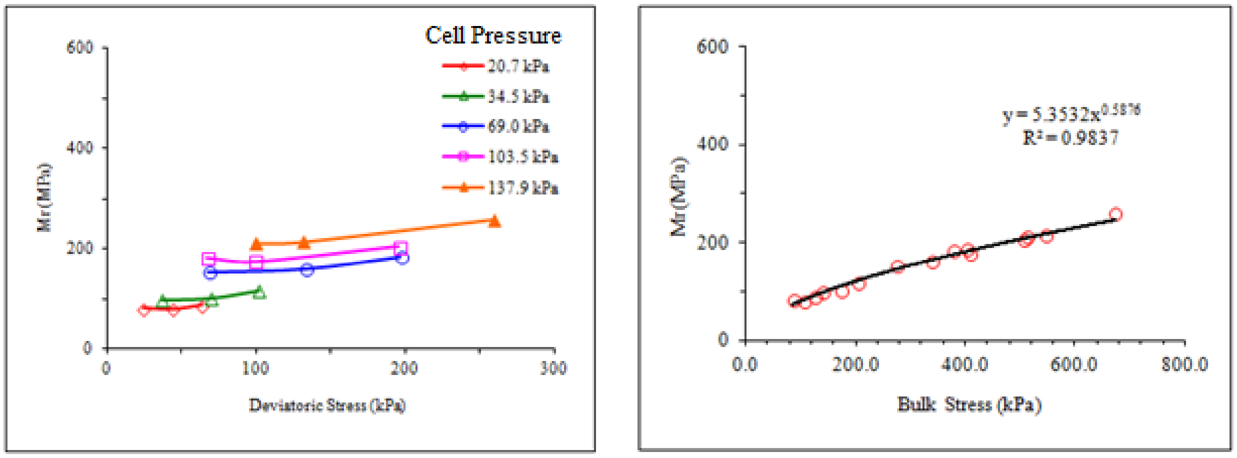

(13) Source 2 Natural Fines @ 2.9% moisture content

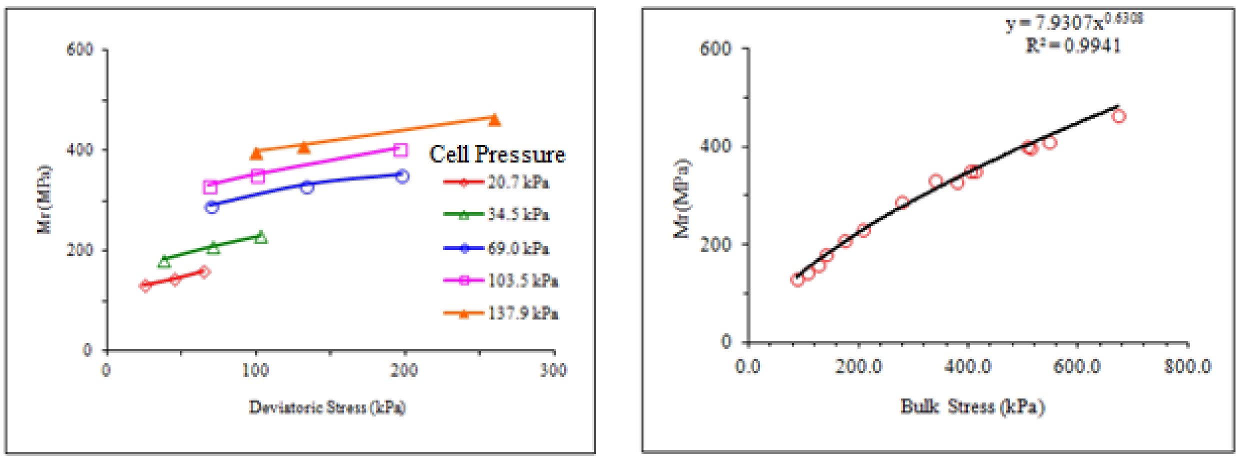

(14) Source 2 Natural Fines @4.9% moisture content

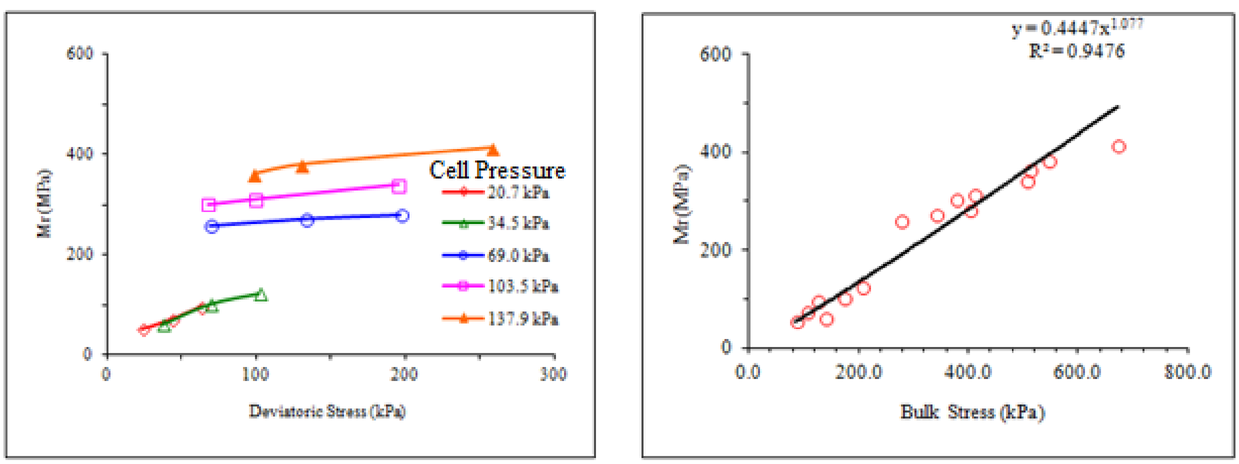

(15) Source 2 Natural Fines @ 6.9% moisture content

Figure C.1 Relationship of resilient modulus with deviatoric and bulk stresses (Cont'd)

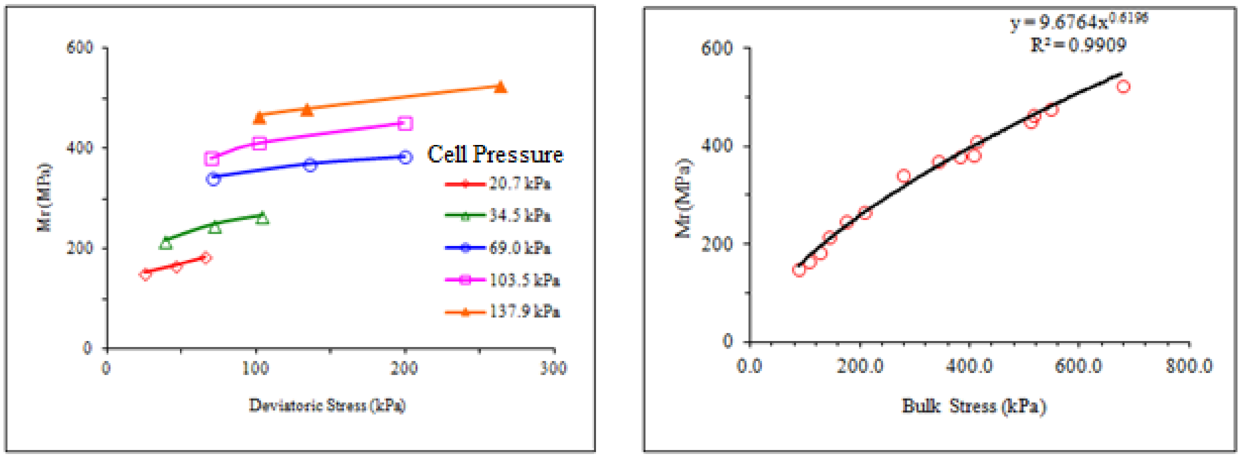

(16) Source 2 0% Fines @ 3% moisture content

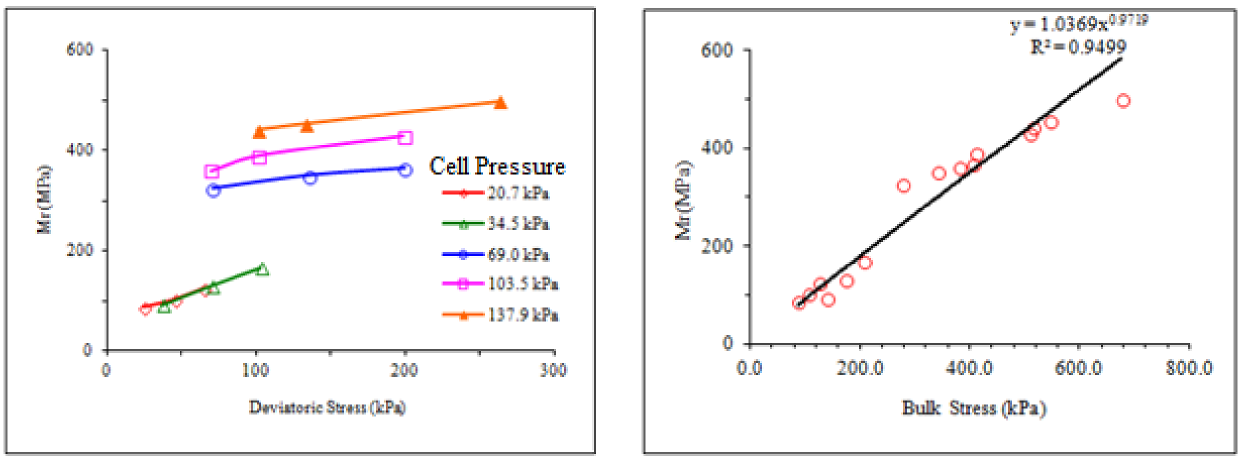

(17) Source 2 0% Fines @ 5% moisture content

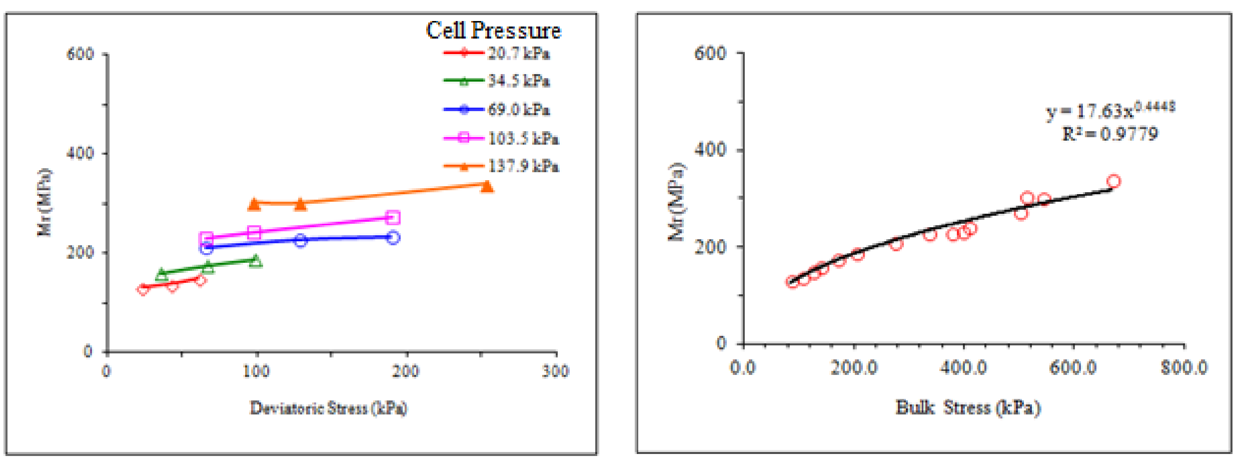

(18) Source 2 10% Natural Fines @ 5% moisture content

Figure C.1 Relationship of resilient modulus with deviatoric and bulk stresses (Cont'd)

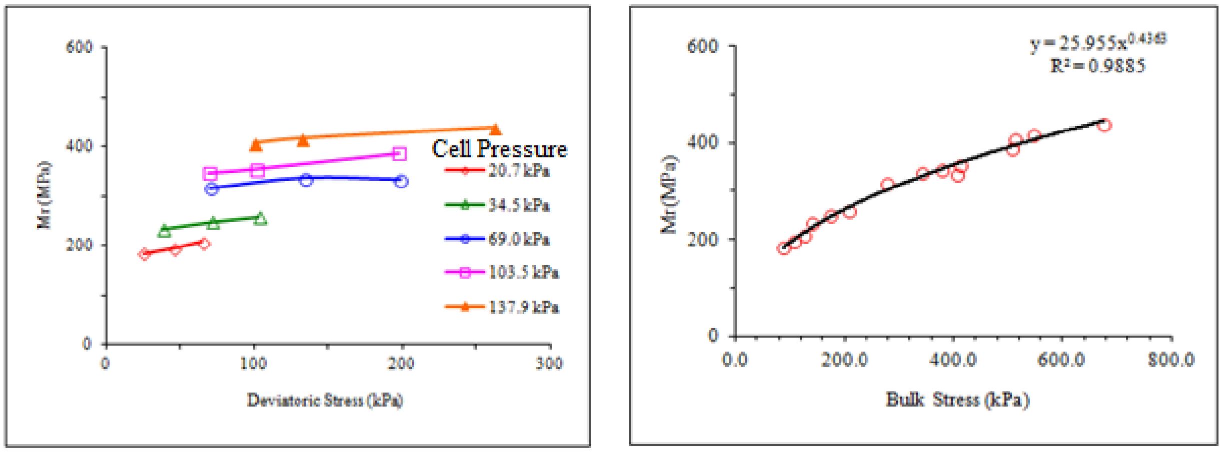

(19) Source 2 5% Substitute Fines @ 3% moisture content

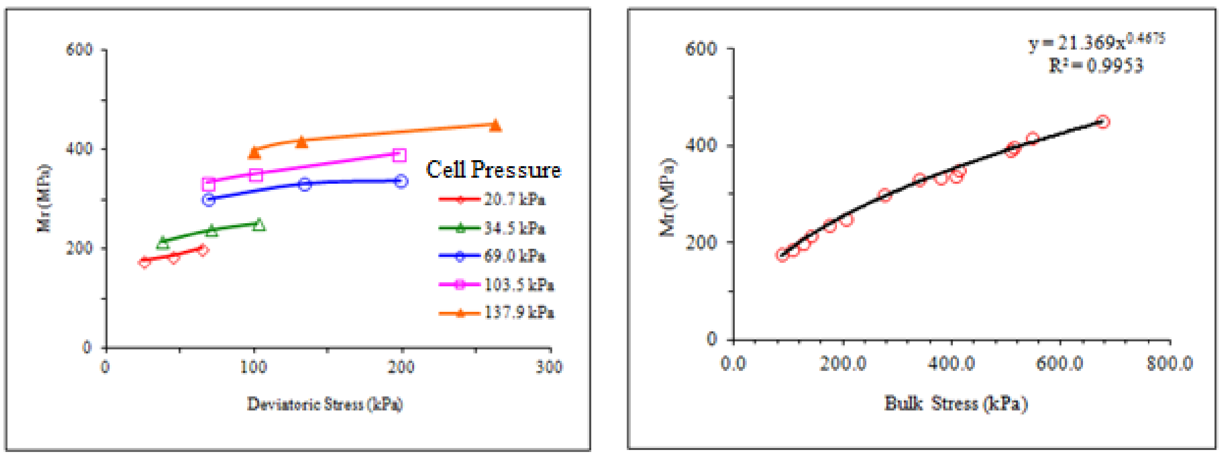

(20) Source 2 5% Substitute Fines @ 5% moisture content

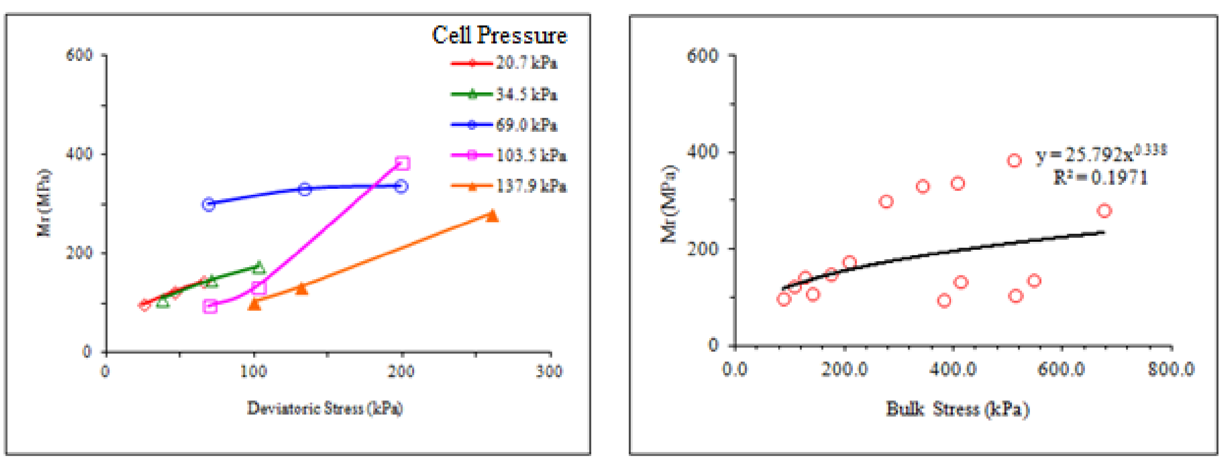

(21) Source 2 5% Substitute Fines @ 7% moisture content

Figure C.1 Relationship of resilient modulus with deviatoric and bulk stresses (Cont'd)

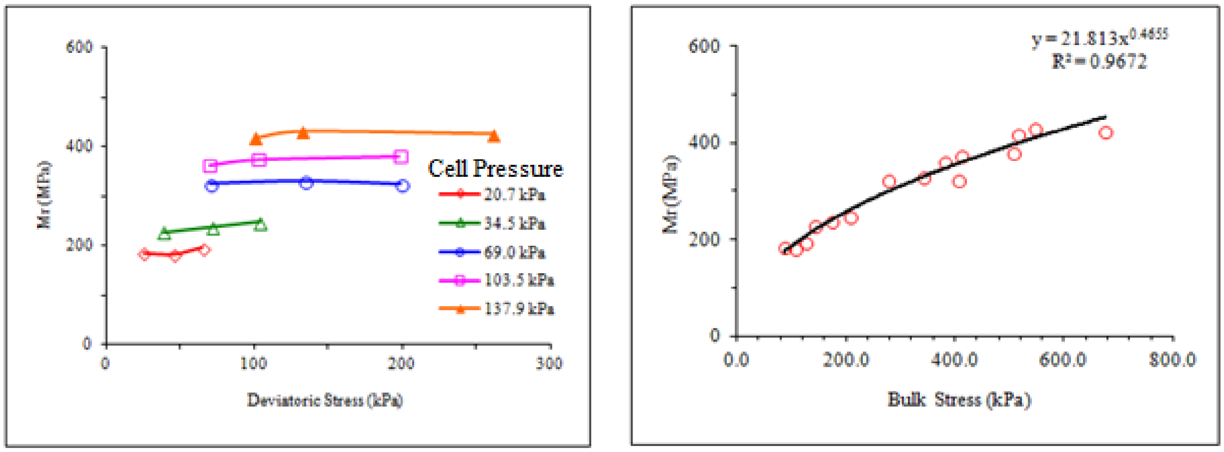

(22) Source 2 10% Substitute Fines @ 3% moisture content

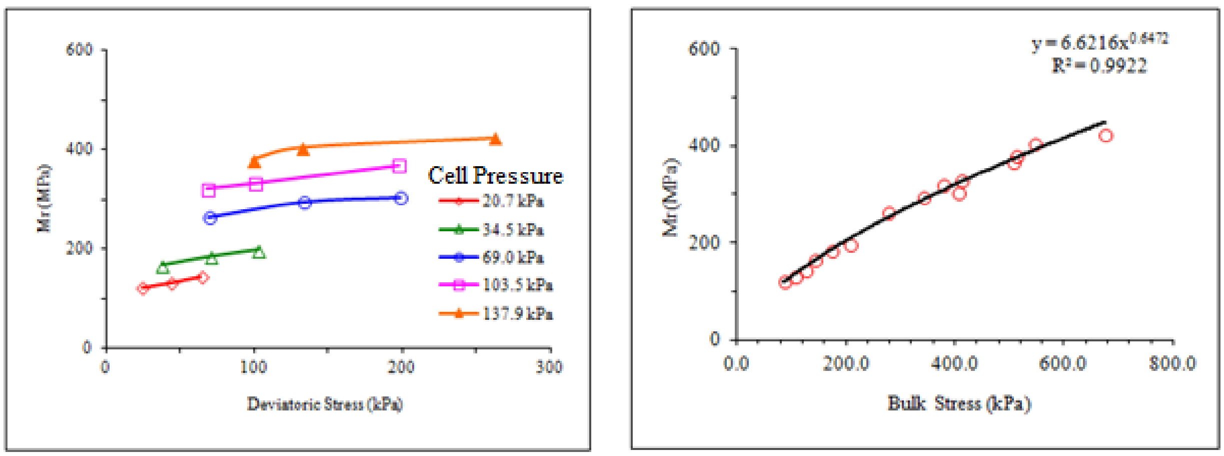

(23) Source 2 10% Substitute Fines @5% moisture content

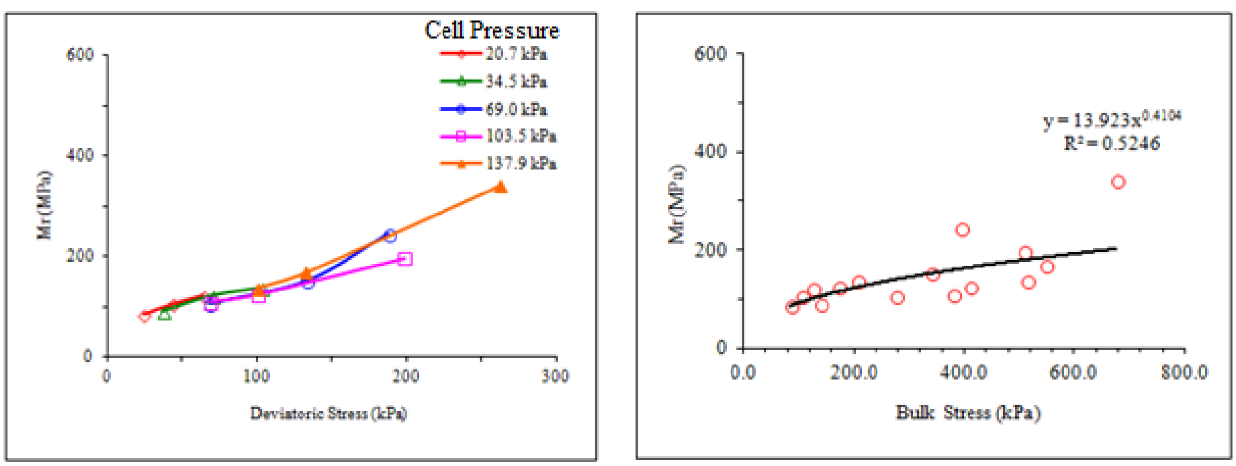

(24) Source 2 10% Substitute Fines @ 7% moisture content

Figure C.1 Relationship of resilient modulus with deviatoric and bulk stresses (Cont'd)

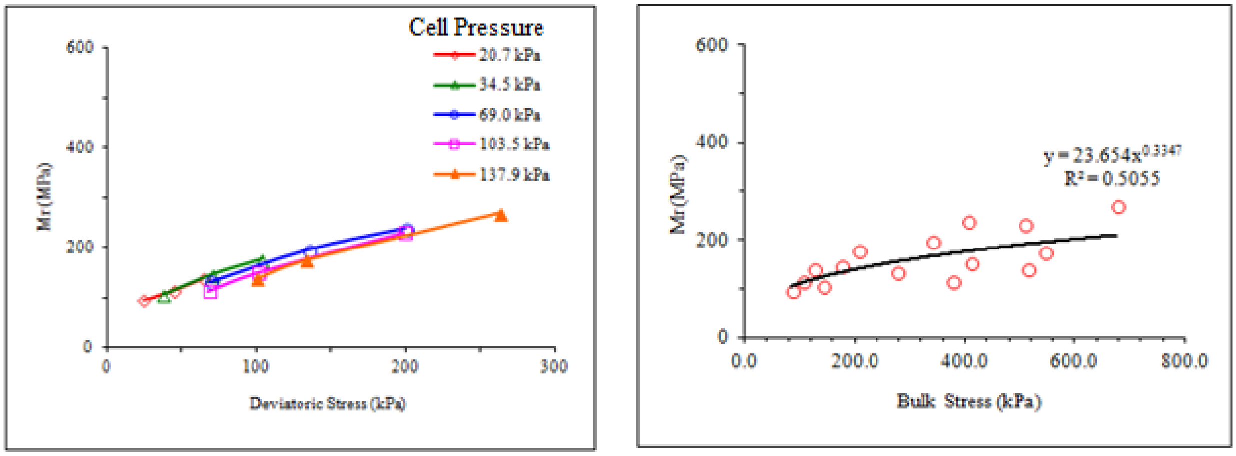

(25) Source 3 Natural Fines @ 5.95% moisture content

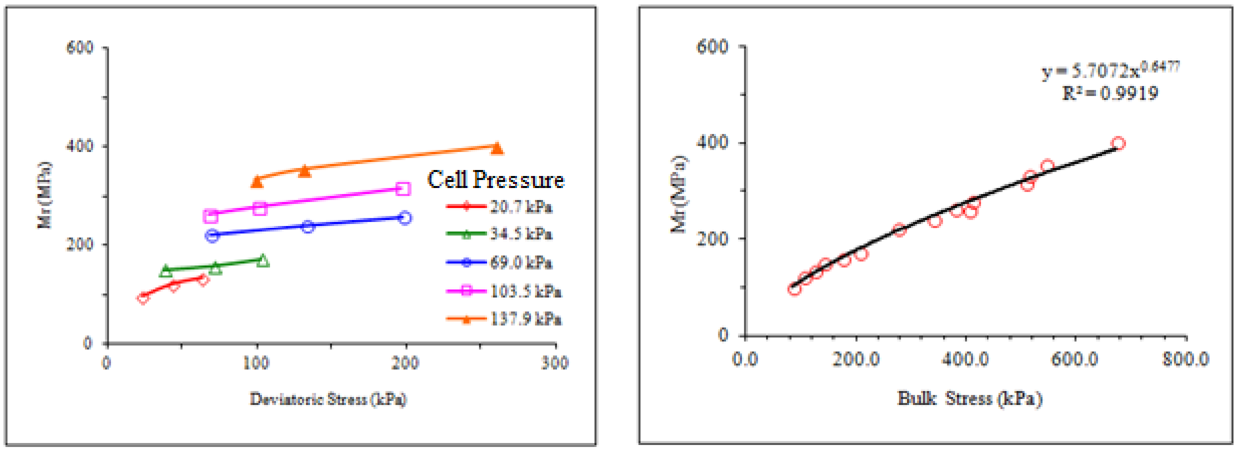

(26) Source 3 Natural Fines @ 7.95% moisture content

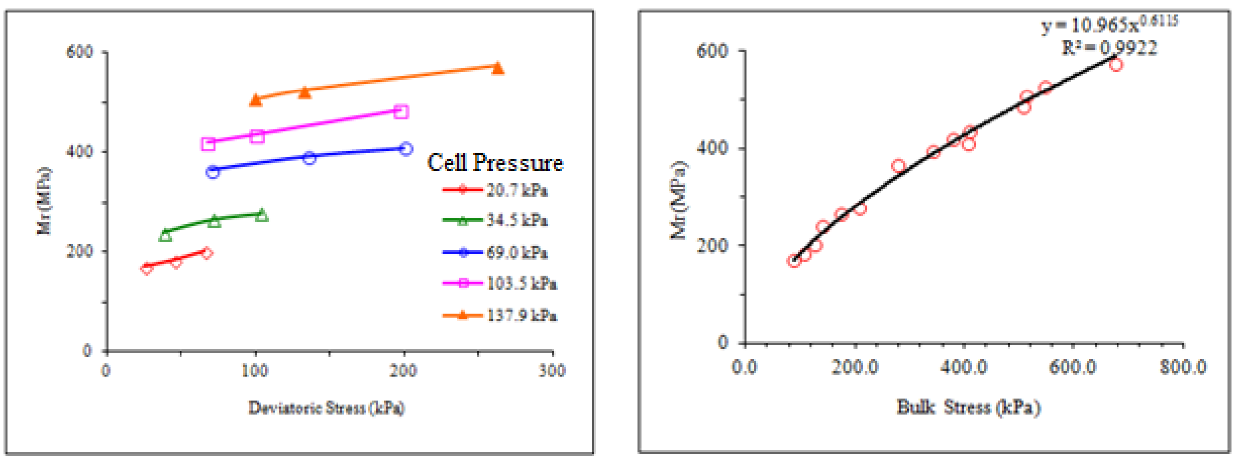

(27) Source 3 0% Fines @ 3% moisture content

Figure C.1 Relationship of resilient modulus with deviatoric and bulk stresses (Cont'd)

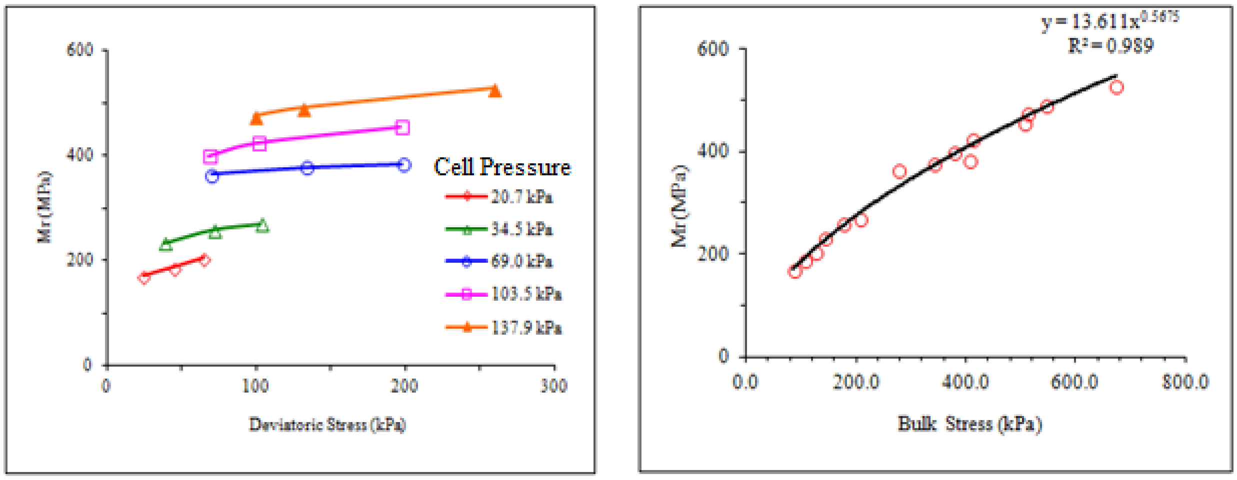

(28) Source 3 0% Fines @ 5% moisture content

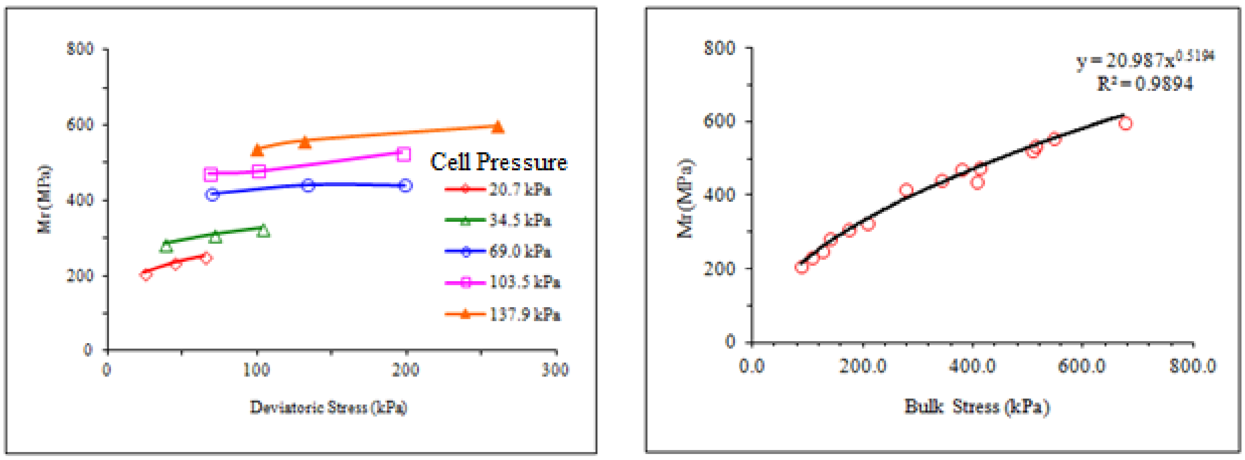

(29) Source 3 0% Fines @ 7% moisture content

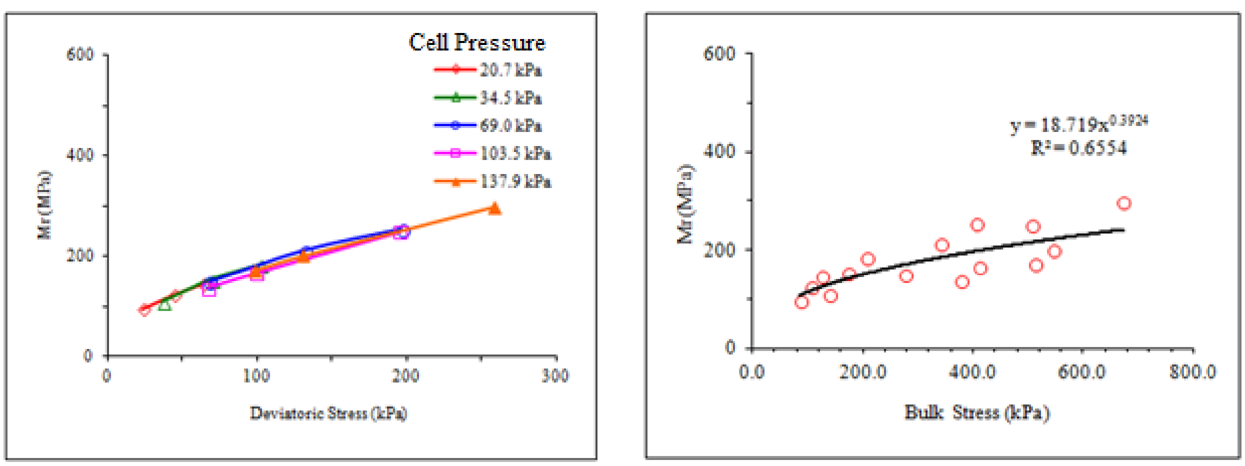

(30) Source 3 10% Natural Fines @ 5% moisture content

Figure C.1 Relationship of resilient modulus with deviatoric and bulk stresses (Cont'd)

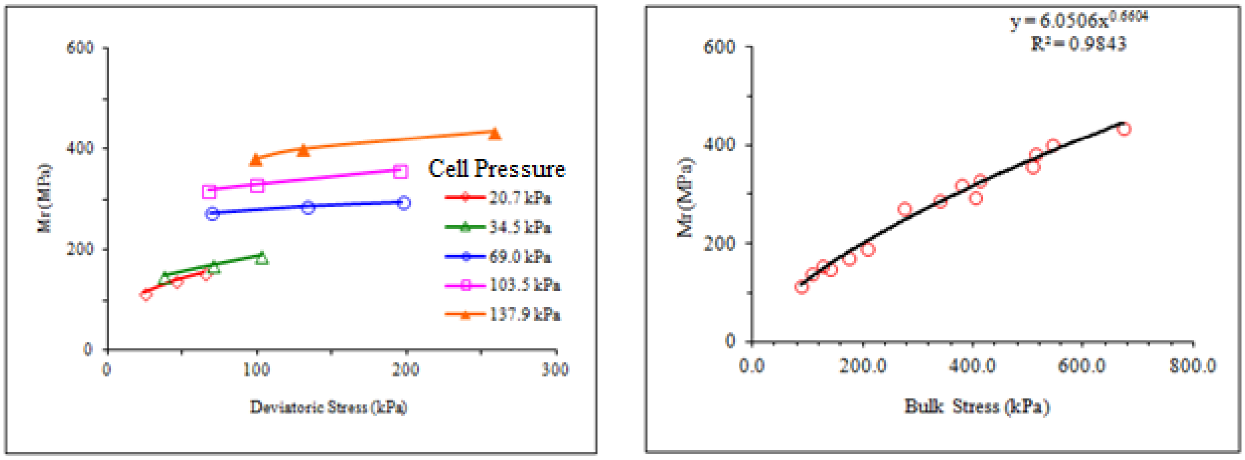

(31) Source 3 10% Natural Fines @ 8% moisture content

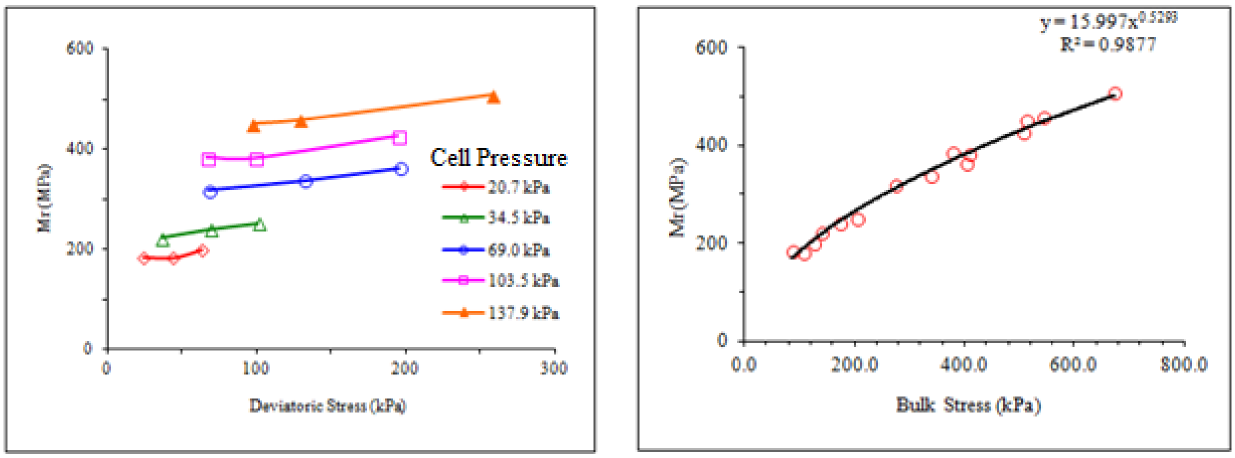

(32) Source 3 5% Substitute Fines @ 3% moisture content

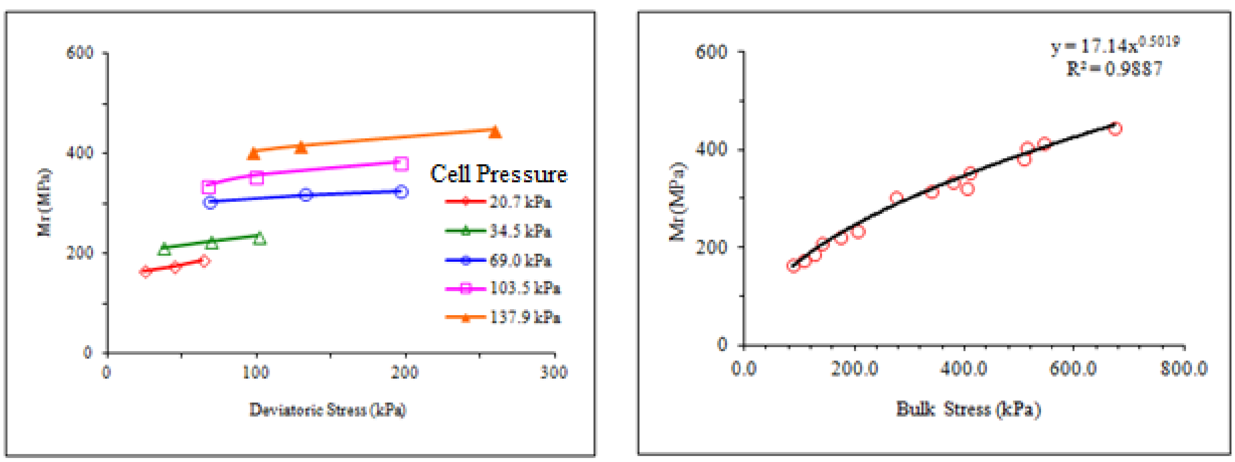

(33) Source 3 5% Substitute Fines @ 5% moisture content

Figure C.1 Relationship of resilient modulus with deviatoric and bulk stresses (Cont'd)

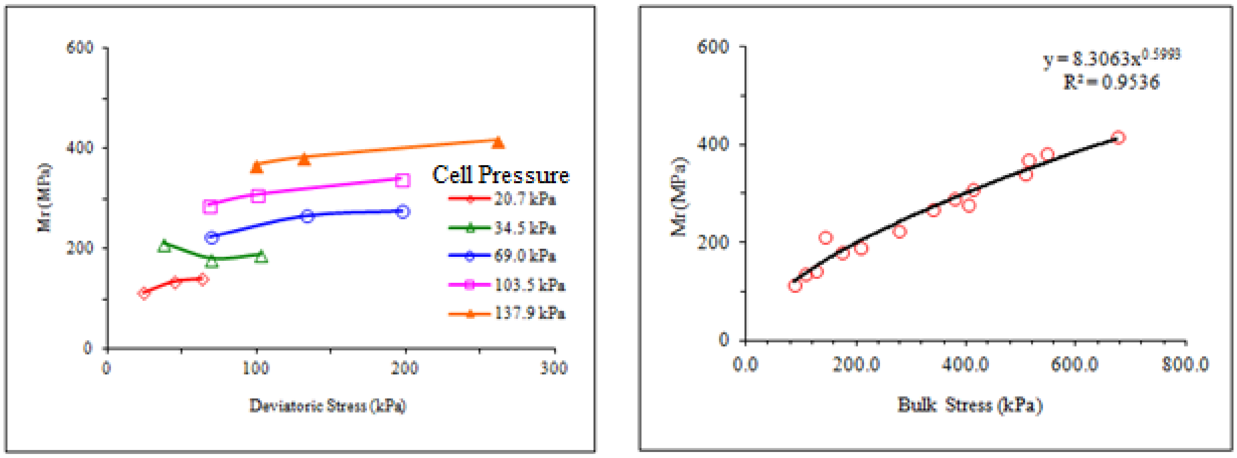

(34) Source 3 5% Substitute Fines @ 7% moisture content

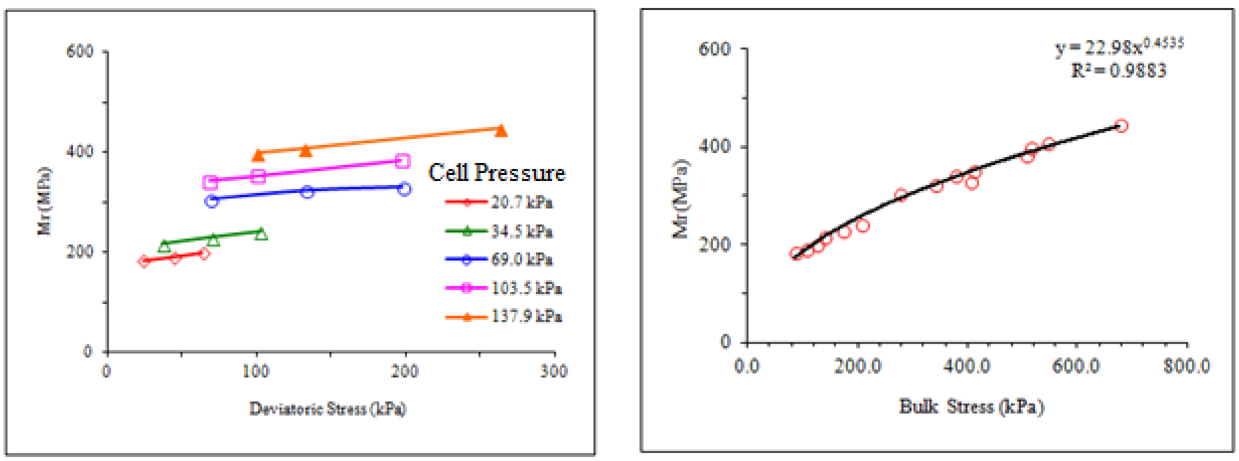

(35) Source 3 10% Substitute Fines @ 3% moisture content

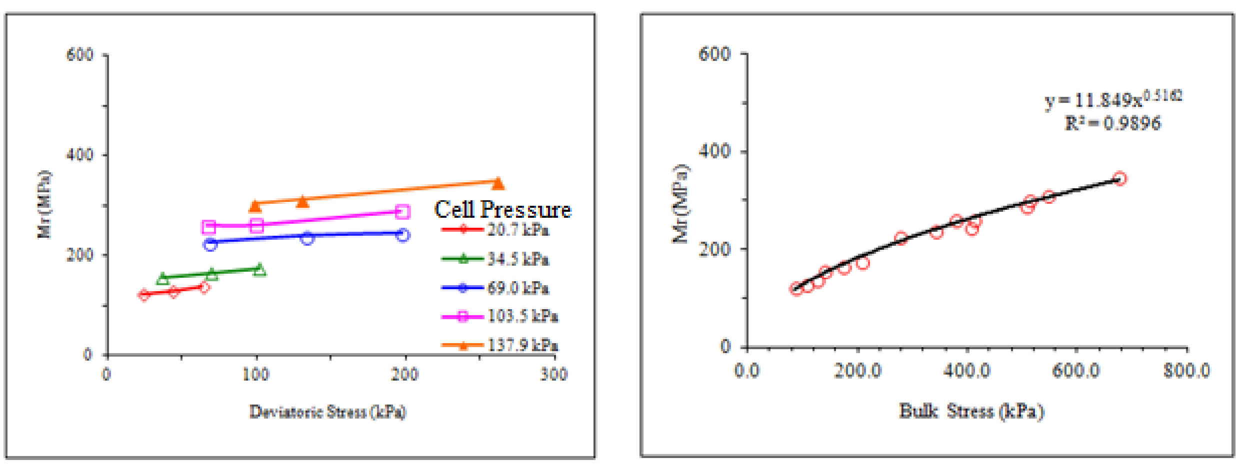

(36) Source 3 10% Substitute Fines @ 5% moisture content

Figure C.1 Relationship of resilient modulus with deviatoric and bulk stresses (Cont'd)

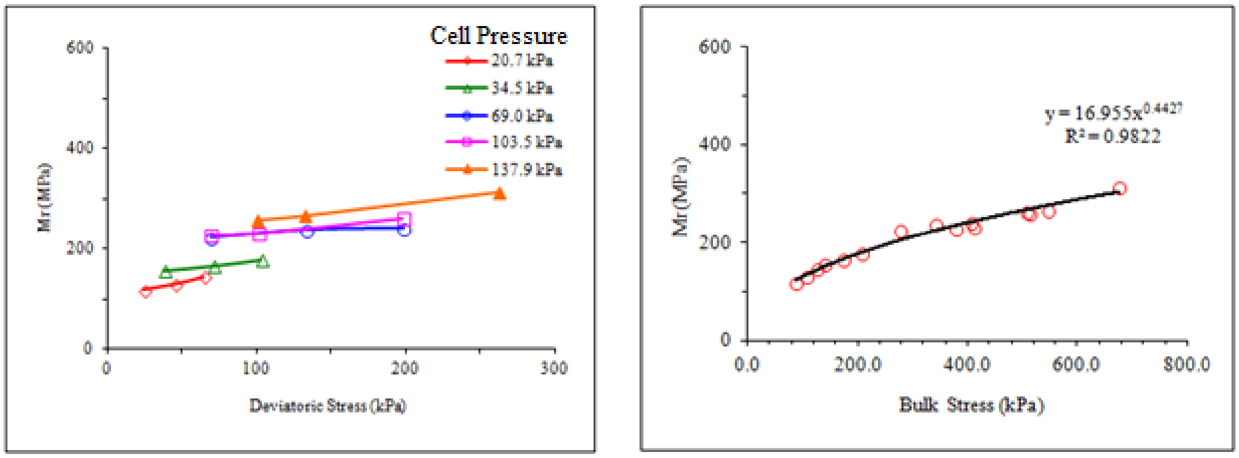

(37) Source 3 10% Substitute Fines @ 7% moisture content

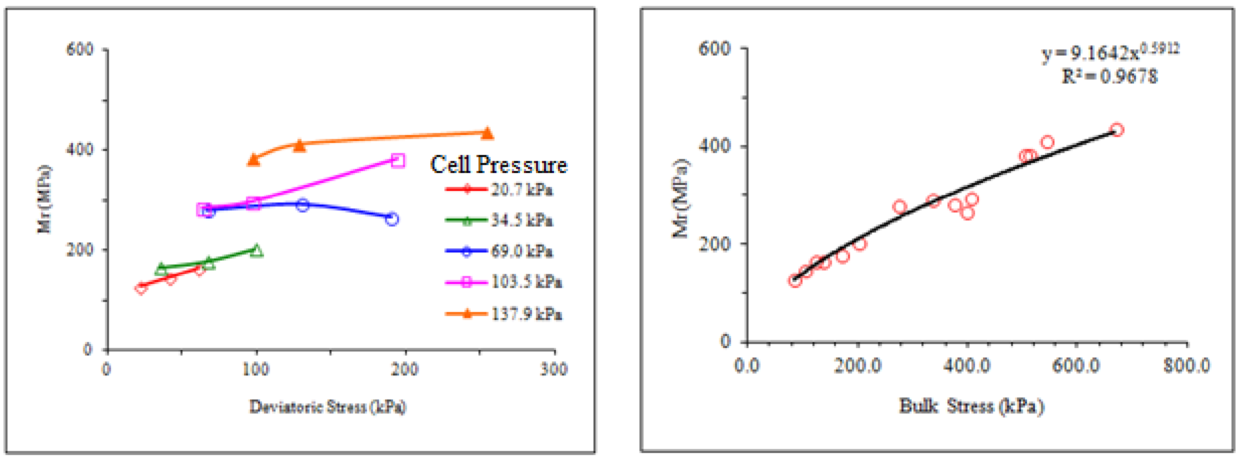

(38) Source 4 Natural Fines @ 4.3% moisture content

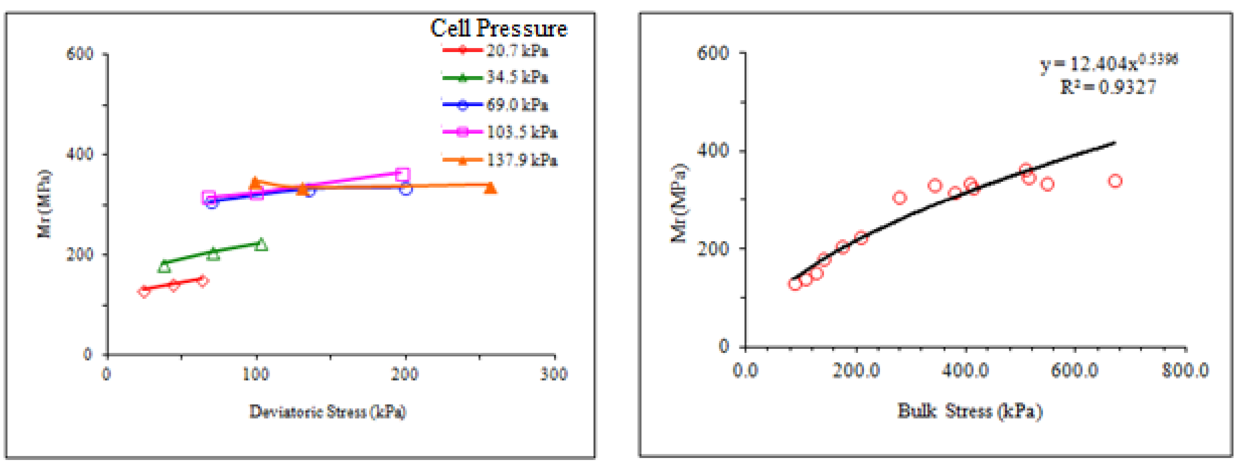

(39) Source 4 Natural Fines @ 6.3% moisture content

Figure C.1 Relationship of resilient modulus with deviatoric and bulk stresses (Cont'd)

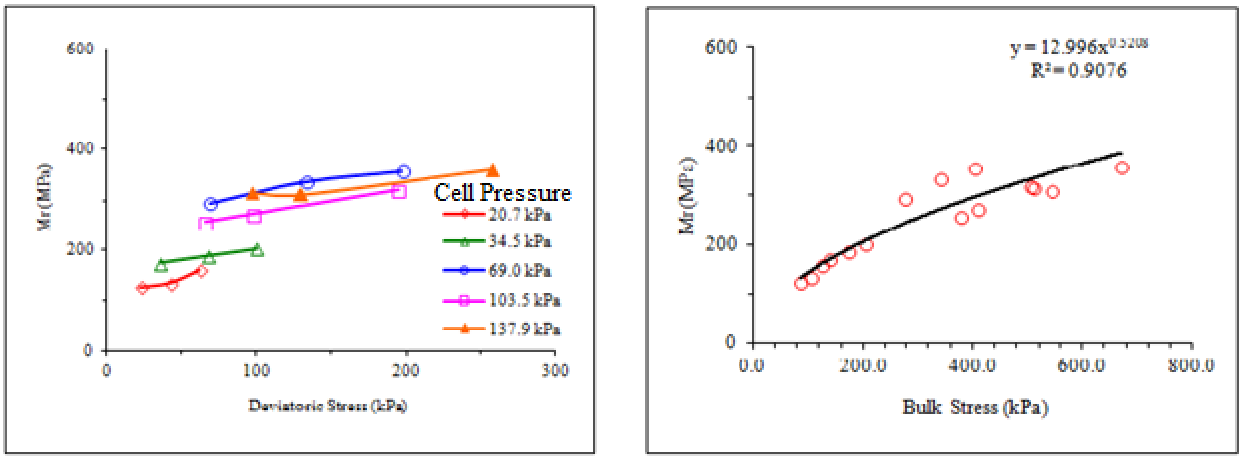

(40) Source 4 10% Natural Fines @ 5% moisture content

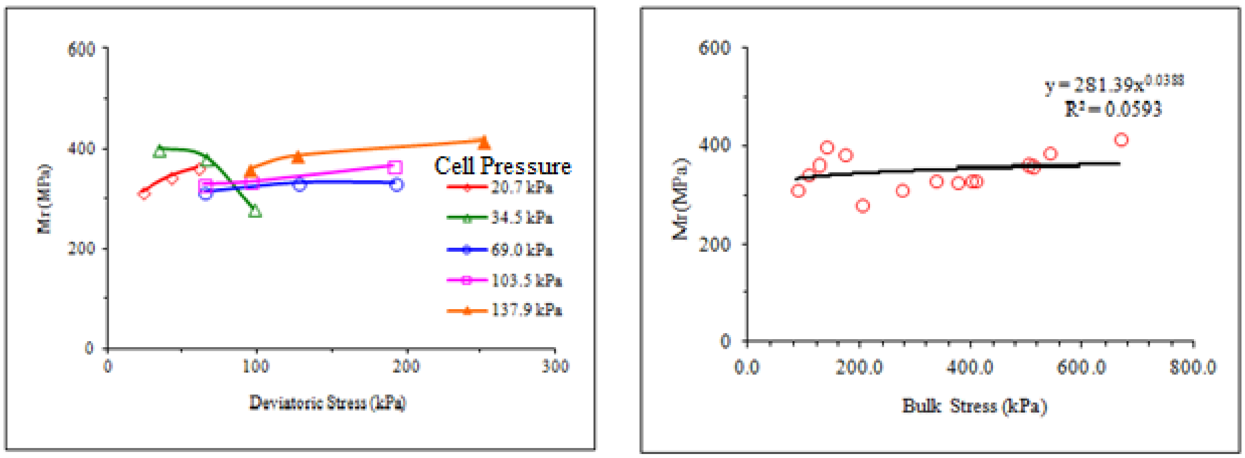

(41) Source 4 5% Substitute Fines @ 3% moisture content

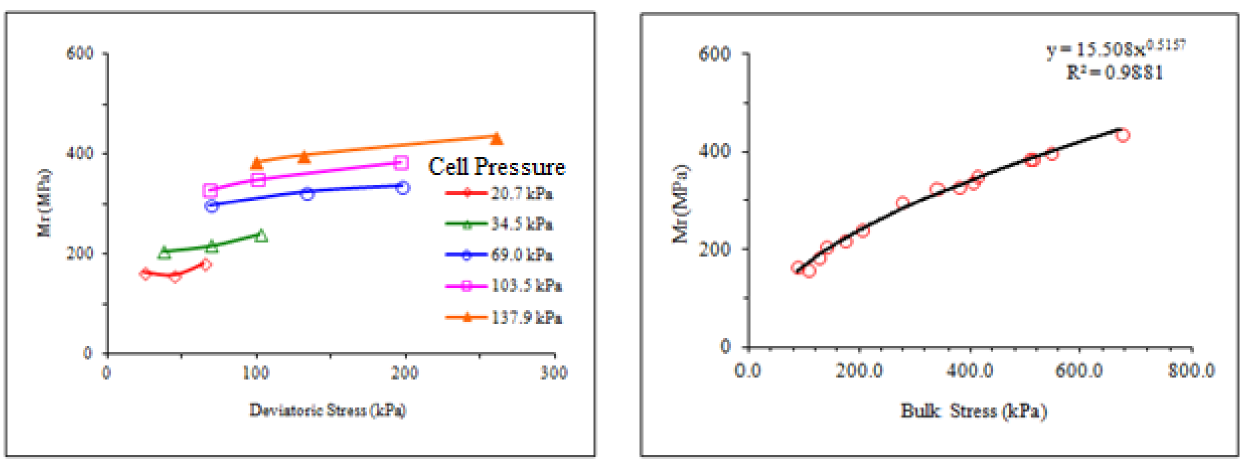

(42) Source 4 5% Substitute Fines @ 5% moisture content

Figure C.1 Relationship of resilient modulus with deviatoric and bulk stresses (Cont'd)

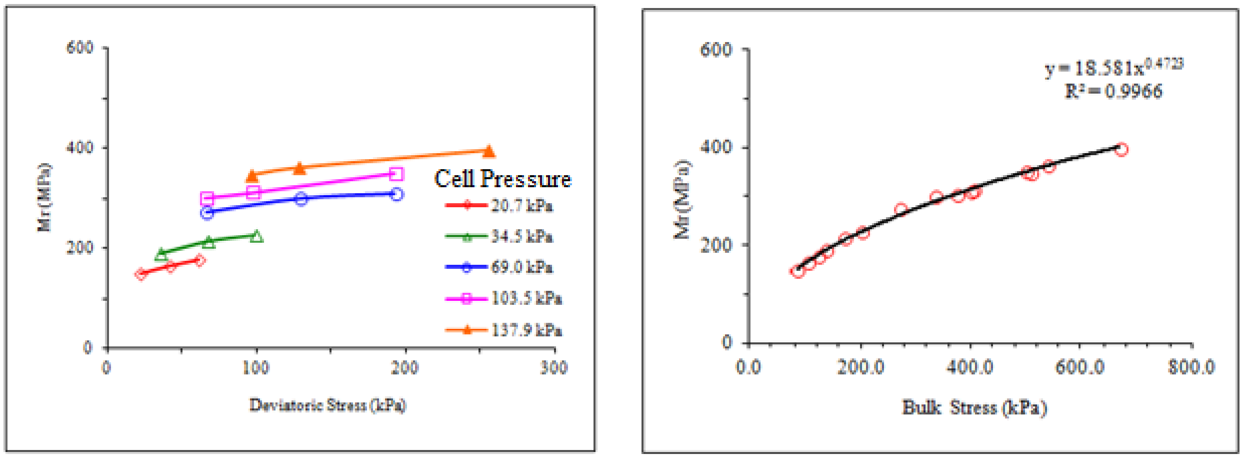

(43) Source 4 5% Substitute Fines @ 7% moisture content

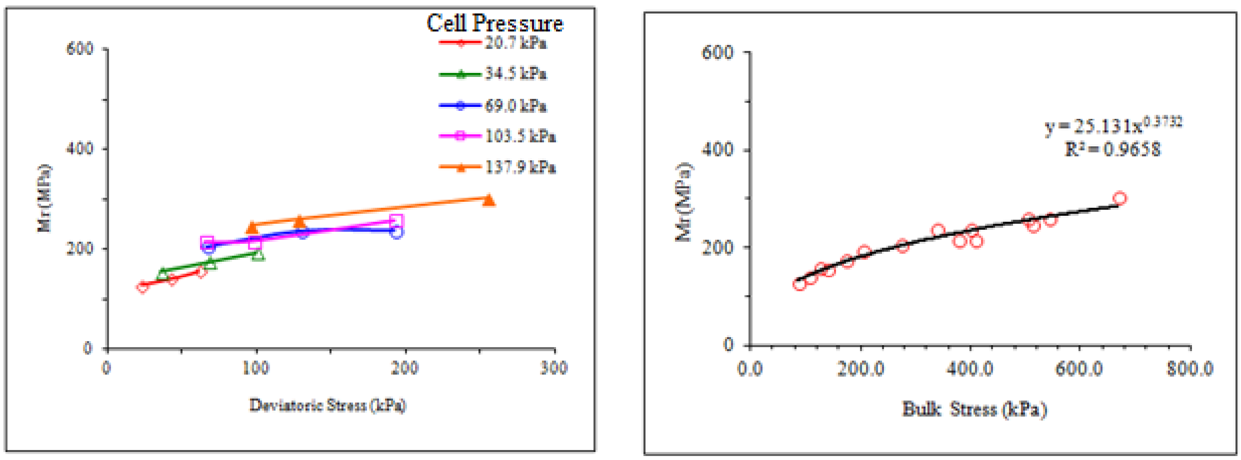

(44) Source 4 10% Substitute Fines @ 3% moisture content

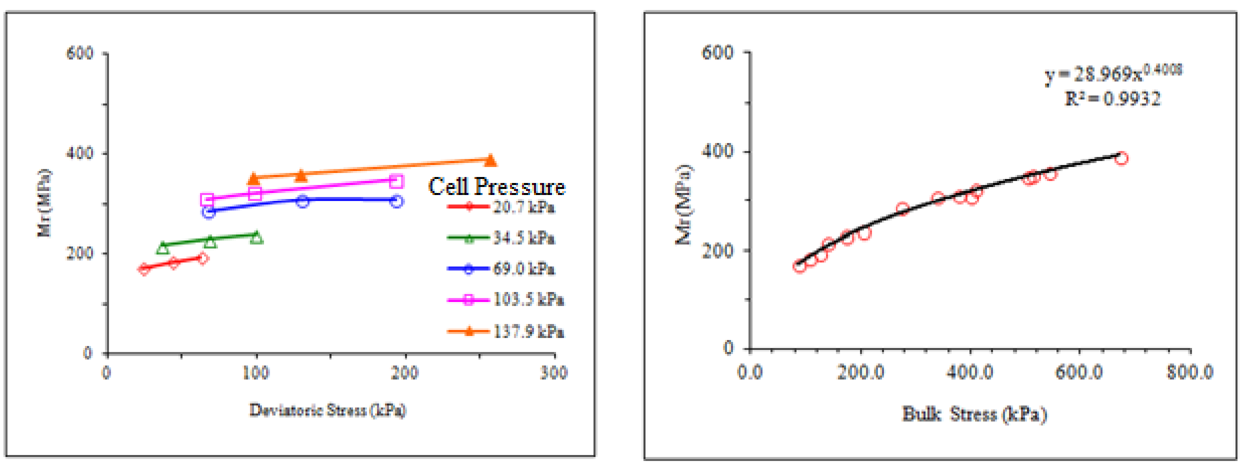

(45) Source 4 10% Substitute Fines @ 5% moisture content

Figure C.1 Relationship of resilient modulus with deviatoric and bulk stresses (Cont'd)

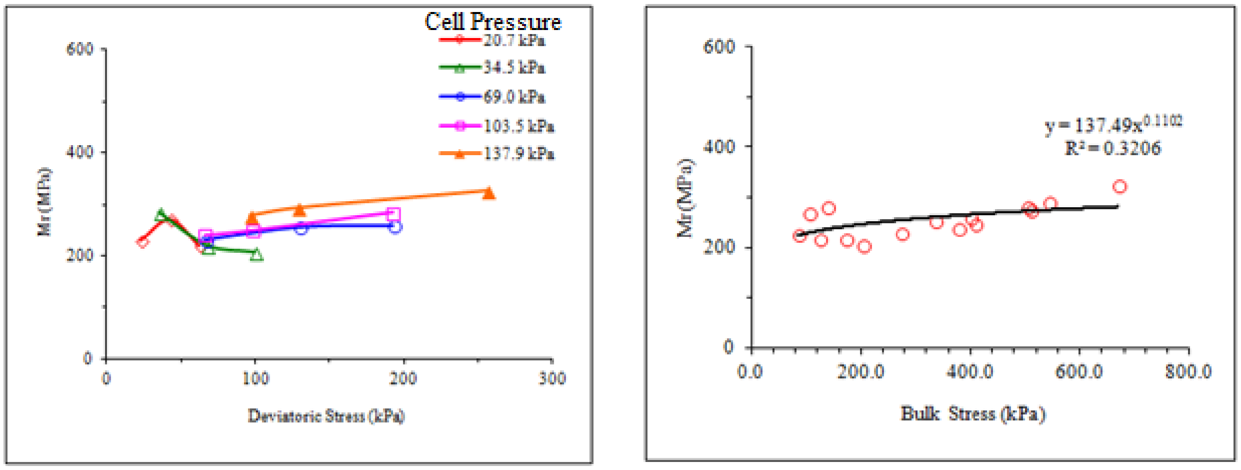

(46) Source 4 10% Substitute Fines @ 7% moisture content

Figure C.1 Relationship of resilient modulus with deviatoric and bulk stresses

Appendix D

D.1 Influence of Water Content

A range of water contents was used to determine the effect of fines on the resilient modulus. For natural fines, the water contents ranged from -2 percent, to +2 percent of $w_{opt.}$ Since vibratory compaction was used for preparing resilient modulus samples, the optimum water content was expected to be lower than the optimum value from the standard Proctor tests. With the optimum water content expected to be lower, 3 percent water content was chosen as the minimum and 7 percent water content was chosen as the maximum because the maximum CBR dry densities occurred when the water content was 7 percent for all sources. Water contents were also selected for the tests performed on 0 and 10 percent fines content.

The effect of water content at different fines content for Sources 1 to 4 is presented in Figure D.1 to D4. There is no systematic variation of M_R with water content as some specimens had higher M_R values at 5 percent water content and others at 7 percent water content. Generally, the resilient modulus was highest when the water content was 5 percent for 3 out of 4 sources. As the water content increased beyond 5 percent the M_R decreased.

As stated in Section 4.2.1, with the water content approaching 7 percent and above, many of the tests failed. The resilient modulus for the tests which did not fail was low with the exception of 7.9 percent F1 fines of Source 1 and 0 percent fines of Source 3. Looking at the CBR values for each source, they were highest when the water content was near 7 percent but because of different compaction methods for CBR and resilient modulus, the water content at 7 percent was wet of optimum resulting in a lower $M_{R.}$ It was also clear that the maximum M_R values for each source, except Source 3, occurred when the water content was below 6 percent. This indicates that when the water content goes above a certain point, the resilient modulus decreases

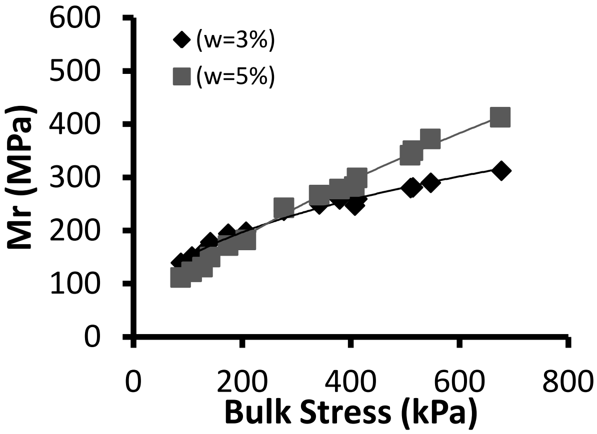

(a) 0 percent fines

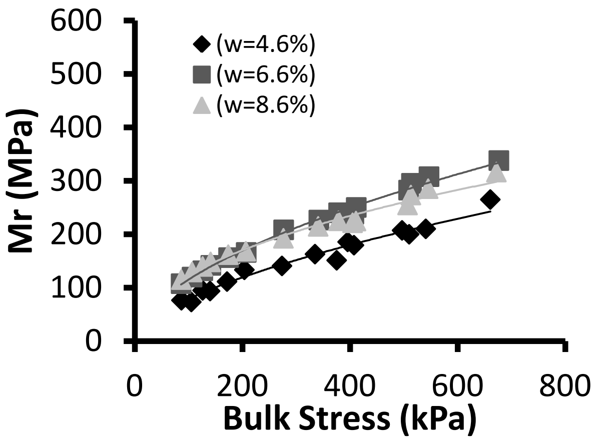

(b) Natural Fines

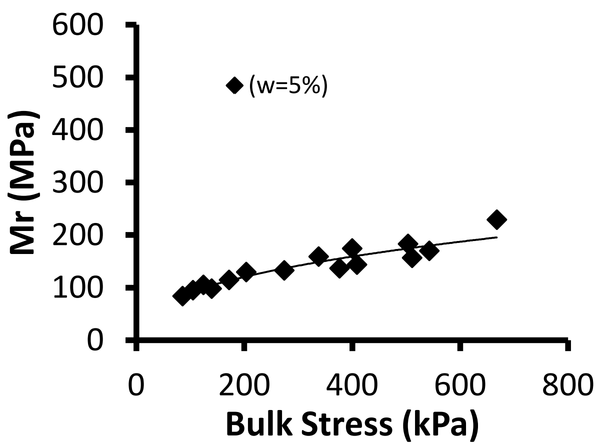

(c) 10 percent Natural fines

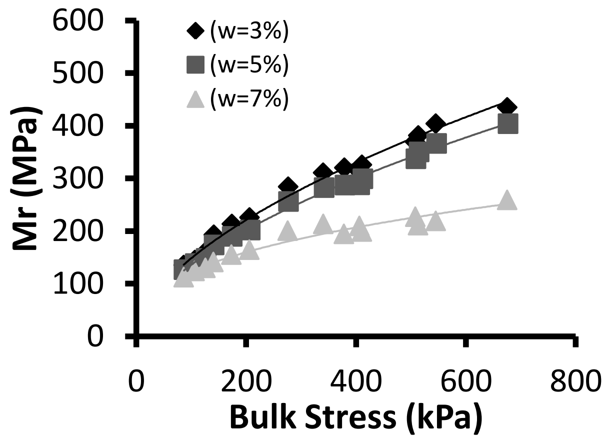

(d) 5 percent Substitute fines

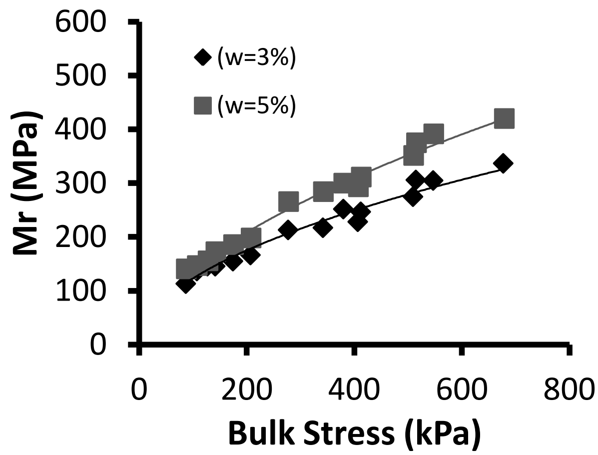

(e) 10 percent Substitute fines

Figure D.1 Source 1 resilient modulus vs. bulk stress

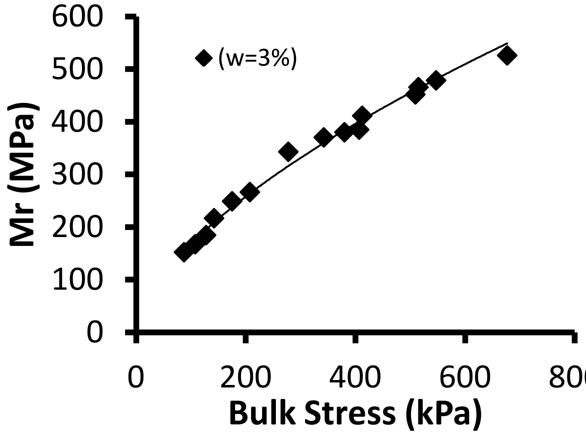

(a) 0 percent fines

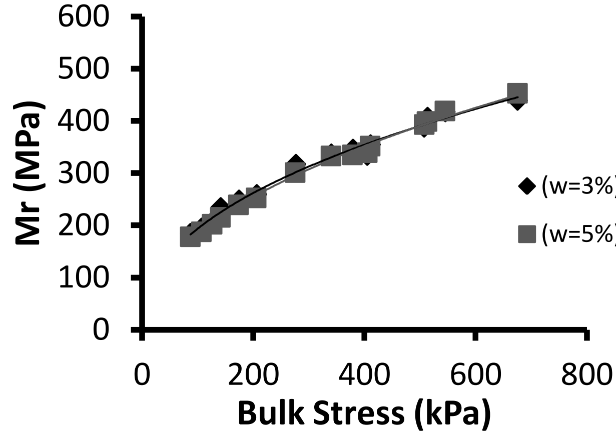

(d) 5 percent Substitute fines

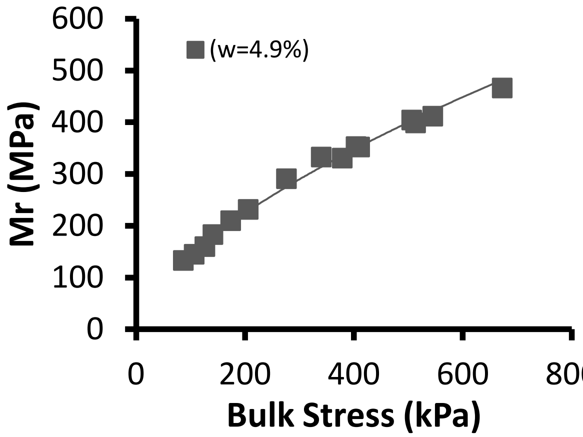

(b) Natural Fines

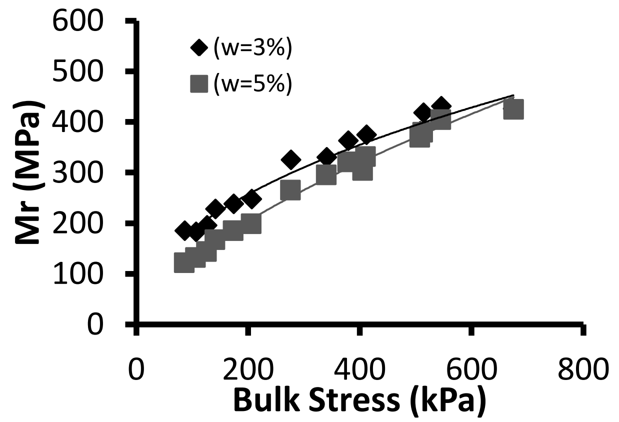

(e) 10 percent Substitute fines

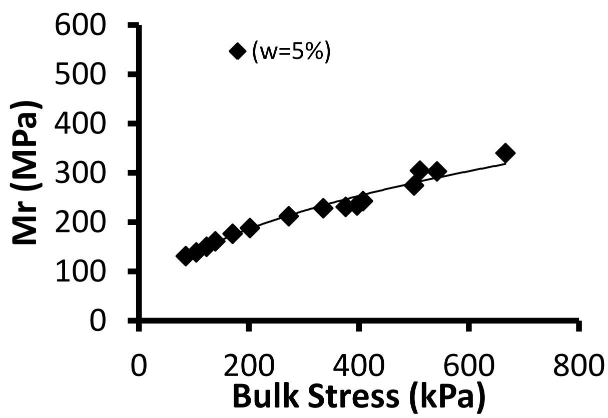

(c) 10 percent Natural fines

Figure D.2 Source 2 resilient modulus vs. bulk stress

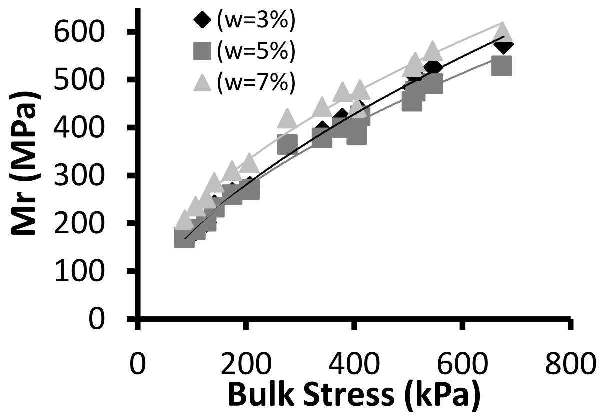

(a) 0 percent fines

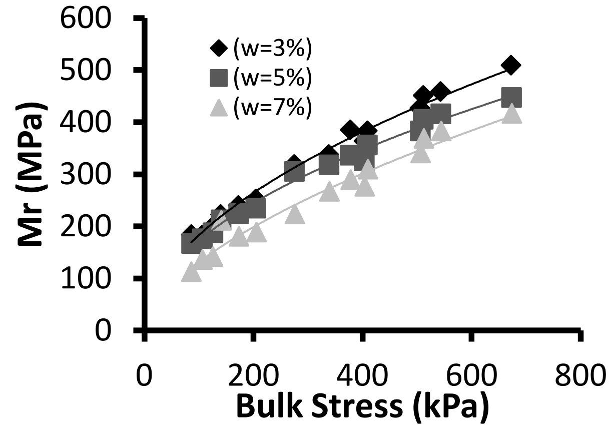

(d) 5 percent Substitute fines

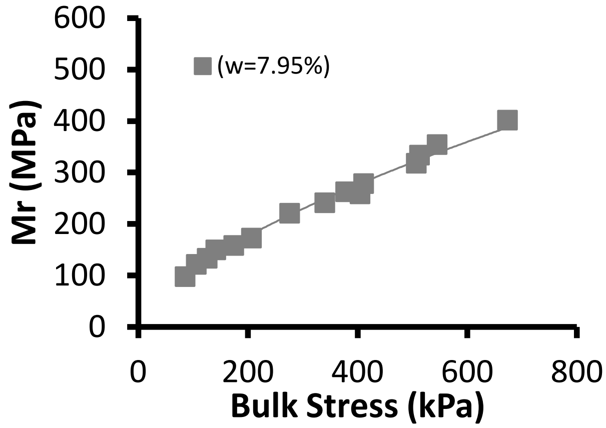

(b) Natural Fines

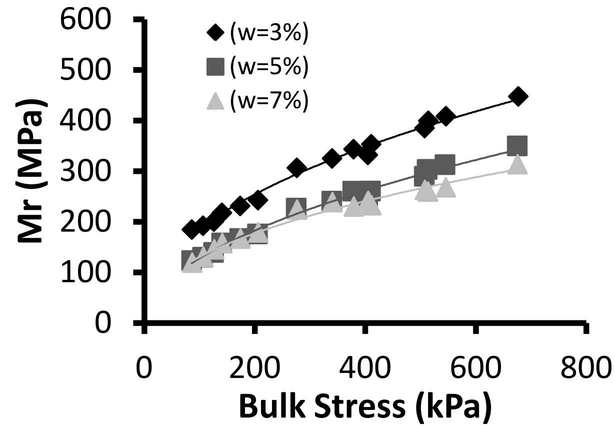

(e) 10 percent Substitute fines

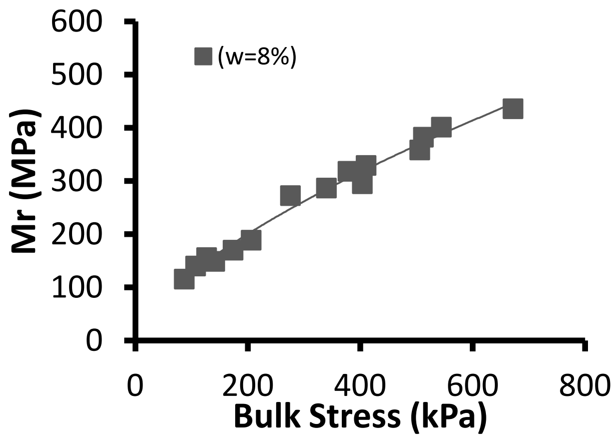

(c) 10 percent Natural fines

Figure D.3 Source 3 resilient modulus vs. bulk stress

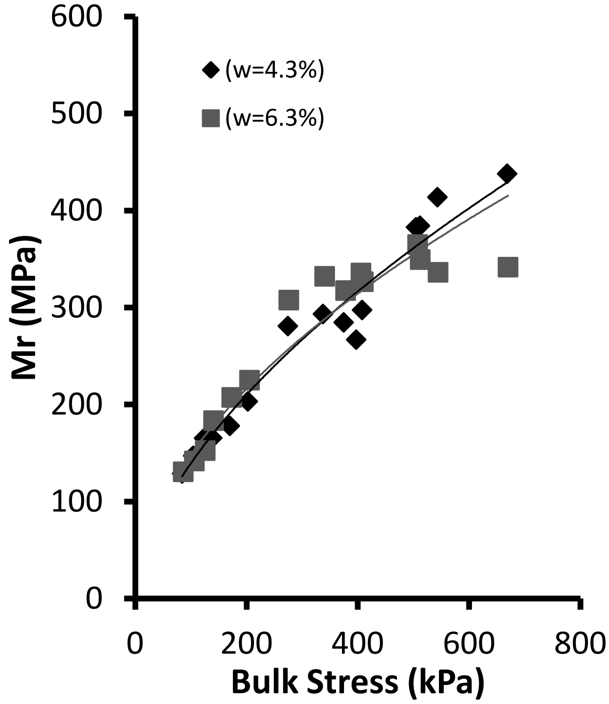

(a) Natural fines

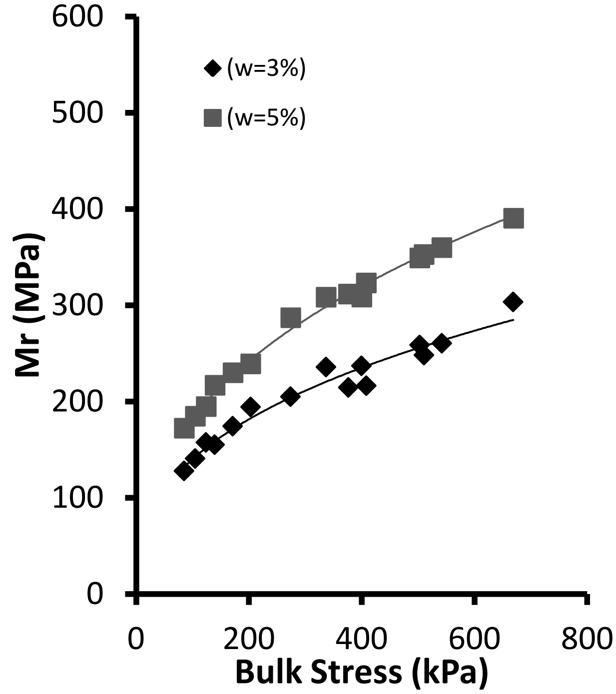

(d) 10 percent Substitute fines

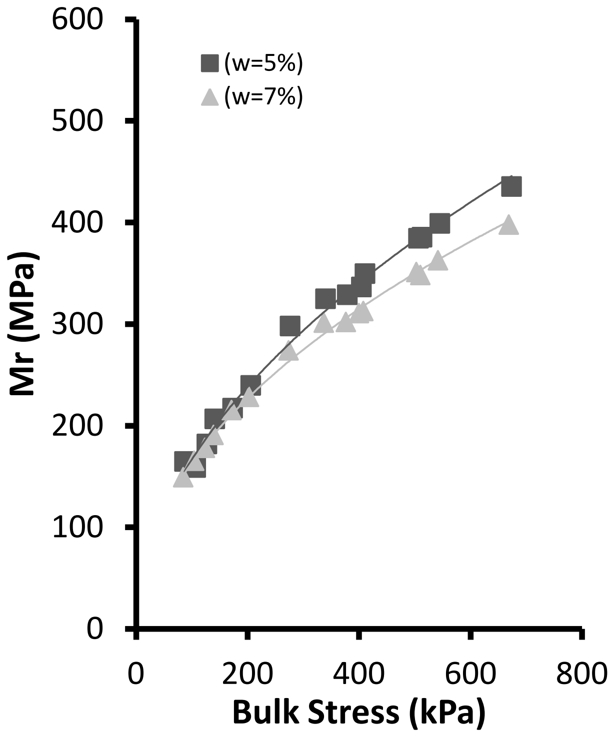

(c) 5 percent Substitute fines

Figure D.4 Source 4 resilient modulus vs. bulk stress

D.2 Influence of Fines content on Regression Coefficients for K_i, i = 1,2 and 3

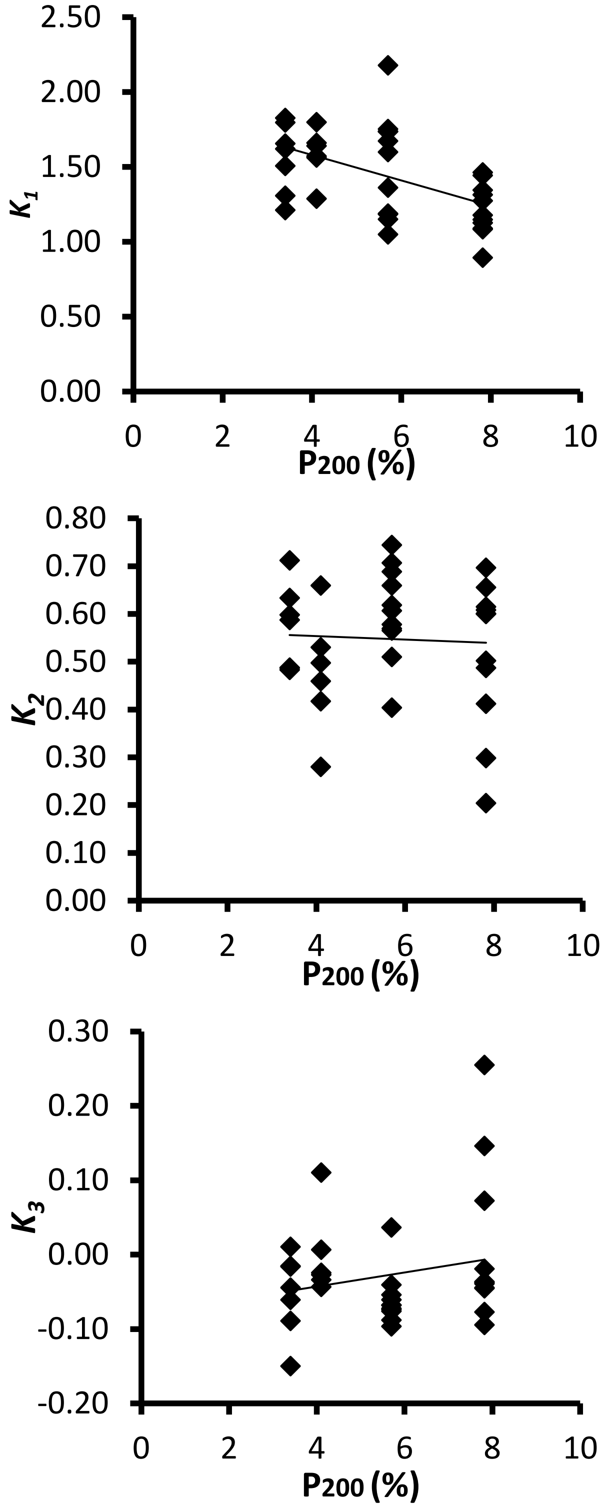

Figure D.5 Variation of *K*-coefficient with fines content for Uzan model

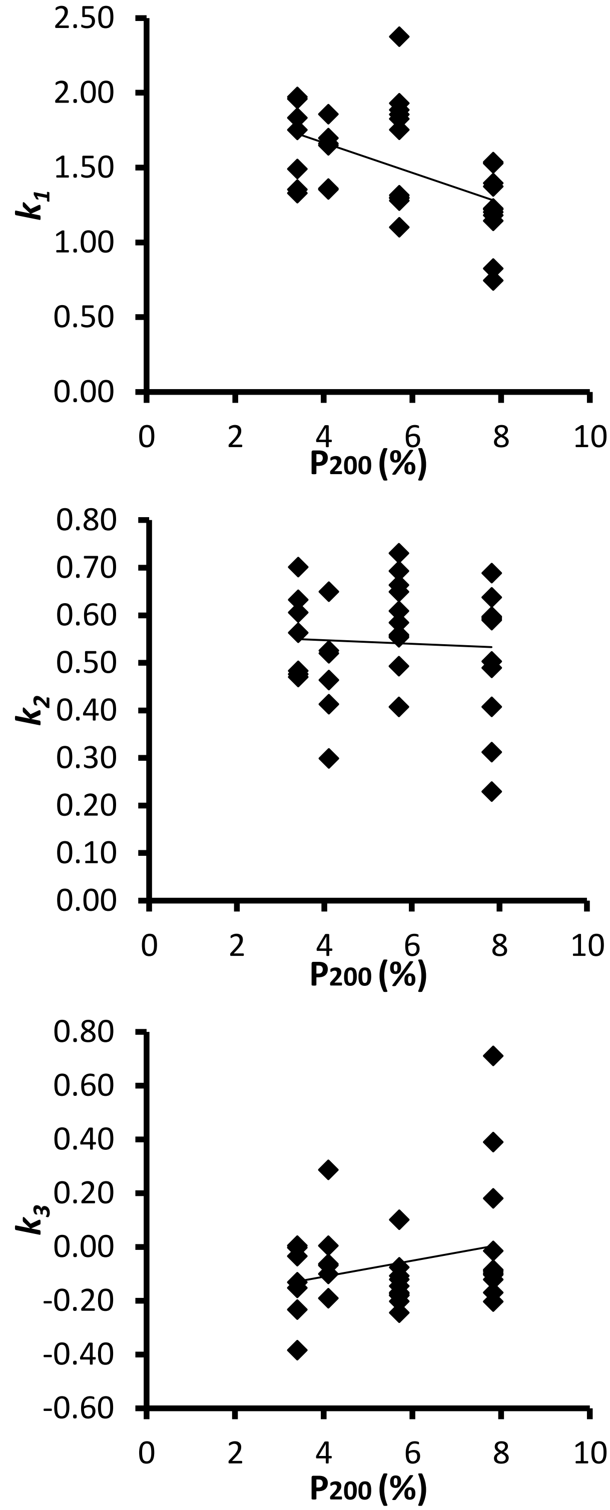

Figure D.6 Variation of *k*-coefficient with fines content for AASHTO model

D.3 Influence on *m* and *b*

Table D.1 *m* and *b* results for natural fines

List	m (MPa/kPa)	b (MPa)
S1/0% Fines (w=3)	0.194	180.5
S1/0% Fines (w=5)	0.457	110.1
S1/7.8% Fines (w=4.6)	0.305	53.7
S1/7.8% Fines (w=6.6)	0.348	108
S1/7.8% Fines (w=8.6)	0.325	99.1
S1/10% Fines (w=5)	0.205	73.3
S2/0% Fines (w=3)	0.489	292.5
S2/3.4% Fines (w=4.9)	0.439	173.9
S2/10% Fines (w=5)	0.355	104.9
S3/0% Fines (w=3)	0.561	204.2
S3/0% Fines (w=5)	0.46	226.8
S3/0% Fines (w=7)	0.490	277.7
S3/5.7% Fines (w=7.95)	0.483	79.2
S3/10% Fines (w=8)	0.450	140
S4/4.1% Fines (w=4.3)	0.503	113.7
S4/4.1% Fines (w=6.3)	0.086	293.4

Table D.2 *m* and *b* results for substitute fines

List	m (MPa/kPa)	b (MPa)
S1/5% Fines (w=3)	0.405	167.3
S1/5% Fines (w=5)	0.390	143.1
S1/5% Fines (w=7)	0.134	154.9
S1/10% Fines (w=3)	0.344	109
S1/10% Fines (w=5)	0.430	137.9
S2/5% Fines (w=3)	0.341	217.5
S2/5% Fines (w=5%)	0.399	189.7
S2/10% Fines (w=3)	0.313	233.9
S2/10% Fines (w=5)	0.429	151.2
S3/5% Fines (w=3)	0.504	178
S3/5% Fines (w=5)	0.396	188.3
S3/5% Fines (w=7)	0.502	93.9
S3/10% Fines (w=3)	0.372	198.6
S3/10% Fines (w=5)	0.323	131.4
S3/10% Fines (w=7)	0.218	154.1
S4/5% Fines (w=5)	0.358	199.5
S4/5% Fines (w=7)	0.318	187.2
S4/10% Fines (w=3)	0.232	138.6
S4/10% Fines (w=5)	0.268	212.4

D.4 Influence of Regression Coefficients

Table D.3 Source 1 regression coefficients

			Uzan			AASHTO			*K-θ*		
SOURCE	w (%)	Fines (%)	K_1	K_2	K_3	k_1	k_2	k_3	K_1	K_2	K_3
S1	4.6	7.8 F1	0.890	0.490	0.150	0.750	0.500	0.390	0.770	0.610	0
S1	6.6	7.8 F1	1.085	0.608	-0.045	1.145	0.597	-0.098	1.135	0.569	0
S1	8.6	7.8 F1	1.178	0.502	-0.019	1.203	0.490	-0.015	1.201	0.485	0
S1	3	0	1.464	0.412	-0.038	1.537	0.408	-0.103	1.519	0.380	0
S1	5	0	1.127	0.697	-0.039	1.182	0.689	-0.090	1.174	0.662	0
S1	5	10 F1	1.149	0.204	0.255	0.826	0.229	0.711	0.893	0.423	0
S1	3	5 F2	1.444	0.601	-0.045	1.529	0.596	-0.121	1.512	0.561	0
S1	5	5 F2	1.315	0.600	-0.037	1.374	0.593	-0.085	1.364	0.568	0
S1	7	5 F2	1.346	0.299	0.072	1.227	0.312	0.181	1.253	0.361	0
S1	3	10 F2	1.089	0.615	-0.095	1.222	0.590	-0.203	1.199	0.532	0
S1	5	10 F2	1.274	0.656	-0.077	1.397	0.638	-0.170	1.376	0.588	0

Table D.4 Source 2 regression coefficients

			Uzan			AASHTO			*K-θ*		
SOURCE	w (%)	Fines (%)	K_1	K_2	K_3	k_1	k_2	k_3	K_1	K_2	K_3
S2	4.9	4.3 F1	1.508	0.598	0.010	1.491	0.606	0.0047	1.492	0.607	0
S2	3	0	1.657	0.634	-0.044	1.752	0.633	-0.131	1.732	0.594	0
S2	5	10 F1	1.308	0.483	-0.015	1.330	0.470	-0.0025	1.329	0.470	0
S2	3	5 F2	1.827	0.487	-0.061	1.973	0.476	-0.152	1.940	0.435	0
S2	5	5 F2	1.797	0.488	-0.012	1.833	0.483	-0.034	1.827	0.474	0
S2	3	10 F2	1.621	0.588	-0.150	1.960	0.563	-0.384	1.879	0.459	0
S2	5	10 F2	1.212	0.712	-0.089	1.354	0.701	-0.233	1.330	0.632	0

Table D.5 Source 3 regression Coefficients

			Uzan			AASHTO			*K-θ*		
SOURCE	w (%)	Fines (%)	K_1	K_2	K_3	k_1	k_2	k_3	K_1	K_2	K_3
S3	7.95	5.7 F1	1.050	0.707	-0.041	1.101	0.693	-0.076	1.100	0.670	0
S3	3	0	1.730	0.660	-0.068	1.886	0.650	-0.170	1.859	0.600	0
S3	5	0	1.753	0.619	-0.076	1.930	0.609	-0.203	1.893	0.552	0
S3	7	0	2.179	0.565	-0.068	2.376	0.556	-0.180	2.332	0.506	0
S3	8	10 F1	1.151	0.744	-0.097	1.296	0.731	-0.245	1.272	0.659	0
S3	3	5 F2	1.674	0.607	-0.073	1.826	0.585	-0.146	1.802	0.544	0
S3	5	5 F2	1.600	0.569	-0.074	1.753	0.554	-0.174	1.723	0.505	0
S3	7	5 F2	1.185	0.689	-0.088	1.316	0.664	-0.180	1.296	0.611	0
S3	3	10 F2	1.738	0.510	-0.054	1.856	0.493	-0.108	1.835	0.463	0
S3	5	10 F2	1.189	0.578	-0.061	1.279	0.559	-0.121	1.265	0.525	0
S3	7	10 F2	1.362	0.404	0.036	1.300	0.408	0.101	1.315	0.435	0

Table D.6 Source 4 regression coefficients

			Uzan			AASHTO			*K-θ*		
SOURCE	w (%)	Fines (%)	K_1	K_2	K_3	k_1	k_2	k_3	K_1	K_2	K_3
S4	4.3	4.1 F1	1.288	0.660	-0.043	1.360	0.650	-0.101	1.350	0.620	0
S4	6.3	4.1	1.573	0.498	-0.034	1.661	0.520	-0.191	1.627	0.468	0
S4	5	5 F2	1.641	0.530	-0.027	1.698	0.526	-0.069	1.686	0.507	0
S4	7	5 F2	1.661	0.459	0.0065	1.649	0.464	0.0045	1.650	0.465	0
S4	3	10 F2	1.563	0.280	0.110	1.354	0.299	0.287	1.399	0.376	0
S4	5	10 F2	1.799	0.417	-0.025	1.857	0.413	-0.063	1.844	0.396	0

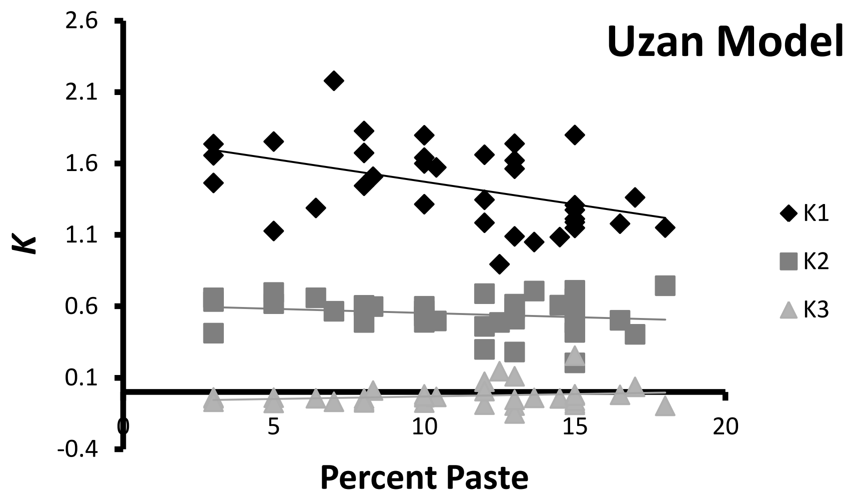

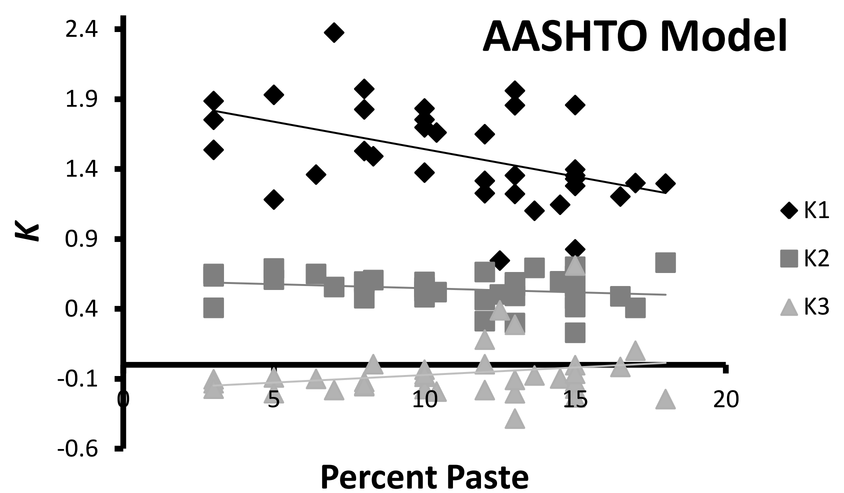

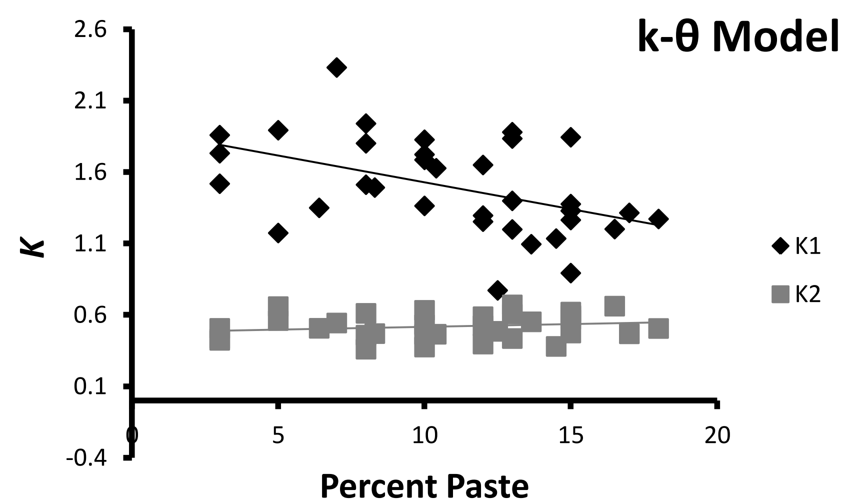

Figure D.7 Regression coefficients vs. percent paste

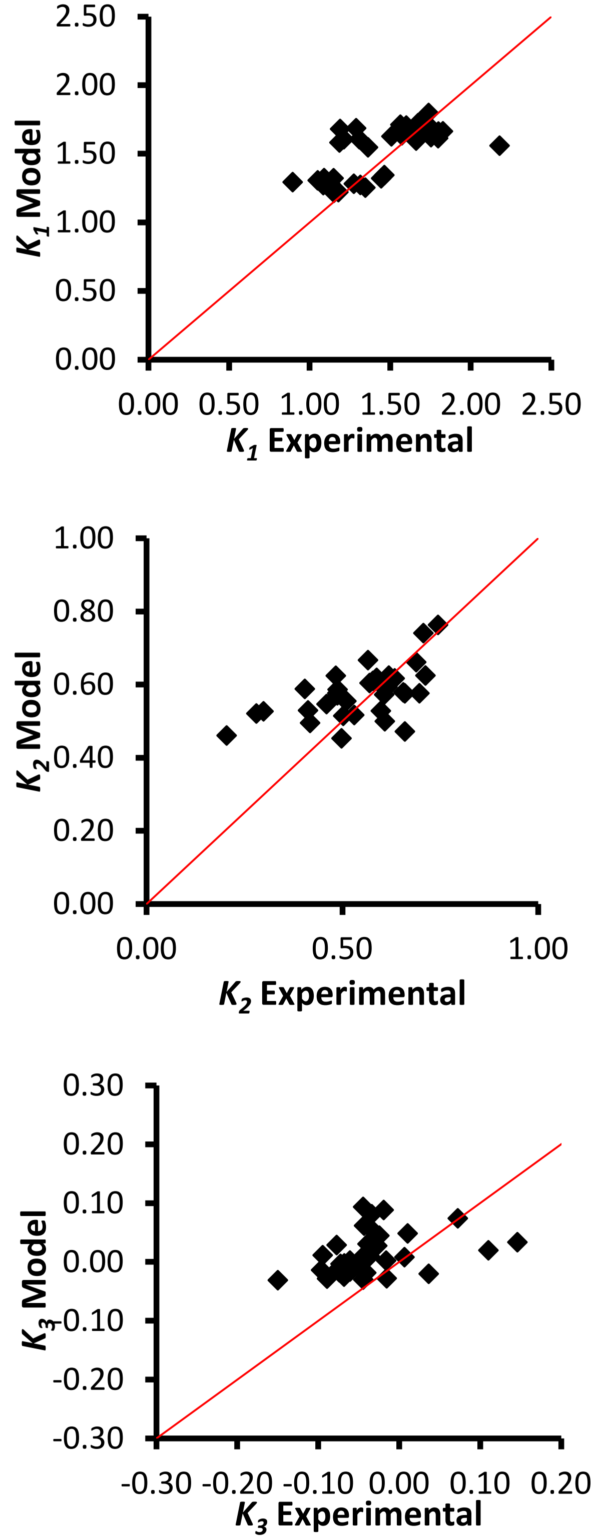

Figure D.8 Uzan model *K*-coefficients from Equation (8) (Guo et al. 2006)

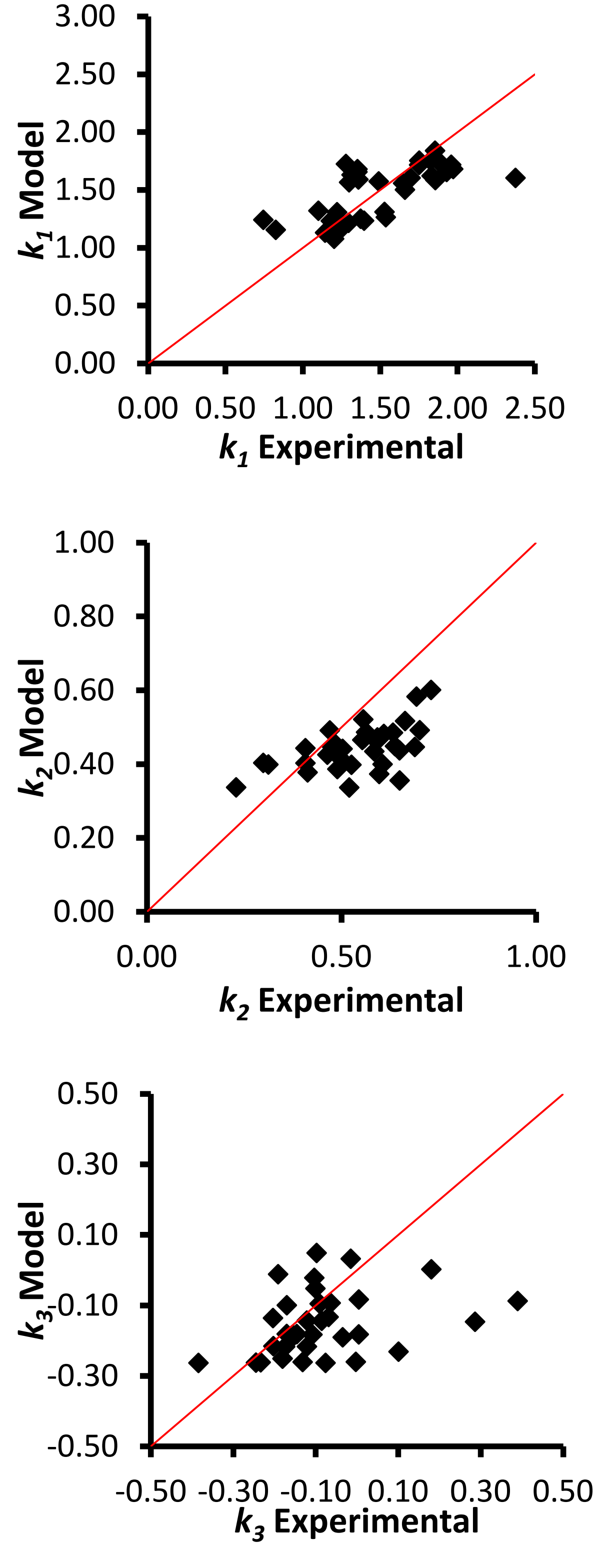

Figure D.9 AASHTO model *K*-coefficients from Equation (8) (Guo et al. 2006)

From Figures D.9 and D.10 it is clear that the K_1 values from Equation 8 closely match the experimental data. The K_2 values have more scatter compared to K_1 for both the Uzan and AASHTO models. The K_3 values for the Uzan model closely match the experimental data, but for the AASHTO model there is a significant amount of scatter amongst the K_3 values.

D.5 Permanent Deformation

Table D.7 Source 1 permanent deformation

			Cell Pressure				
			20.7 kPa	34.5 kPa	69 kPa	103.5 kPa	137.9 kPa
Source	Water (%)	Fines (%)	Strain				
S1	4.6	7.8 F1	0.00065	0.00041	0.0012	0.00048	0.00068
S1	6.6	7.8 F1	0.00047	0.00067	0.0022	0.00060	0.00094
S1	8.6	7.8 F1	0.00034	0.00039	0.0017	0.00056	0.00092
S1	3	0 F1	0.00035	0.00029	0.0011	0.00036	0.00058
S1	5	0 F1	0.00029	0.00028	0.00077	0.00028	0.00045
S1	5	10 F1	0.0016	0.00070	0.0029	0.0011	0.0013
S1	3	5 F2	0.000091	0.00016	0.00053	0.00023	0.00039
S1	5	5 F2	0.00019	0.00018	0.00058	0.00025	0.00041
S1	7	5 F2	0.00024	0.00031	0.0015	0.00053	0.001
S1	3	10 F2	0.00048	0.00077	0.0013	0.00045	0.00063
S1	5	10 F2	0.00021	0.00023	0.00092	0.00031	0.00053

Table D.8 Source 2 permanent deformation

			Cell Pressure				
			20.7 kPa	34.5 kPa	69 kPa	103.5 kPa	137.9 kPa
Source	Water (%)	Fines (%)	Strain				
S2	4.9	3.4 F1	0.00019	0.00016	0.00031	0.00011	0.00017
S2	3	0 F1	0.0002	0.00019	0.00045	0.00016	0.00025
S2	5	10 F1	0.00022	0.00026	0.0011	0.00031	0.00042
S2	3	5 F2	0.00015	0.00015	0.00052	0.00025	0.00062
S2	5	5 F2	0.00012	0.00017	0.00056	0.0002	0.00035
S2	3	10 F2	0.000053	0.00015	0.0011	0.00038	0.0015
S2	5	10 F2	0.00021	0.00025	0.00094	0.00031	0.00068

Table D.9 Source 3 permanent deformation

			Cell Pressure				
			20.7 kPa	34.5 kPa	69 kPa	103.5 kPa	137.9 kPa
Source	Water (%)	Fines (%)	Strain				
S3	7.95	5.7 F1	0.00077	0.00058	0.0013	0.00042	0.00051
S3	3	0 F1	0.00025	0.00019	0.00028	0.000095	0.00014
S3	5	0 F1	0.00032	0.00021	0.00034	0.00012	0.00015
S3	7	0 F1	0.00010	0.00013	0.00028	0.00012	0.00017
S3	8	10 F1	0.00055	0.00048	0.00048	0.00019	0.00029
S3	3	5 F2	0.00013	0.00010	0.00015	0.00010	0.00012
S3	5	5 F2	0.00018	0.00024	0.00057	0.00021	0.00029
S3	7	5 F2	0.00047	0.00039	0.00072	0.00026	0.00037
S3	3	10 F2	0.00016	0.00017	0.00042	0.00018	0.00030
S3	5	10 F2	0.00045	0.00026	0.00082	0.00029	0.00043
S3	7	10 F2	0.00015	0.00035	0.0013	0.00047	0.00071

Table D.10 Source 4 permanent deformation

			Cell Pressure				
			20.7 kPa	34.5 kPa	69 kPa	103.5 kPa	137.9 kPa
Source	Water (%)	Fines (%)	Strain				
S4	4.3	4.1 F1	0.00011	0.00022	0.00075	0.00019	0.00027
S4	6.3	4.1 F1	0.00021	0.00015	0.00048	0.00027	0.00076
S4	5	5 F2	0.00014	0.00011	0.00032	0.000138	0.00024
S4	7	5 F2	0.00015	0.00019	0.00058	0.00022	0.00032
S4	3	10 F2	0.00028	0.00035	0.0016	0.00042	0.00059
S4	5	10 F2	0.00014	0.00018	0.00069	0.00019	0.00032